Bacterial Energy Metabolism Laboratory

Instituto de Tecnologia Química e Biológica - António Xavier

Universidade Nova de Lisboa

Av. da República, Estação Agronómica Nacional

2780-157 Oeiras, Portugal

http://www.itqb.unl.pt

http://www.itqb.unl.pt/labs/bacterial-energy-metabolism

Table of contents

Chapter 6 – Concluding remarks

Acknowledgments

The work present here was only possible due to the help and cooperation of several people to whom I am very thankful.

First I must acknowledge my supervisor, Doctor Inês Cardoso Pereira. When I first came to ITQB as a master graduate, I presented all my qualities and limits to Doctor Inês and still, she believed in my passion for science and my desire to obtain a PhD. For the past five years, Doctor Inês helped me to overcome some of my limits and to become the scientist that I am today, still not perfect but much better. Doctor Inês was always present to discuss my results and to guide me in the right strategy. For all of the above I am very grateful for the attention and dedication that Doctor Inês gave me, as well as for the revision of this thesis. Thank you Doctor Inês!

To Sofia Venceslau for all the discussions and for the cooperation in my work. As a biologist I had not had a lot of experience in working with proteins and Sofia was the one that introduced me to this world, as well as the daily routine of the laboratory. She was always available to discuss and to help during my Ph.D.

To all my lab colleagues and friends that I made during my Ph.D: to Marta and Mónica for the support and friendship, and to Américo for the discussions as well as for the cooperation in his work. Also, I thank Isabel Pacheco for the purification of the hydrogenase and the pyruvate ferredoxin oxidoreductase and for her support in the laboratory.

To Doctor Christiane Dahl, for receiving me to work in her laboratory at Bonn University for three periods. With her I learned a lot, she was always very kind to me making me feel like at home. During my stay in Bonn I got the chance to meet several people with whom I became friends: Yvonne, Thomas, Kevin, Jeanette, Renate, Julia, Konrad, Tobias and Anja. To all a great thanks for always being available to spend time with me, again making me feel at home. With them I never felt a foreigner but a member of the group.

To Fabian Grein, for teaching me several molecular biology techniques, and also for being a close friend to whom I am very thankful. Fabian was always present, often by Skype, and always available to discuss my work. I must say that he was my support during my stay in Bonn, helping me to find a home and also making me feel very, very good. A final remark, the rubber “For BIG mistakes” is always with me, and I know that it can also be used for “a lot of small ones”. To Fabian: You are the best!

To Doctor Ricardo Louro and Doctor Margarida Archer, for accepting to be part of my scientific thesis committee, and for the helpful discussions.

To Luís Gafeira, from the Cell Physiology & NMR Lab for the discussions about *Archaeoglobus fulgidus,* which helped me to understand better this organisms and led me to improve my work.

To Eng. João Carita for the bacterial growths and also for the rides to the train station.

To William Leavitt, who introduced me to the chemical techniques to detect sulfur compounds. I must refer that working with him improved my ability to organize my work.

To Cláudia for her friendship and for always being there! I must say that the best thing about Cláudia is being the type of friend that I like: honest, not saying what we want but what she thinks! I cannot forget to thank Cláudia for introducing to me a very good friend that I have now: César! Thank you both for your friendship.

To all the friends that I made in ITQB, really nice people that made me believe that it is possible to go through tough times.

To Doctor Ricardo Louro and to Doctor Catarina Paquete for the discussions about NMR and cytochromes and for the support and patience with all my questions.

To Eng Paula Chicau and Eng Cristina Leitão for the introduction to the HPLC equipment, for all the discussions on HPLC problems and for their friendship and support, helping me in the maintenance of the equipment.

To my friends: Pedro, Luís (Pascoal), Victor (Grijó), Ricardo (Pombinha), Alexandre (Jagu), Andréia (Jaga), Juliano and Jorge for always being present in the good and the bad moments to cheer me.

To my family, and specially to my cousins Paulo, Sílvia and Francisco, for the late nights of talking and amusement.

To my Parents, that made this journey possible by always believing that I was capable of different things.

To my sister and to my brother in law, for the support and most importantly for giving birth to my two beloved nephews.

Finaly to my wife, Inês, I must say that this was only possible due to you. You were the one that pushed me further and supported me even when I was really down. You always understood the five hours of trains per day, the lack of humor and the times where frustration was my main face.

Always supporting me to go abroad and for the main sentence “you can do it”! Thanks my love, you make everything possible.

To ITQB-AX UNL for the amazing conditions to work, and also to the staff that are formidable people.

Fundação para a Ciência e Tecnologia is acknowledged for the financial support, by awarding me a PhD fellowship (SFRH/BD/ /77940/2011)

Thank you

This thesis is dedicated to my beloved wife, Inês Silva

Thesis outline

The present work contributes to clarify decades of debate concerning the last step of the dissimilatory sulfate reduction pathway, the reduction of sulfite to sulfide. This work focused on proteins involved in the dissimilatory reduction of sulfite such as DsrAB, the soluble sulfite reductase, DsrC (crucial for DsrAB function), and DsrJ, a membrane-bound cytochrome *c* that belongs to DsrMKJOP membrane complex. In addition, we tried to find the physiological electron donor for the DsrAB enzyme.

This thesis begins with a short general introduction on sulfate reducing prokaryotes and their physiological properties. The second chapter contains the detailed characterization of the dissimilatory sulfite reductases of *Desulfovibrio vulgaris* and *Archaeoglobus fulgidus* as well as the description of the *A. fulgidus* DsrC mutants produced. This is followed by a third chapter concerning the reduction of sulfite by DsrAB and its interaction with DsrC, which revealed the important role of this small protein in the process. The fourth chapter includes studies to find the physiological electron donor for DsrAB testing several oxidoreductases such as pyruvate ferredoxin-oxidoreductase (Por), aldehyde oxidoreductase (Aor), the carbon monoxide dehydrogenase (CODH) and also NADH oxidase (NoxA-3). Chapter five covers the ongoing investigation about the heme protein DsrJ, a very special cytochrome that contains an unusual His/Cys distal axial heme *c* ligation, where several techniques were used to determine the nature and function of this ligation. Finally, the sixth chapter is a general conclusion that includes some considerations on the future perspectives of this work.

List of publications

A protein trisulfide couples dissimilatory sulfate reduction to energy conservation

André A. Santos*, Sofia S. Venceslau*, Fabian Grein, William D. Leavitt, Christiane Dahl, David T. Johnston and Inês A. C. Pereira
(2015) *Science* **350**: 1541-1545.

* co-first authors

Sulfur Isotope Effects of Dissimilatory Sulfite Reductase

William D. Leavitt, Alexander S. Bradley, **André A. Santos**, Inês A. C. Pereira and David T. Johnston
(2015) *Frontiers in Microbiology* **6**.

Electron Transfer between the QmoABC Membrane complex and Adenosine 5´-Phosphosulfate Reductase

Américo G. Duarte, **André A. Santos** and Inês A. Cardoso Pereira
(2015) submitted to BBA – Bioenergetics – under review

Abstract

Life on Earth is extremely diverse, as organisms had to adapt to a panoply of different environmental niches. There are several mechanisms by which organisms grow in the absence of oxygen, one of which is the dissimilatory reduction of sulfate to sulfide, performed by sulfate reducing prokaryotes (SRP). This is thought to be one of the most ancient biological metabolisms to have developed on earth. In SRP sulfate is first imported to the cytoplasm where it is activated by Sulfate adenylyl transferase to adenosine 5′-phosphosulfate (APS) in an ATP consuming process. After, the adenylyl-sulfate reductase is the enzyme responsible for the reduction of APS to sulfite. The next step involves the reduction of sulfite to sulfide, but the mechanism involved in this process is not clear. There are two proposals that have been made for this step: an earlier one based on *in vitro* assays (the trithionate pathway) and a more recent one based on crystallographic information (DsrAB + DsrC pathway).

The work developed in this thesis aimed to contribute to the understanding this last step of sulfate reduction. The work was divided in three main tasks: i) the study of the interaction of DsrAB with DsrC in the reduction of sulfite, ii) the search for the physiological electron donor to DsrAB and iii) the characterization of the cytochrome *c* type DsrJ present in the DsrMKJOP complex.

The first task validated the DsrAB-DsrC pathway in which we proved that DsrC is crucial to the activity of sulfite reduction by DsrAB, being used as a co-substrate along with sulfite. Our work showed that the product of sulfite reduction by DsrAB is a DsrC trisulfide. This implies that in the energy conservation accomplished by the dissimilatory reduction of sulfide, four electrons are pooled from the reduced

menaquinone pool through the DsrMKJOP membrane complex to reduce the DsrC-trisulfide.

In the second task we aimed to disclose the physiologic electron donor of the first two electrons needed by DsrAB for the reduction of sulfite. To access this question we used three ferredoxin oxidoreductases (Aldehyde oxidoreductase, Pyruvate ferredoxin oxidoreductase and Carbon monoxide dehydrogenase) and one NADH oxidase (recombinant NoxA-3). These candidates were used in *in vitro* activity assays with DsrAB/sulfite and also in protein-protein interaction studies (surface plasma resonance). None of the candidates tested demonstrated to interact with DsrAB, but further experiments have to be carried out to discard them completely as electron donors.

The last task involved the analysis of the distal axial heme ligands of the DsrJ subunit of the DsrMKJOP complex, and was a continuation of previous work developed by Grein and coworkers. DsrJ is a protein that contains three heme binding motifs in which the corresponding ligands are proposed to be Histidine/Histidine, Methionine/Histidine and the unusual Cysteine/Histidine. Here we generated several variations on the *dsrJ* gene from *Allochromatium vinosum* in the potential distal axial ligands and analyzed these variants by several techniques: Electron paramagnetic resonance (EPR), Resonance Raman (RR), Nuclear magnetic resonance (NMR), Mass spectrometry (MS) and UV-visible. Although we generated more than ten variants, we were not able to identify the correct distal axial heme ligand for the three hemes present in the DsrJ protein. These results suggested that: i) there might be something during the protein purification that can bind to the modified heme in the absence of correct distal axial ligand or ii) that the protein is not correctly folded due to the absence of the other subunits of the membrane complex DsrMKJOP, although by MS the recombinant

protein and the tested mutants have the correct weight including three hemes.

The work presented here demonstrates the crucial role of the DsrC protein in DsrAB sulfite reduction, leading to energy conservation by the membrane complex DsrMKJOP. On the other hand, work on finding the physiological electron donor for the first two electrons needed by DsrAB has to be continued as it is extremely important to fully understand the dissimilatory sulfite reduction mechanism. The role of the DsrMKJOP complex, and more specifically of DsrJ, remains a mystery to be solved for both SRP and sulfate oxidizing bacteria (SOB), where it was proven to be essential for the oxidation of sulfur globules.

Sumário

A vida na Terra é extremamente diversificada, principalmente devido à adaptação de micro-organismos a diferentes nichos ambientais. Existem vários mecanismos pelos quais os micro-organismos conseguem obter energia na ausência de oxigénio, sendo um deles a redução dissimilativa do sulfato a sulfureto, realizada por organismos procariontes redutores de sulfato (SRP). Este poderá ser um dos mecanismos biológicos de obtenção de energia mais antigos, tendo aparecido muito antes da disponibilidade de oxigénio na atmosfera. Nestes organismos o sulfato é primeiro importado para o citoplasma, onde é ativado pela sulfato adenilil-transferase a adenosina 5'-fosfosulfato (APS), num processo com consumo de ATP. Seguidamente, a APS reductase é a enzima responsável pela redução de APS a sulfito. O próximo passo envolve a redução de sulfito de sulfureto, mas o mecanismo envolvido neste processo não é claro. Existem duas propostas para esta etapa: uma baseada em ensaios *in vitro* (a via do tritionato) e outra, mais recente, com base em informações cristalográficas (via da DsrAB + DsrC).

O trabalho desenvolvido nesta tese teve como objetivo contribuir para a compreensão deste passo da redução do sulfato. O trabalho foi dividido em três tarefas principais: i) o estudo da interação da DsrAB com DsrC na redução de sulfito, ii) a pesquisa do dador de eletrões fisiológico para DsrAB e iii) a caracterização de DsrJ, um citocromo tipo *c*, presente no complexo membranar DsrMKJOP.

A primeira tarefa validou a via DsrAB-DsrC na qual se provou que a DsrC é crucial para a atividade de redução de sulfito pela DsrAB, sendo utilizada como um co-substrato juntamente com sulfito. O nosso trabalho mostrou que o produto de redução do sulfito pela DsrAB é um

trissulfureto associado à DsrC. Este facto implica que, na conservação de energia associada à redução dissimilativa de sulfato, quatro eletrões serão provenientes da menaquinona membranar através do complexo DsrMKJOP reduzindo o DsrC-trissulfureto.

A segunda tarefa teve como objetivo descobrir o doador fisiológico dos dois primeiros eletrões requeridos pela DsrAB para a redução de sulfito. Para tal, foram utilizadas três ferredoxina oxidoreductases (aldeído oxidoreductase, piruvato ferredoxina oxidoreductase e desidrogenase de monóxido de carbono) e uma NADH oxidase (NOXA-3). Estes possíveis dadores foram testados em ensaios de atividade *in vitro* com DsrAB/sulfito e também em estudos de interação proteína-proteína (Ressonância plasmónica de superfície). Nenhum dos possíveis dadores testados demonstrou interagir com DsrAB, porém mais testes deverão ser realizadas de modo verificar estas conclusões.

A última tarefa envolveu a análise dos ligandos axiais distais dos hemos presentes na subunidade DsrJ do complexo membranar DsrMKJOP, tendo este trabalho sido uma continuação de trabalho anterior desenvolvido por Grein e colaboradores. A DsrJ é uma proteína que contém três motivos de ligação a hemos tipo *c*, nos quais os ligandos propostos são Histidina/Histidina, Metionina/Histidina e uma invulgar Cisteína/Histidina. De modo a verificar a identidade destes ligandos, produzimos vários mutantes da proteína DsrJ de *Allochromatium vinosum* com alterações nos potenciais ligandos axiais distais e analisámo-los através de várias técnicas: Ressonância paramagnética eletrônica (EPR), Ressonância de Raman (RR), Ressonância magnética nuclear (RMN), espectrometria de massa (MS) e UV-visível. Embora tenhamos gerado mais de dez variantes, não foi possível identificar os ligandos axiais distais dos hemos presentes na proteína DsrJ. Estes resultados sugerem que: i) poderá existir algo que

durante a purificação das proteínas se ligue aos hemos modificados na ausência do ligando axial distal original ou ii) que as proteínas recombinantes poderão não estar corretamente estruturadas devido à ausência das outras subunidades do complexo de membrana DsrMKJOP, embora pela técnica de MS a proteína recombinante e os mutantes testados tivessem a massa molecular correta incluindo três hemos.

O trabalho aqui apresentado demonstra o papel crucial da proteína DsrC na redução do sulfito pela DsrAB, ligando este mecanismo à conservação de energia através da interação com o complexo membranar DsrMKJOP. Por outro lado, o objetivo de encontrar o doador fisiológico de eletrões para os dois primeiros eletrões necessários pela DsrAB não foi conclusivo e deverá ser continuado, uma vez que é extremamente importante para compreender o mecanismo de redução dissimilativa do sulfito. O papel do complexo membranar DsrMKJOP- mais especificamente da DsrJ- permanece inconclusivo, sendo necessário ser resolvido tanto para SRP como para as bactérias oxidantes de sulfato, onde o papel desta proteína foi demonstrado ser essencial para a oxidação dos glóbulos de enxofre.

List of abbreviations

AOR	Aldehyde oxidoreductase
ATP	Adenosine triphosphate nucleotide
APS	Adenosine-5'-phosphosulfate
ApsBA	Adenosine-5'-phosphosulfate reductase
aSiR	Assimilatory sulfite reductase
CODH	Carbon monoxide dehydrogenase
D.	*Desulfovibrio*
D. vulgaris	Desulfovibrio vulgaris Hildenborough
Dsr	Dissimilatory sulfite reductase
DTT	Dithiothreitol
e^-	electron
EPR	Electron paramagnetic resonance
Fdx	ferredoxin
Fe-S	iron-sulfur cluster
g	EPR g-value
GSA	gel shift assay
Hdr	heterodisulfide reductases
HEPES	*N*-(2-hydroxyethyl)-*N'*-2-ethanesulfonic acid
Hmc	high molecular mass cytochrome complex
HPLC	high performance liquid chromatography
PPi	inorganic pyrophosphate
IPTG	isopropyl-β-D-thiogalactoside
LGT	lateral gene transfer
MALDI-TOF	matrix-assisted laser desorption ionization/time-of-flight
MalPEG	methoxy-polyethylene glycol maleimide
MIC	Microbially influenced corrosion
MS	Mass spectrometry
MQ	menaquinone
MQH_2	menaquinol

Nar	nitrate reductase
Nrf	nitrite reductase
Nhc	nine-heme cytochrome complex
NMR	Nuclear magnetic resonance
NoxA-3	NADH oxidase from *A. Fulgidus*
Ohc	octaheme cytochrome complex
PAGE	polyacrylamide gel electrophoresis
PAPS	phosphoadenosine phosphosulfate
Qmo	quinone-interacting membrane oxidoreductase complex
Rnf	*Rhodobacter* nitrogen fixation complex
RR	Resonance Raman
Sat	Sulfate adenylyl transferase
SDS	sodium dodecyl sulfate
Sox	sulfur oxidation enzymes
SiR	sulfite reductases
SiRHP	aSiR siroheme-containing subunit
SiRFP	aSiR flavin-containing protein
PFOR	Pyruvate ferredoxin oxidoreductase
SOB	sulfur oxidizing bacteria
SPR	Sulfate reducing prokaryotes
SRP	Surface plasmon resonance
Tricine	*N*-[2-hydroxy-1,1-bis(hydroxymethyl)-ethyl]glycine
Tris	tris(hydroxymethyl)-aminomethane
UV	ultra-violet
Wt	wild type

Chapter 1

Introduction

Introduction

Sulfur is one of the most versatile nonmetallic elements on Earth, due to its broad range of oxidation states that go from -2 (sulfide) to +6 (sulfate). Sulfur can be found in minerals such as pyrite (FeS_2) or gypsum ($CaSO_4$) or in biological compounds like amino acids, nucleosides, protein cofactors, co-enzymes, vitamins, metabolites, sulfolipids and hormones (Ehrlich & Newman, 2008). Sulfur compounds can also be oxidized or reduced microbiologically and the sulfur cycle is crucial for the maintenance of the life on Earth, being connected to other cycles such as that of carbon and nitrogen (Muyzer & Stams, 2008). As a major biogeochemical cycle in nature (Luptakova, 2007), it has been shown that 75% of the crustal sulfur has been cycled biologically and that per year $4\text{-}5\times10^{12}$ kg of sulfate is cycled by living cells (Skyring & Donnelly, 1982).

The microorganisms capable of reducing sulfate are known as sulfate reducing prokaryotes (SRP), which can be present in a wide variety of anaerobic environments (Peck *et al.*, 1982). SRP are more abundant in marine settings, the biggest reservoir of sulfate (Vairavamurthy *et al.*, 1995), where it is the second most abundant anion after chloride. An historical overview of research in SRP is available in Rabus *et al.*, 2006. Interest in sulfate reduction began after 1864 when Meyer realized that the remarkable concentrations of hydrogen sulfide in aquatic systems were produced biologically through the reduction of sulfate (Meyer, 1864). In 1895 the first sulfate-reducing bacterium was isolated and named *Spirillum desulfuricans* by Beijerinck's co-workers. The first real evidence for a sulfur reduction mechanism as the main energy source for microbial growth was found by Pelsh in 1936, with *Desulfuromonas acetoxidans* being the first organism grown by sulfur

reduction (Pelsh, 1936). The initial breakthrough studies into the biochemistry of the SRP occurred mainly during the 1950s and 1960s. *Desulfovibrio* was then identified as the first anaerobe with a cytochrome, which previously was only believed to be associated with aerobic respiration. In 1956 Postgate discovered a green protein that reduced sulfite to sulfide and named it desulfoviridin (Postgate, 1956). Later, in 1958, Lipmann reported on the main differences between the assimilatory and dissimilatory sulfate reduction pathways (Lipmann, 1958). The dissimilatory sulfate reduction was than showed by Jørgensen and coworkers to be responsible for the mineralization of about half of the organic carbon in marine sediments (Jørgensen & Fenchel, 1974). The 1980s were the decade for the revolution on understanding the enzymatic reactions and bioenergetics of sulfate reduction. ATP balances with hydrogen were accurately measured with chemostat studies (Badziong & Thauer, 1978, Nethejaenchen & Thauer, 1984) and three different types of hydrogenases ([Fe-Fe], [Ni-Fe] and [Ni-Fe-Se]) were detected (Huynh *et al.*, 1984, Rieder *et al.*, 1984, Fauque *et al.*, 1988). Another essential development was the beginning of molecular studies in *Desulfovibrio* species that made possible the analysis in more detail of several crucial metabolic enzymes. The first 16S rRNA comparative analysis of a sulfate reducing bacteria was performed by Oyaizu and Woese (Oyaizu *et al.*, 1985). They exposed the relationships of *Desulfovibrio desulfuricans* with *Myxococcus* and photosynthetic purple bacteria. This revolutionized the phylogenetic organization of sulfate reducing prokaryotes. In the 1990s, improvements in the study of single proteins, genes and environmental impact led to a better understanding of SRP at metabolic and physiologic levels. In 1997, the first completely sequenced genome of an SRP from the archaeon *Archaeoglobus fulgidus*, was achieved by Klenk and collaborators (Klenk *et al.*, 1997). The genome of *Desulfovibrio vulgaris*

Hildenborough, one of the most studied SRP, was fully sequenced in 2004 by Heidelberg and coworkers (Heidelberg *et al.*, 2004).

Sulfate can be anaerobically respired using gaseous hydrogen as the energy source or heterotrophically when using organic substrates like pyruvate, formate, lactate, malate, succinate or ethanol (Muyzer & Stams, 2008). SRP are divided into two major groups regarding the degradation of organic compounds: those that degrade organic compounds incompletely to acetate and those that degrade it completely to carbon dioxide (Muyzer & Stams, 2008). They are also known for their ability to grow on diverse substrates besides the simple ones mentioned above. These substrates include: sugars, amino acids, one-carbon compounds (such as methanol, carbon monoxide and methanethiol), benzoate and phenol, aromatic hydrocarbons, short and long-chain alkanes (Muyzer & Stams, 2008). Moreover, many SRP are able to grow by disproportionating thiosulfate, sulfite and sulfur, resulting in the formation of sulfate and sulfide (Bak & Pfennig, 1987, Bottcher *et al.*, 2005). Being anaerobes, SRP were considered to be unable to use oxygen as energy source, but many can tolerate oxygen for periods of time, and include terminal oxidase genes in their genomes (Dolla *et al.*, 2007). Lobo *et* al demonstrated that, from a variety of SRP that can tolerate oxygen, *D. desulfuricans* ATCC 27774 has the ability to grow in a lactate/nitrate medium (absence of sulfur compounds) under nearly atmospheric oxygen levels (Lobo *et al.*, 2007). SRP are distributed in a variety of environments ranging from marine to freshwaters, hot environments (such as hydrothermal vents and mud volcanoes), extreme pH habitats (acid-mine drainage sites with pH as low as 2-3) and soda lakes (pH high as 10) (Rabus *et al.*, 2015). They can also be part of microbial consortia with microorganisms such as methanotrophic archaea or with sulfur oxidizing bacteria (Muyzer & Stams, 2008).

SRP can be found in four bacteria phyla (Proteobacteria - class *Deltaproteobacteria*, *Nitrospirae*, *Firmicutes* and *Thermodesulfobacteria*) and two archaeal phyla (*Euryarchaeota* and *Crenarchaeota*) (Müller *et al.*, 2015). These groups of organisms have been taxonomically characterized by several techniques such as cultivation (which can detect less than 1% of the total microorganisms), analysis of the phospholipid fatty acids and 16S ribosomal RNA (rRNA) (Muyzer & Stams, 2008). Comparative analysis of the *dsrAB* genes is a commonly used technique to identify novel lineages of SRP (Wagner *et al.*, 2005, Hansel *et al.*, 2008, Loy *et al.*, 2008, Müller *et al.*, 2015). The DsrAB enzymes are assumed to be ancient, with an ancestor present before the division of the domains *Bacteria* and *Archaea* (Wagner *et al.*, 1998, Dhillon *et al.*, 2005, Loy *et al.*, 2009). The distribution of the *dsrAB* genes among prokaryotes is now known to have involved divergent speciation, functional diversification and lateral gene transfer (LGT) (Loy *et al.*, 2008). The *dsrAB* genes present in the genus *Archaeoglobus, Thermodesulfobacterium* and in few low-GC content Gram-positive bacteria of the phylum *Firmicutes* have been shown to derive from *Deltaproteobacteria* donor, proving the existence of LGT even across domains (Larsen *et al.*, 1999, Klein *et al.*, 2001, Stahl *et al.*, 2002, Zverlov *et al.*, 2005). This makes the comparative *dsrAB* gene analysis an important technique for the detection of new SRP and sulfur oxidizing microorganisms even in environmental samples. However, it must be noted that other organisms besides SRP and sulfur oxidizing bacteria may also contain *dsrAB* genes. This includes sulfur disproportionators and organisms that reduce sulfite, thiosulfate or organosulfonates.

Sulfur species can be easily oxidized to sulfate in the presence of oxygen, with the levels of atmospheric oxygen being crucial for this process. It is known that the atmospheric oxygen levels only arose

around 2.45 billion years ago, after the Great oxygenation event (Holland, 2006). This event increased marine sulfate to the levels present of today (~28mM) (Canfield *et al.*, 2000). The understanding of the evolution of the sulfate reservoir, as a proxy for atmospheric oxygen levels, can be achieved by measuring the ratio of stable sulfur isotopes present in sulfur-bearing minerals. Sulfur has the ability to exist in 4 stable isotopes: ^{32}S and ^{34}S (the two most abundant), and ^{33}S and ^{36}S (minor isotopes) (Johnston, 2011). Sulfur isotope discrimination has been used to study dissimilatory sulfate reduction performed by SRP, as this metabolic process induces a large mass-dependent fractionation between sulfate and sulfide that is preserved in geological records (Johnston, 2011). This occurs because SRP favors light sulfur isotopes (^{32}S) instead of heavier ones (^{34}S) (Wing & Halevy, 2014). This can be explained by the fact that S-O bonds of lighter isotopes are easier to brake during sulfate reduction (Lyons & Gill, 2010). Through isotope analysis Shen and coworkers found evidence that microbial sulfate respiration had evolved 3.47 Gyr ago (Shen *et al.*, 2001). Culture experiments with SRP were one of the first metabolisms to be isotopically characterized (Thode H. *et al.*, 1951). Through these experiments, isotope fractionation has been inversely correlated with cell sulfate reduction rates, and directly with extracellular concentrations of sulfate (Harrison & Thode, 1958, Kaplan & Rittenberg, 1964, Chambers *et al.*, 1975, Leavitt *et al.*, 2013).

Sulfate respiration is of great importance for the biogeochemical sulfur cycle, and sulfur isotope fractionation has been used for decades as a proxy for atmospheric oxygenation leading to a better understanding of Earth history (Rabus *et al.*, 2015).

1.1 Biological and economic impact of SRP

SRP can have very important biotechnological applications. Recently, Rabus and coworkers reviewed on the major biotechnological/environmental impact of SRP in the last 20 years (Rabus *et al.*, 2015). SRP are known to be extremely important for bioremediation of heavy and radioactive metals and organic compounds (oxidation of monoaromatic hydrocarbons, dehalorespiration and nitroaromatic respiration) and for the reduction of azo dyes (Barton & Fauque, 2009, Rabus *et al.*, 2015). Due to their high tolerance to metal contamination, they are used for the removal of heavy metals from acidic mine drainage waters (Martins *et al.*, 2009, Martins *et al.*, 2011, Sánchez-Andrea *et al.*, 2011, Sánchez-Andrea *et al.*, 2014). Moreover, SRP are used in waste water and off gas treatments to remove metals, sulfate and CO (in off gas) (Rabus *et al.*, 2015). There are three processes accomplished by SRP that allows them to be used for bioremediation: growth by sulfate reduction (precipitation of metals that react with sulfide), uranium reduction and mercury methylation (Rabus *et al.*, 2015). On the other hand, SRP are associated in major economic and health issues. SRP are implicated in the biocorrosion of ferrous metals, corrosion of concrete and stonework and also have a major impact on the petroleum industry (Barton & Fauque, 2009, Rabus *et al.*, 2015). Microbially influenced corrosion (MIC) by SRP can be accomplished through three mechanisms: the chemical attack of iron by hydrogen sulfide, the use of the cathodic hydrogen (generated through slowly chemical oxidation of Fe^0) or by directly taking up of the electrons from the metallic iron (Beech & Sunner, 2007, Rabus *et al.*, 2015). In the oil industry SRP cause problems not only in pipeline corrosion but also because of their growth in crude oil and the production of hydrogen sulfide in crude oil (a process called souring of oil fields) that

contaminates this expensive and extremely important raw material for our society (Voordouw, 2011). Concerning human health, it was long demonstrated that SRP are present in the human gut (Gibson *et al.*, 1988). SRP are present in all humans and, although not being part of the dominant intestinal flora, are now known as belonging to the human microbiome (Carbonero *et al.*, 2012). These SRP have been implicated with the onset or perpetuation of chronic inflammatory bowel diseases such as Crohn's disease and ulcerative colitis (Loubinoux *et al.*, 2002). However, it remains to be revealed if SRP are the cause of the inflammatory process or if they are opportunistic colonizers of the inflamed area (Verstreken *et al.*, 2012). SRP have been also implicated with clinical severity of human periodontitis (Langendijk *et al.*, 2000). Furthermore, SRP have been isolated from profound abscesses (abdominal and brain), urine and blood (Tee *et al.*, 1996, McDougall *et al.*, 1997, La Scola & Raoult, 1999, Loubinoux *et al.*, 2000). Recently it was hypothesized that these SRP can also be involved in the development of autism spectrum disorders (Weston *et al.*, 2015). It is difficult to grow and isolate SRP specimens from clinical samples, but this can be overcome with molecular techniques for SRP identification such as 16S rRNA gene sequencing or the identification of specific genes like *apsBA* or *dsrAB* (Nakao *et al.*, 2009, Müller *et al.*, 2015).

1.2 Sulfate reduction mechanism: Assimilatory vs Dissimilatory pathways

There are two biological pathways for sulfate reduction: it can be assimilated and transformed into several biological molecules, a capacity found in prokaryotes, fungi and plants or it can be dissimilated (a respiratory process) where it acts as electron acceptor. Sulfur compounds of intermediate oxidation state can also be disporportionated by some SRP and other highly specialized-bacteria. In this case, elemental sulfur, sulfite or thiosulfate function simultaneously as electron donor and acceptor, for the generation of energy (Tang *et al.*, 2009). The dissimilatory mechanism is considered a true respiratory process accomplished by several prokaryotes (*Bacteria* and *Archaea*). In both assimilatory and dissimilatory mechanisms sulfate is reduced in the cytoplasm. In the assimilatory pathway sulfate is imported by a sulfate permease (SulT family in prokaryotes and SulP/SLC26 family in eukaryotes) (Pilsyk & Paszewski, 2009), and in the dissimilatory pathway by electroneutral proton-anion symport in freshwater microorganisms (Cypionka, 1987) or sodium ion gradient produced by Na^- antiport in marine strains (Kreke & Cypionka, 1994). Thermodynamically, the redox potential for the sulfate/bisulfite couple is -516 mV, too low to allow reduction by a physiological electron donor such as ferredoxin (~- 400 mV) or NADH (~-320 mV). Therefore sulfate needs to be activated before it can be reduced (Thauer *et al.*, 2007). Once inside the cytoplasm sulfate is activated by Sulfate adenylyl transferase (Sat) with the consumption of ATP molecules to adenosine 5′-phosphosulfate (APS) and inorganic pyrophosphate (PPi) (Ullrich *et al.*, 2001). This results in an increase of the redox potential from -516 mV for the sulfate/sulfite couple to - 60 mV for the APS/sulfite couple (Thauer *et al.*, 2007). PPi must be further hydrolyzed to 2 Pi to pull the reaction to the

direction of APS (Ehrlich & Newman, 2008). This hydrolysis can be accomplish by soluble inorganic pyrophosphatases (most cases) or, in some SRP, it can be performed by membrane-associated proton translocating pyrophosphatases, coupling this reaction to energy conservation (Pereira *et al.*, 2011). The differences between assimilatory and dissimilatory pathways start here (Figure 1.1). In the dissimilatory pathway APS is then reduced by adenylyl-sulfate reductase (ApsBA) to sulfite and adenosine monophosphate (AMP). In contrast, in most assimilatory pathways, APS is further phosphorylated to 3′-phosphoadenosine 5′-phosphosulfate (PAPS) by APS-kinase activity, which is only then reduced by PAPS reductase to sulfite. The final step is the reduction of sulfite to sulfide, which has a redox potential of

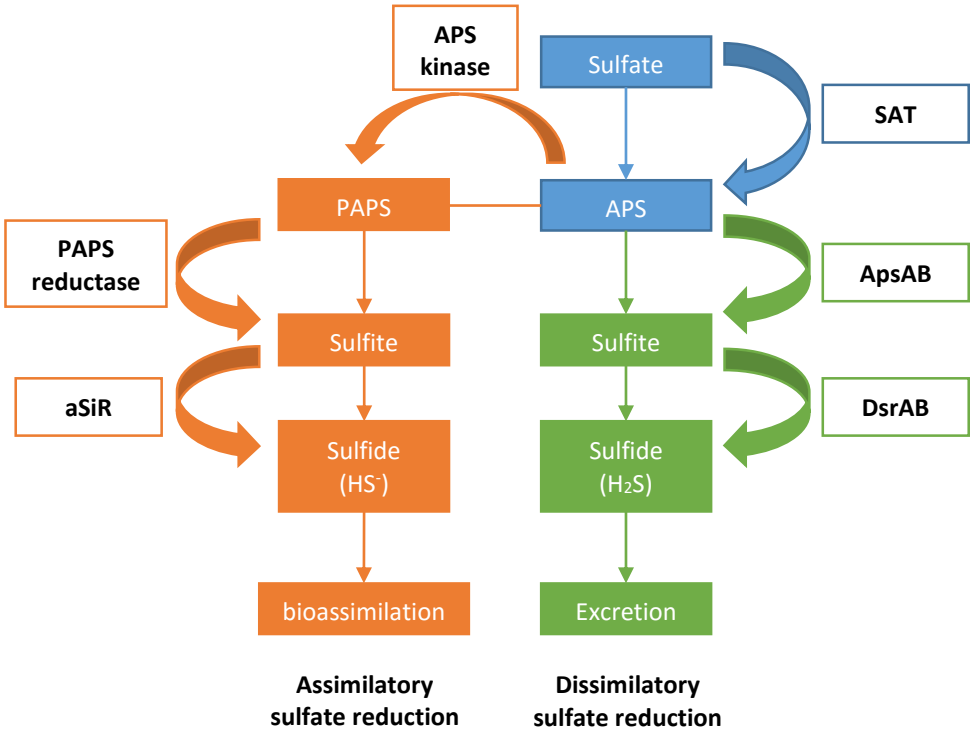

Figure. 1.1. Schematic representation of the difference between the assimilatory and dissimilatory pathways for sulfate reduction. Blue – common pathway; Green – Dissimilatory pathway; Orange – Assimilatory pathway.

- 116 mV (Muyzer & Stams, 2008). In the assimilatory reduction, the aSiR is capable of reducing sulfite in one single step to sulfide, without the formation of other products (Crane & Getzoff, 1996). On the other hand, it was shown that in *in vitro* assays with DsrAB and sulfite, DsrAB produces a mixture of compounds with thiosulfate, trithionate and sulfide being formed (Lee & Peck, 1971, Akagi, 1983).

1.3 Sulfite reductases

The assimilatory and dissimilatory pathways involve two forms of sulfite reductases (SiR): the assimilatory sulfite reductase (aSiR) and the dissimilatory sulfite reductase (DsrAB). The SiR are proteins thought to be present in LUCA (Last Universal Common Ancestor) which plays a crucial role in the reduction of sulfite to sulfide (Wagner *et al.*, 1998, Castresana & Moreira, 1999, Larsen *et al.*, 1999). These enzymes are not only considered ancient but crucial for the biologic conversions of sulfur compounds in the anoxic and extremely reduced primordial Earth (Wagner *et al.*, 1998). The reduction of sulfite to sulfide and nitrite to ammonia are the only examples of single-step six-electron reductions found in nature (Stroupe & Getzoff, 2009). Through comparative studies it is known that among the SiR, the basic framework has been conserved. The motif Cys-X_5-Cys-X_n-Cys-X_3-Cys is found to be highly conserved in all SiRs (Karkhoff-schweizer *et al.*, 1995). This motif harbors the catalytic center, a unique cofactor that includes a siroheme (iron-sirohydrochlorin) bound to an iron-sulfur [4Fe-4S] cluster (Figure 1.2) (Crane *et al.*, 1997). It has been found that the biosynthetic pathway for siroheme is more ancient than that of cytochromes and are closely related to cobalamin (vitamin B12) (Stroupe & Getzoff, 2009, Lobo *et al.*,

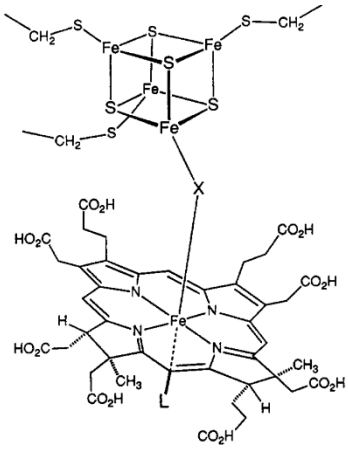

Figure. 1.2. scheme of the siroheme bound to the [4Fe-4S] cluster (Tan & Cowan, 1991)

2012). This supports the hypothesis of an ancestral origin for sulfite reduction, in early prokaryotes period, long before aerobic respiration. Moreover, the analysis of the structure and sequence identity between the aSiR siroheme-containing subunit (SiRHP) with the α and β subunits of DsrAB indicates that they are phylogenetically related and the aSiR diverged from a gene-duplication event followed by gene fusion of an ancestral sulfite reductase gene present in a very early life form (Crane *et al.*, 1995, Oliveira *et al.*, 2008, Rabus *et al.*, 2015). The siroheme has a structural organization that allows it to *push* electrons into the substrate. On the other hand, the distorted geometry and carboxylate side chains of the siroheme promotes the stabilization of an high effective proton concentration overhead the substrate which indirectly *pulls* electrons from the substrate facilitating its reduction (Crane & Getzoff, 1996). Among SiR there are several variances in the oligomeric state, the number of prosthetic groups and the electron delivery system (Schiffer *et al.*, 2008).

Assimilatory sulfite reductase. The aSiRs are widespread among prokaryotes, fungi and plants. The aSiR from *E. coli* is a heavy oligomer (> 700 kDa) containing eight copies of a flavin-containing protein (SiRFP; 66 kDa) and four copies of the siroheme-containing hemoprotein (SiRHP; 64 kDa) (Siegel *et al.*, 1974, Crane & Getzoff, 1996). In this holoenzyme the SiRFPs are responsible for accepting electrons from NADPH and the SiRHPs (Figure 1.3) contain the catalytic

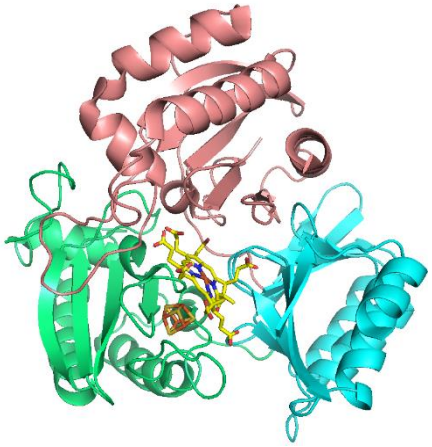

Figure. 1.3. E. coli SiRHP (pdb 1AOP) cartoon with the 3 domains represented by the cyan, salmon and green color and the siroheme (yellow) with the iron-sulfur cluster (orange) (Crane et al., 1995). Cartoon generated by Pymol program.

centers that accept the electrons from the flavoprotein subunits and reduce the substrate (Figure 1.4 (B)) (Crane & Getzoff, 1996). The first crystallographic structure of an aSiR from *Escherichia coli* (PDB code 1AOP) was solved in 1995 by Crane and coworkers (Crane *et al.*, 1995). This structure showed that SiRHP is formed by a tri-lobed protein with a pseudo two-fold symmetry. A siroheme-[4Fe-4S] cofactor is present in the junction of the three domains (Crane *et al.*, 1995). On the other hand, the aSiR from *Arabidopsis thaliana* is a monomeric protein containing only the SiRHP unit which can accept electrons from an NADPH:ferredoxin reductase or photosystem I through a ferredoxin (Figure 1.4 (A)) (Nakayama *et al.*, 2000). It is well documented that aSiR

can catalyze the six-electron reduction of sulfite to sulfide in one single-step (Crane & Getzoff, 1996, Smith & Stroupe, 2012)

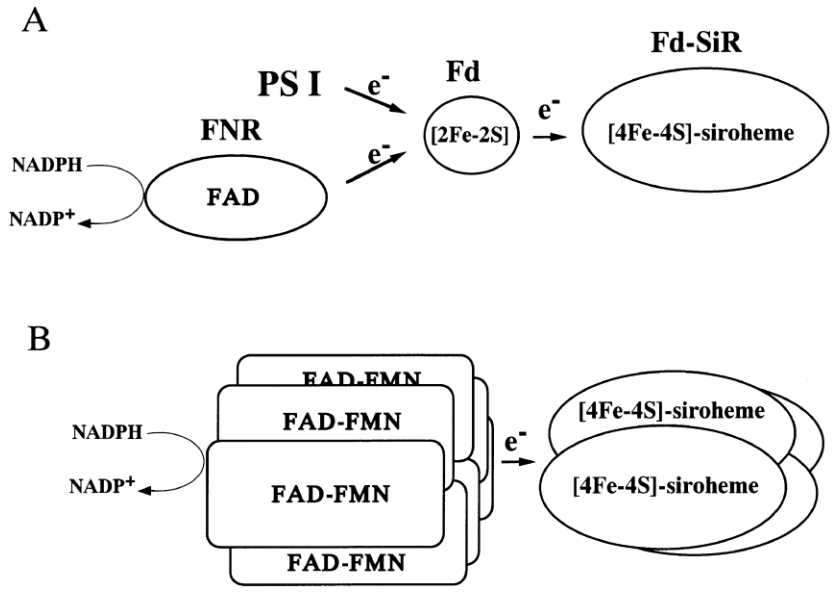

Figure. 1.4. Schematic representation of the electron donors of the sulfite reduction system in plants (A) and E. coli (B). Electrons are donated to plant SiR from Fd reduced by photosystem I (PS I) or the NADPH/FNR/Fd cascade. E. coli NADPH-SiR is a complex hemoflavoprotein with a subunit structure of $\alpha_8\beta_4$: the α subunit is a flavoprotein containing FAD and FMN and the β subunit is a hemoprotein containing siroheme and a [4Fe–4S] cluster (Nakayama et al., 2000)

Dissimilatory sulfite reductase. The *dsrAB* genes are widespread among SRP and encode the proteins responsible for the reduction of sulfite in anaerobic respiration. It can also be present in several organisms that reduce thiosulfate, sulfite or organosulfonates, in syntrophic bacteria and organisms that disproportionate sulfur compounds (Simon & Kroneck, 2013). All dissimilatory sulfate organisms known to data have the *dsrAB* genes (Zverlov *et al.*, 2005). The *dsrAB* genes can also be present in sulfite-reducing organisms such as *Desulfitobacterium*, *Desulfitibacter* and *Pyrobaculum* (Simon & Kroneck, 2013), sulfur-disproportionating bacteria, organosulfonate metabolizing organisms, and some sulfur-oxidizing bacteria (SOB), where the *reversible* DsrAB is essential for the oxidation of sulfur globules (Pott & Dahl, 1998, Loy *et al.*, 2009). The DsrAB proteins are $\alpha_2\beta_2$ heterotetramers with molecular masses between 145 and 225 kDa (Rabus *et al.*, 2006) and with the α subunit larger (about 50 kDa) than the β subunit (typically 40 kDa). According to their characteristic UV-visible spectrum, DsrAB proteins were classically divided in four classes: desulforubidin (Lee *et al.*, 1973), desulfofuscidin (Moura *et al.*, 1988), *P*-582 (Trudinge.Pa, 1970) and desulfoviridin (Lee *et al.*, 1973). Nowadays, it is known that these small changes in the UV-visible spectrum are not correlated with the significant structural differences to justify a division of the DsrAB proteins in classes, being referred only as DsrAB (Rabus *et al.*, 2015). Although, in the case of desulfoviridin there is an extra peak in the UV-visible spectrum at the 630 nm area that reveals a different feature. This characteristic peak is due to the presence of a sirohydrochlorin, which is a siroheme without Fe (Figure 1.5). Another difference between Dsr proteins is that, in some cases (ex.: *D. vulgaris* and *D. desulfuricans*), the oligomeric state of the purified proteins is $\alpha_2\beta_2\gamma_2$. This third γ protein was suggested to be a subunit of the desulfoviridin proteins. However, this protein corresponds to DsrC,

whose gene is not in the same transcriptional unit as the *dsrAB* genes, and their expression is not coordinated (Karkhoff-Schweizer *et al.*, 1993). This indicates that DsrAB and DsrC are two different proteins that, in the case of *D. vulgaris* and *D desulfuricans*, can form a tight complex. The DsrC protein was proposed to be involved in the mechanism of sulfite reduction (Oliveira *et al.*, 2008) (see further discussion in chapter 1.4).

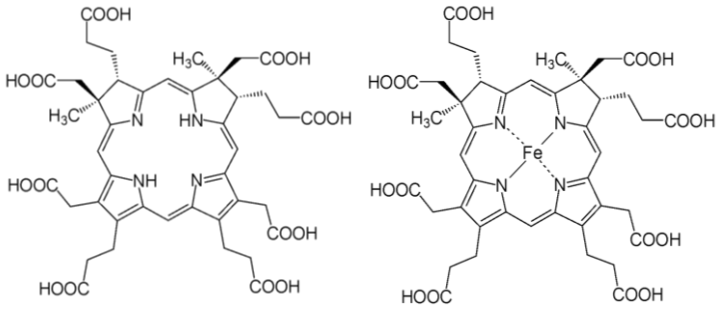

Figure. 1.5. Scheme of sirohydrochlorin and siroheme

Only with the determination of the crystal structure of DsrAB in 2008, from *D. vulgaris* (Oliveira *et al.*, 2008) and *A. fulgidus* (Schiffer *et al.*, 2008), was the cofactor composition of this enzyme truly elucidated (Figure 1.6). The structures showed that the DsrAB proteins only have two catalytic siroheme-[4Fe-4S] cofactors, one per each αβ unit, present

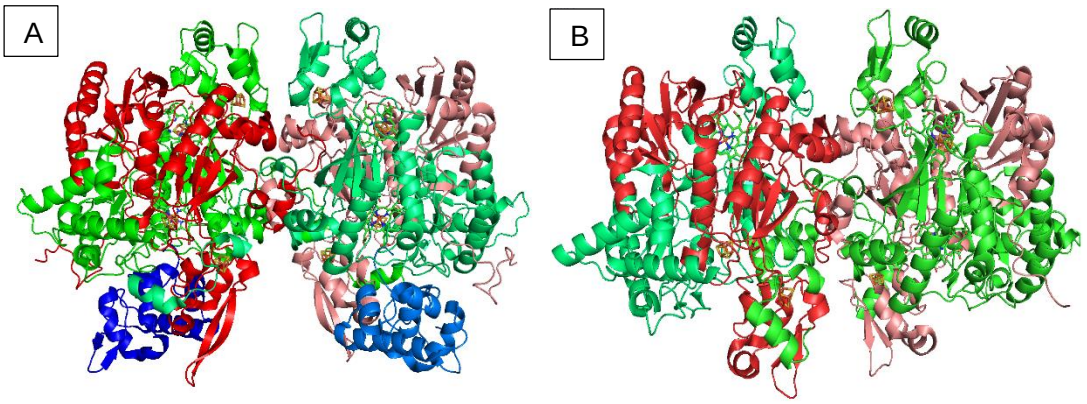

Figure. 1.6. (A) D. vulgaris DsrAB (pdb 2V4J) and (B) A. fulgidus (pdb 3MM5) cartoon with the subunit α (red and salmon), subunit β (green and light green), subunit γ (blue and light blue). Cartoons generated by Pymol program.

in DsrB. There is also one siroheme (in the case of *A. fulgidus*) or sirohydrochlorin (in the case of *D. vulgaris*) per each DsrA subunit, but these are non-catalytic. In the case of the siroheme in *A. fulgidus*, there is a tryptophan residue blocking the possible sulfite binding site. This tryptophan is not conserved among all DsrAB proteins but it is conservatively exchange by a phenylalanine in the DsrA subunit. Moreover, in the DsrA subunit the amino acids surrounding the siroheme are different from those present in the catalytic cavity of DsrB subunit, forcing the negatively charged acetate and propionate groups to repel incoming anions (Schiffer *et al.*, 2008). Concerning the sirohydrochlorin in *D. vulgaris*, the absence of the Fe obviously precludes any catalytic activity and the positive electrostatic potential at the possible substrate channel that facilitates the entrance of the negatively charged sulfite

(present in the catalytic center in DsrB) is absent in the DsrA subunits. Also, the existence of an arginine and a tryptophan near the sirohydrochlorin cavity in DsrA blocks its access by sulfite (Oliveira *et al.*, 2008). Overall, this shows that the DsrAB proteins have evolved to lose the catalytic site in DsrA. A similar situation is observed for the assimilatory proteins where the second cofactor is no longer even present.

It was already referred that the DsrAB proteins do not reduced sulfite exclusively to sulfide. Several authors verified that the *in vitro* formation and relative proportion of the several sulfur products was connected with the concentration of electron donor (methyl viologen or hydrogenase) and the concentration of substrate (sulfite) (Akagi, 1995). They verified that higher concentrations of electron donor and low concentration of substrate led to production of more sulfide and less trithionate/thiosulfate, and that the opposite (less electron donor and high substrate concentrations) produced more trithionate than sulfide (Kobayash.K *et al.*, 1972, Kobayash.K *et al.*, 1974, Jones & Skyring, 1975, Drake & Akagi, 1977, Akagi, 1983, Akagi, 1995). These results led to the proposal of an alternative pathway for the dissimilatory reduction of sulfite. This pathway was named the trithionate pathway, where it was proposed that the DsrAB reduces sulfite to a mixture of thiosulfate, trithionate and sulfide. Further details of this mechanism were proposed by Parey and coworkers through the analysis of the *A. fulgidus* DsrAB crystal structure complexed with SO_3^{2-}, S^{2-}, NO^{2-}, CO and CN^- (Parey *et al.*, 2010) (Figure 1.7). In this proposal, they divided the process into three two-electron transfer steps, each one involving the acceptance of two protons and release of one H_2O molecule. The proposed mechanism starts with the bisulfite (the form of sulfite at pH 6) being reduced at the catalytic siroheme-[4Fe-4S] cofactor to form an S(II) intermediate. From

here, two things can happen: this intermediate can react with more bisulfite forming thiosulfate that can further react with another bisulfite releasing trithionate, or it can be further reduced to an S(0) intermediate. Again, this S(0) intermediate can react with free bisulfide releasing thiosulfate, or it can be further reduced to sulfide as the end product (Parey *et al.*, 2010).

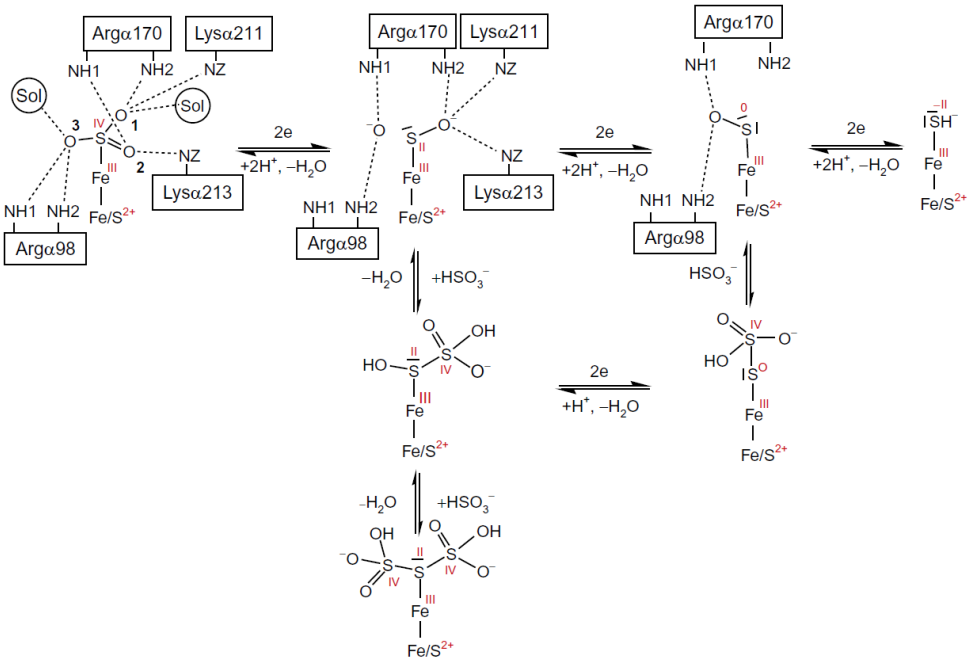

Figure. 1.7. Scheme of the six-electron reduction of sulfite to trithionate, thiosulfate and sulfide. Only residues that directly interact with the siroheme iron-bound sulfur-oxygen adduct are noted. The process is subdivided into three two-electron transfer steps each accompanied by acceptance of two protons and release of one H_2O molecule. Trithionate and thiosulfate might be produced if the S(II) and S(0) intermediates are sufficiently long-living to be attacked by sulfite; these side reactions are supported by high sulfite concentrations that are unlikely to exist within the cell.(Parey et al., 2010)

Nevertheless it has been questioned whether this trithionate pathway is truly physiologically relevant. This pathway would require the

existence of trithionate and thiosulfate reductases in all SRP, which have not been shown to be present in all SRP (Pereira *et al.*, 2011). There is another proposed mechanism by Oliveira and coworkers for dissimilatory sulfite reduction in which the DsrC protein is considered fundamental for the reduction of sulfite into the single product sulfide (Oliveira *et al.*, 2008) (see chapter 1.4).

1.4 DsrC, the missing link in dissimilatory sulfite reduction

In 2008, Oliveira and coworkers revealed new insights into the pathway of sulfite reduction through the analysis of the structure of the *D. vulgaris* Hildenborough DsrAB in complex with DsrC. Here, they pointed out the crucial role of DsrC. DsrC was first described by Pierik in 1992 (Pierik *et al.*, 1992) as a third subunit of the DsrAB enzyme from *Desulfovibrio vulgaris* Hildenborough which have a $\alpha_2\beta_2\gamma_2$ structure. In 1993, it was shown that these three genes were not co-regulated and additionally the *dsrC* gene was not present in the same operon as *dsrAB* genes (Karkhoff-schweizer *et al.*, 1993). Other purified DsrAB proteins from SRP (ex.: *Pyrobaculum aerophilum* and *A. fulgidus*) do not contain DsrC, having a $\alpha_2\beta_2$ rearrangement, suggesting that DsrC protein is an independent protein rather than a third subunit of DsrAB (Dahl *et al.*, 1993, Cort *et al.*, 2001, Mander *et al.*, 2005, Cort *et al.*, 2008). It is established that DsrC belongs to TusE/DsrC/DsvC family (Venceslau *et al.*, 2014). This family contains proteins with 12-14 kDa, with a helix-turn-helix (HTH) motif, and a highly conserved C-terminal arm. The HTH motif is associated with protein or DNA binding but can also be observed in protein-protein interactions (Aravind *et al.*, 2005, Venceslau *et al.*, 2014).The family can be divided in three major protein groups: DsrC, TusE and RspA (Venceslau *et al.*, 2014). DsrC proteins have two

conserved cysteines in their C-terminal arm corresponding to the Cys_B-X_{10}-Cys_A motif, in which the Cys_A is the penultimate amino acid in the C-terminal sequence and Cys_B is eleven residues before (Figure 1.8). Accordingly to the NMR structure of *P. aerophilum* DsrC, the C-terminal is flexible, switching between the retrated and estended form (Cort *et al.*, 2001). A crystal structure of DsrC from *A. fulgidus* in the retracted form showed that the two conserved cysteins are not in close enough proximity to form a disulfide bond (Mander *et al.*, 2005). However, it is

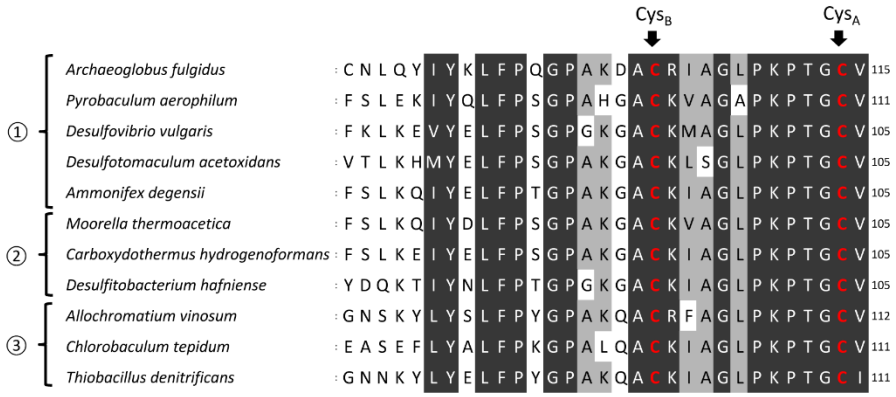

Figure. 1.8. Alignment of the DsrC C-terminal arm. DsrC from sulfate reducing organisms (1), organisms that reduce sulfite or thiosulfate (2) and sulfur oxidizing bacteria (3) are included. Strictly conserved residues are in black. The key DsrC CysA and CysB residues are highlighted in red.

possible, in the presence of oxidizing agents, to produce a disulfite bond between Cys_B and Cys_A (Venceslau *et al.*, 2013).

The TusE proteins have only the conserved Cys_A and the RspA (stands for regulatory sulfur-related proteins) have no conserved cysteines in the C-terminal arm, but have the HTH motif (Venceslau *et al.*, 2014). According to Venceslau *et* al. the *dsrC* gene is present in all organisms that have the *dsrAB* genes, but the reverse is not verified, which reinforces the hypothesis that DsrC is essential for the function of DsrAB (Venceslau *et al.*, 2014). In fact, the expression of DsrC is equal

or higher than that of other dissimilatory sulfate reduction proteins, suggesting an important role in cell metabolism (Wall *et al.*, 2008). The structural homology of DsrC to the Tet repressor TetR (a DNA binding protein that regulates the expression of the TetA, enzyme responsible for tetracycline antibiotic resistance (Kisker *et al.*, 1995)) suggests that DsrC could be involved in transcriptional regulation (Cort *et al.*, 2001, Venceslau *et al.*, 2014). This was supported by Grimm and coworkers which demonstrated that DsrC from *A. vinosum* is able to bind to a promoter region upstream of the *dsrA* gene (Grimm *et al.*, 2010). On the other hand, the homology of DsrC with TusE supports the idea that DsrC could be implicated in sulfur related reactions (Ikeuchi *et al.*, 2006, Oliveira *et al.*, 2011, Venceslau *et al.*, 2014). The TusE protein is involved in a sulfur-relay mechanism in which its terminal cysteine is decisive for the biosynthesis of thiouridine (Ikeuchi *et al.*, 2006). This mechanism starts with the activation of the S-atom of cysteine by the cysteine desulfurase IscS which forms an enzyme-bound persulfide. After that, the sulfur is carried by three small proteins: TusA, TusBCD

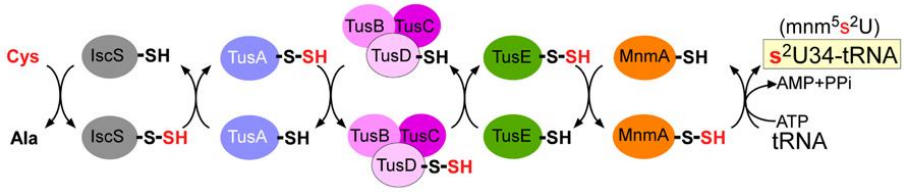

Figure. 1.9. Biosynthesis pathway of 2-thiouridine In E. coli, Tus proteins relay the persulfide sulfur of IscS to a modification enzyme, MnmA. In the green circle is represented the TusE protein receiving the sulfur from the TusD and transferring it to the MnmA (Shigi, 2014).

and TusE. In TusE, the last cysteine of the C-terminal arm forms a persulfide and transfers the sulfur to MnmA, which finaly incorporates it into tRNA (Figure 1.9) (Ikeuchi *et al.*, 2006, Shigi, 2014).

DsrC proteins have already been implicated in two crucial pathways in SRP and SRO (Oliveira *et al.*, 2008, Stockdreher *et al.*, 2012). In the sulfate reduction pathway, DsrC is proposed to be decisive for the reduction of sulfite. It was shown by Oliveira et al (2008) (Figure 1.10) that the C-terminal arm of DsrC binds inside a pocket between the DsrA and DsrB subunits (Oliveira *et al.*, 2008). This brings the Cys_A residue right next to catalytic active site allowing the involvement of Cys_A in catalysis. In the *D. vulgaris* structure, DsrC is covalently linked to the siroheme-[4Fe-4S], which is also observed in the structures of

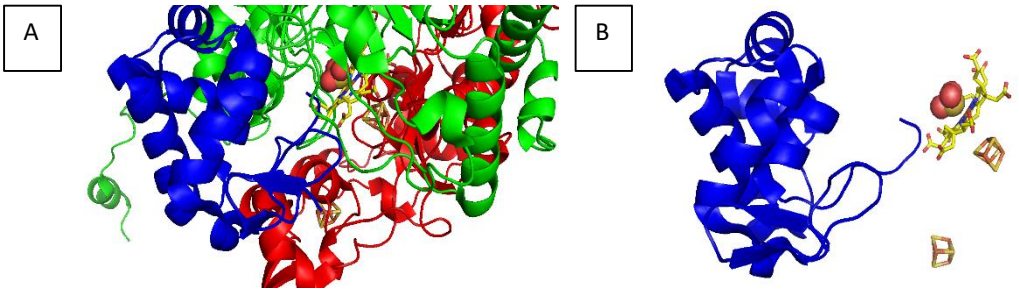

Figure. 1.10. Cartoons representing the interactions of DsrC with the sulfite present at the catalytic siroheme-[4Fe-4S] in DsrAB from D. vulgaris (Oliveira et al., 2008). (A) αβγ subunits (pdb 2V4J) showing the pocket for γ (DsrC) interaction with siroheme-[4Fe-4S] (B) only γ subunit (DsrC- blue) interacting with sulfite in the siroheme-[4Fe-4S] (yellow). All cartoons were performed with Pymol program.

D. norvegicum and *D. gigas* DsrAB (Oliveira *et al.*, 2008, Oliveira *et al.*, 2008, Hsieh *et al.*, 2010, Oliveira *et al.*, 2011). This covalent bond is most likely formed after aerobic purification due to the oxidation of a π-cation radical species at the siroheme. This ability to produce π-cation radical species permits the generation of an extra electron at the active site, which may be one of the reasons for which sirohemes have been selected for the reduction of sulfite (Crane & Getzoff, 1996, Oliveira *et al.*, 2008). Moreover, it was also shown by mass spectrometry that in solution the DsrAB from *D. norvegicum*, is present in several forms, having no ($\alpha_2\beta_2$), one ($\alpha_2\beta_2\gamma$) or two ($\alpha_2\beta_2\gamma_2$) DsrC proteins coupled to

DsrAB (Oliveira *et al.*, 2011). Oliveira et al proposed a mechanism for sulfite reduction in which they suggest that DsrAB would reduce sulfite to an S^0 valence state that would bind to the Cys_A of the C-terminal arm of DsrC resulting in a persulfide (Oliveira *et al.*, 2008). This DsrC persulfide would then suffer an internal reaction with Cys_B with the release of hydrogen sulfide (H_2S) and with the formation of a disulfide bond between Cys_A and Cys_B. This disulfide would then react with DsrK (from the DsrMKJOP membrane complex), becoming reduced to enter in another cycle of sulfite reduction (Figure 1.11) (Oliveira *et al.*, 2008).

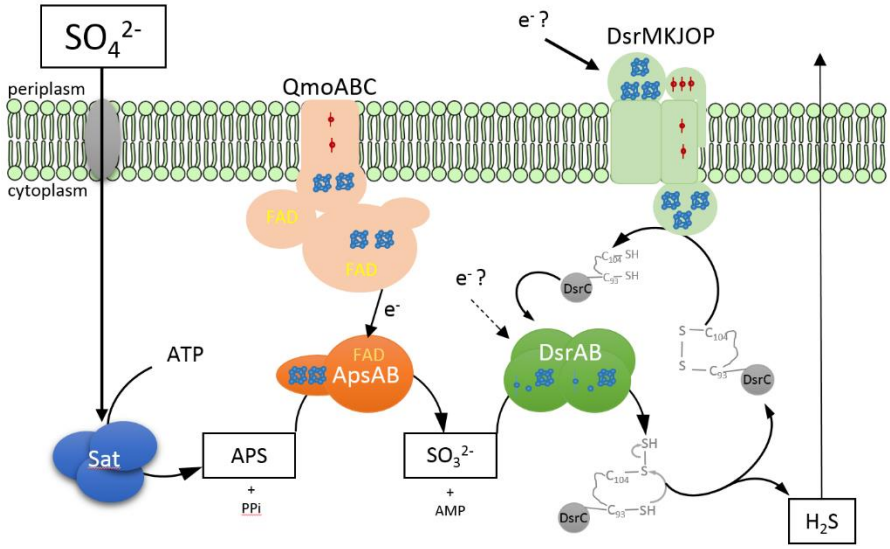

Figure. 1.11. Schematic representation of the proposed sulfate reduction mechanism. Sat, sulfate adenylyltransferase; ApsAB, adenosine phosphosulfate reductase; QmoABC, membrane complex that is the probable electron donor to ApsAB. C-SH represents the thiol group of Cys 93, C-S-SH a persulfide group of Cys 104, and C- S- S-C the disulfide bond between the two Cys. (From Oliveira et al. 2008)

This proposal brought a new perspective to sulfite reduction since it linked this reaction to energy conservation through the DsrMKJOP complex. According to Oliveira *et* al. (2008) two electrons, from the total

of six electrons needed for the reduction of sulfite to sulfide, would come from the DsrC reduced terminal cysteines. These cysteines are converted to a disulfide bond state after reacting with the S^0 valence state and releasing H_2S. This DsrC disulfide form would then be reduced by DsrMKJOP membrane complex from which two electrons from the menaquinone pool would be needed. This proposal rejects the trithionate pathway and suggests that the subproduct formation of trithionate and thiosulfate were only *in vitro* products caused by the absence of DsrC in the cavity of DsrAB and the excess of sulfite (Oliveira *et al.*, 2008, Parey *et al.*, 2010).

In the sulfur oxidation pathway it was shown that a mutant with a deletion in the *dsrC* gene was genetically unstable and unable to grow even in the absence of sulfur compounds (Cort *et al.*, 2008). Moreover, is was shown by Stockdreher and coworkers that, in *in vitro* assays, DsrC is extremely important for sulfur oxidation as it receives sulfur from the DsrE protein (Stockdreher *et al.*, 2012). In more detail, during

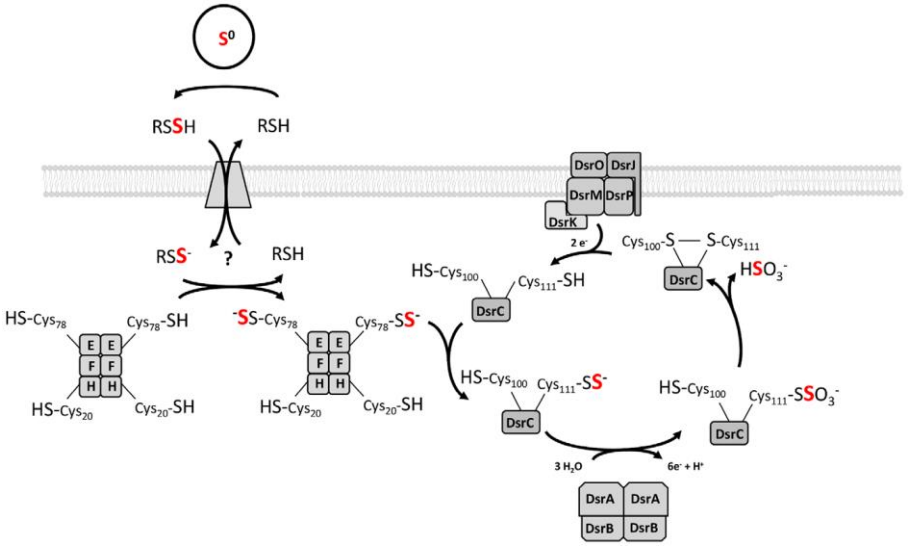

Figure. 1.12. Model of sulfur oxidation in A. vinosum integrating a sulfur transfer function for DsrEFH and a substrate donating function for DsrC (Stockdreher et al., 2012).

oxidation, sulfur is first accumulated in sulfur globules, and then imported into the cytoplasm were it reacts with Cys_{78} of DsrE (that belongs to DsrEFH cytoplasmic complex) (Stockdreher *et al.*, 2012). This sulfur in DsrE is then proposed to be transferred to the Cys_A of DsrC forming a persulfide which transfers it to the reverse DsrAB forming an intramolecular disulfide bond between Cys_B and Cys_A. This process is proposed to finalize in the DsrMKJOP complex where the oxidized disulfide DsrC form can be reduced, ready to enter in another cycle of sulfur relay (Figure 1.12) (Stockdreher *et al.*, 2012).

1.5 How is dissimilatory sulfate reduction linked to energy conservation?

All SRP share a group of proteins known to be directly involved in sulfate reduction which include, Sat, ApsBA and DsrAB. However, these are cytoplasmic proteins and cannot be directly involved in the generation of a proton-motive force. To accomplish energy conservation the terminal reductases (ApsBA and DsrAB) must be linked to a membrane complex. There are several membrane complexes present in SRP that can be linked to energy conservation such as QmoABC, DsrMKJOP, Qrc and the Hmc/Tmc/Nhc family (Pereira *et al.*, 2011). However, according to Pereira *et* al. only two membrane complexes are conserved in all SRP and also present in many SOB (Pereira, 2008, Frigaard & Dahl, 2009, Pereira *et al.*, 2011). These are the “quinone-interacting membrane-bound oxidoreductase” (QmoABC) and the dissimilatory sulfite reductase membrane complex (DsrMKJOP). These two complexes are thought to be implicated in energy conservation of SRP and have subunits that are homologous to subunits of heterodisulfide reductases (Hdr) of methanogens, complex responsible for the last step of methanogenesis: the reduction of heterodisulfide of

two thiol coenzymes (CoMSH and CoBSH) formed upon the release of methane (Thauer *et al.*, 2008).

The Qmo membrane complex is generally composed of three subunits QmoA and QmoB (cytoplasmic subunits) and QmoC (membrane subunit), and is usually found in a *sat-aprBA-qmoABC* gene cluster (Meyer & Kuever, 2007, Pereira *et al.*, 2011). However, in many clostridial SRP the *qmoC* gene is absent (Pereira, 2008, Pereira *et al.*, 2011), and is proposed to be substituted by the *hdrBC* genes found in the vicinity of the *qmoAB* genes, suggesting a possible interaction (Pereira *et al.*, 2011). The Qmo complex contains two FAD groups, two hemes *b* and several iron-sulfur centers. The two hemes *b* present in QmoC can be reduced by quinols. In 2010, Zane and coworkers verified that a *D. vulgaris* Hildenborough *qmoABC* mutant was not able to grow on sulfate but it grew on sulfite or thiosulfate (Zane *et al.*, 2010). This confirmed that the QmoABC complex is essential for the conversion of APS to sulfite in the dissimilatory sulfate reduction mechanism. It was recently shown by Kaster and coworkers that, in methanogens, HdrABC forms a complex with MvhADG (methyl-viologen-reducing [NiFe]-hydrogenase) coupling the favorable H_2 reduction of CoM-S-S-CoB to the unfavorable reduction of ferredoxin (Kaster *et al.*, 2011). They named this mechanism flavin-based bifurcation. Taking into account the homology between Qmo/Hdr and based on the bifurcating mechanism, Ramos *et* al. recently proposed a confurcation mechanism where QmoABC couples the oxidation of menaquinol (by QmoC) and the oxidation of a cytoplasmic reductant with low redox potential (via QmoB),

both acting as electrons donors to Qmo, to confurcate electrons to reduce ApsAB through QmoA (Figure 1.13) (Ramos *et al.*, 2012).

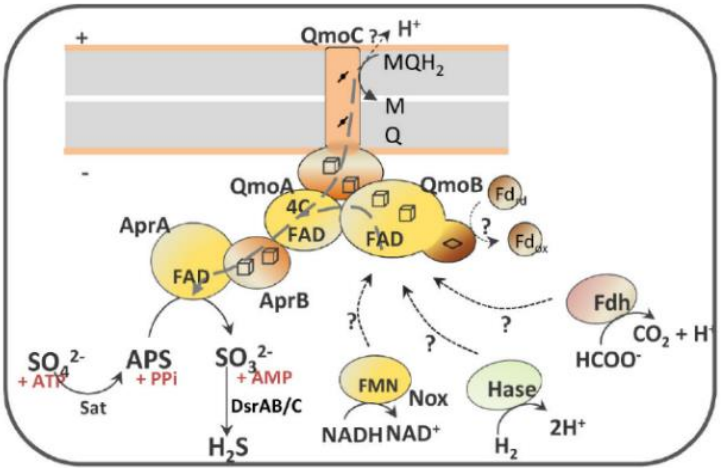

Figure. 1.13. The hypothesis of an electron confurcating mechanism where several possible co-electron donors for the Qmo complex are considered: ferredoxin (Fd), hydrogenase (Hase), formate dehydrogenase (Fdh) or NADH dehydrogenase (Nox) (from Ramos et al. 2012)

The other membrane complex present in SRP and SOB, which proved to be essential for sulfur oxidation (Pott & Dahl, 1998), is DsrMKJOP. This complex was first identified in *Allochromatium vinosum*, a purple SOB, as part of the *dsr* locus responsible for the intracellular oxidation of sulfur (Pott & Dahl, 1998). The Dsr complex was first purified and characterized from the archaeon *A. fulgidus*, where it was named Hme for Hdr-like menaquinol-oxidizing enzyme (Mander *et al.*, 2002).It was also shown that this complex is essential for sulfur globule oxidation in SOB (Sander *et al.*, 2006). DsrMKJOP is a transmembrane complex with two subunits in the periplasm (DsrJ and DsrO), two in the membrane (DsrM and DsrP) and one cytoplasmic (DsrK). According to the subunit organization this complex can be divided in two modules: DsrMK (strictly conserved among SRP) and the DsrJOP (absent in some SRP, mainly *Firmicutes*) (Pereira *et al.*, 2011, Grein *et al.*, 2013, Rabus *et al.*, 2015). The DsrJOP module is predicted to be involved in electron transfer

between the periplasm and the menaquinone pool. The DsrJ protein contains three heme *c*-type binding motif (CXXCH), proposed to have three different distal axial ligands: His/His, His/Met and His/Cys. A His/Cys distal axial ligation is very unusual and has only been found in three other proteins, TsdA (Denkmann *et al.*, 2012), PufC (Alric *et al.*, 2004) and SoxXA (Reijerse *et al.*, 2007). Grein and coworkers observed that the *A. vinosum* mutant lacking DsrJ was unable to oxidize intracellular sulfur, indicating that DsrJ is crucial for sulfur oxidation. Also, when this mutant was complemented with the *dsrJ* gene from *D. vulgaris*, it was able to fully restore the phenotype of the wild type, even though these genes only share 34% of identity, indicating that DsrJ might perform the same function in both organisms with opposite sulfur mechanisms (Grein *et al.*, 2010). The individual midpoint redox potentials of DsrJ from *A. vinosum* are -20, -200 and -220 mV (Grein *et al.*, 2010). These values are close to the calculated values for the His/Cys-ligated heme of PufC -160 mV (Alric *et al.*, 2004), but far from -432 mV value reported for the SoxXA heme (Reijerse *et al.*, 2007). Pires *et* al also reported that the His/Cys-ligated heme present in DsrMKJOP complex from *D. desulfuricans* was not fully reduced even at -400 mV (Pires *et al.*, 2006). Overall, the DsrJ protein still remains an enigmatic protein with no clear attributed function. DsrO contains, by sequence analysis, four iron-sulfur clusters (three in the case of *Desulfovibrio* spp (Pires *et al.*, 2006)) and a Tat signal peptide for translocation across de membrane. DsrP is an integral membrane protein with ten predicted transmembrane helixes, probably responsible for menaquinome/menaquinol interaction, as it belongs to the quinone-interacting NrfD/PsrC protein family (Grein *et al.*, 2010). The DsrMK module is homologous to the membrane-bound HdrED. The HdrED complex is present in methylotrophic methanogens, and it is responsible

for the reduction of CoM-S-S-CoB to CoM-SH and CoB-SH (Figure 1.14) (Deppenmeier, 2004). An isolated DsrMK complex has been isolated

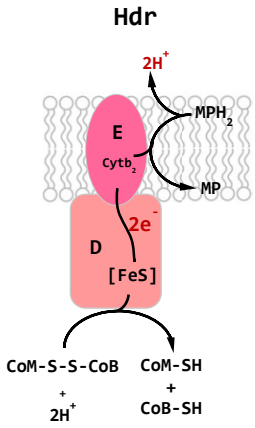

Figure. 1.14. Scheme of the function of the HdrED complex from methylotrophic methanogens (Kulkarni et al., 2009).

from *Archaeoglobus profundus* (Mander *et al.*, 2004). DsrM is an integral membrane protein, but smaller than DsrP, with two *b*-type hemes and only five predicted transmembrane helices. It shares similarity with heme *b*-containing NarI of bacterial nitrite reductases and HdrE of Hdr from methanogenic archaea, which suggests an ability to oxidize the menaquinol pool (Grein *et al.*, 2010). Also, it was shown that the DsrM hemes *b* can be reduced with menaquinol analogues (Pires *et al.*, 2006). Finally in the cytoplasm resides DsrK. The homology of DsrK to the HdrD protein immediately argues that it should be a catalytic subunit of DsrMKJOP complex. The HdrD subunit is responsible for reducing the CoM–S–S–CoB (Figure 1.14) (Hedderich *et al.*, 2005). DsrK and HdrD share a CCG domain that contains the conserved sequence CX_nCCGX_mCXXC that binds the [4Fe-4S] center responsible for heterodisulfide reduction. Moreover, DsrK has no transmembrane helix but was suggested to be membrane anchored by Grein and coworkers, through an amphipathic α-helix at the N- terminus (Grein *et al.*, 2010), because in *A. vinosum* purifications DsrK was only found in the

membrane fractions. As already referred in chapter 1.4, DsrK has the ability to interact with DsrC and due to this it is considered the link between the reduction of sulfite by DsrAB and energy conservation in SRP (Figure 1.15) (Pires *et al.*, 2006, Oliveira *et al.*, 2008, Pereira *et al.*, 2011).

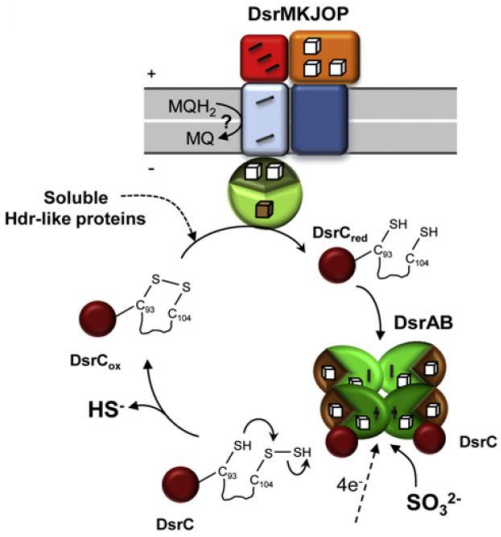

Figure. 1. 15. The reduction of sulfite by DsrAB generates a S^0 intermediate that reacts with Cys_A of DsrC resulting in a persulfide, which by displacement of sulfide forms an intramolecular disulfide bridge, $DsrC_{ox}$. This oxidized form of DsrC is reduced by the DsrK protein of the DsrMKJOP complex (Grein et al., 2013)

References

Akagi JM (1983) Reduction of Bisulfite by the Trithionate Pathway by Cell-Extracts from Desulfotomaculum-Nigrificans. *Biochemical and Biophysical Research Communications* **117**: 530-535.

Akagi JM (1995) Respiratory Sulfate Reduction. *Sulfate-Reducing Bacteria,* Vol. 8 (Barton L, ed.) p.^pp. 89-111. Springer US.

Alric J, Tsukatani Y, Yoshida M, Matsuura K, Shimada K, Hienerwadel R, Schoepp-Cothenet B, Nitschke W, Nagashima KVP & Vermeglio A (2004) Structural and functional characterization of the unusual triheme cytochrome bound to the reaction center of Rhodovulum sulfidophilum. *Journal of Biological Chemistry* **279**: 26090-26097.

Aravind L, Anantharaman V, Balaji S, Babu MM & Iyer LM (2005) The many faces of the helix-turn-helix domain: Transcription regulation and beyond. *Fems Microbiology Reviews* **29**: 231-262.

Badziong W & Thauer RK (1978) Growth Yields and Growth-Rates of Desulfovibrio-Vulgaris-(Marburg) Growing on Hydrogen Plus Sulfate and Hydrogen Plus Thiosulfate as Sole Energy-Sources. *Arch Microbiol* **117**: 209-214.

Bak F & Pfennig N (1987) Chemolithotrophic Growth of Desulfovibrio-Sulfodismutans Sp-Nov by Disproportionation of Inorganic Sulfur-Compounds. *Arch Microbiol* **147**: 184-189.

Barton LL & Fauque GD (2009) Biochemistry, physiology and biotechnology of sulfate-reducing bacteria. *Adv Appl Microbiol* **68**: 41-98.

Beech IB & Sunner JA (2007) *Sulphate-reducing bacteria and their role in corrosion of ferrous materials*. Cambridge University Press, Sulphate-reducing Bacteria.

Bottcher ME, Thamdrup B, Gehre M & Theune A (2005) S-34/S-32 and O-18/O-16 fractionation during sulfur disproportionation by Desulfobulbus propionicus. *Geomicrobiol J* **22**: 219-226.

Canfield DE, Habicht KS & Thamdrup B (2000) The Archean sulfur cycle and the early history of atmospheric oxygen. *Science* **288**: 658-661.

Carbonero F, Benefiel AC & Gaskins HR (2012) Contributions of the microbial hydrogen economy to colonic homeostasis. *Nat Rev Gastroenterol Hepatol* **9**: 504-518.

Castresana J & Moreira D (1999) Respiratory chains in the last common ancestor of living organisms. *J Mol Evol* **49**: 453-460.

Chambers LA, Trudinger PA, Smith JW & Burns MS (1975) Fractionation of sulfur isotopes by continuous cultures of Desulfovibrio desulfuricans. *Can J Microbiol* **21**: 1602-1607.

Cort JR, Selan U, Schulte A, Grimm F, Kennedy MA & Dahl C (2008) Allochromatium vinosum DsrC: solution-state NMR structure, redox properties, and interaction with DsrEFH, a protein essential for purple sulfur bacterial sulfur oxidation. *J Mol Biol* **382**: 692-707.

Cort JR, Mariappan SVS, Kim CY, Park MS, Peat TS, Waldo GS, Terwilliger TC & Kennedy MA (2001) Solution structure of Pyrobaculum aerophilum DsrC, an archaeal homologue of the gamma subunit of dissimilatory sulfite reductase. *European Journal of Biochemistry* **268**: 5842-5850.

Crane BR & Getzoff ED (1996) The relationship between structure and function for the sulfite reductases. *Curr Opin Struc Biol* **6**: 744-756.

Crane BR, Siegel LM & Getzoff ED (1995) Sulfite Reductase Structure at 1.6 Angstrom - Evolution and Catalysis for Reduction of Inorganic Anions. *Science* **270**: 59-67.

Crane BR, Siegel LM & Getzoff ED (1997) Structures of the siroheme- and Fe4S4-containing active center of sulfite reductase in different states of oxidation: Heme activation via reduction-gated exogenous ligand exchange. *Biochemistry* **36**: 12101-12119.

Cypionka H (1987) Uptake of Sulfate, Sulfite and Thiosulfate by Proton-Anion Symport in Desulfovibrio-Desulfuricans. *Arch Microbiol* **148**: 144-149.

Dahl C, Kredich NM, Deutzmann R & Truper HG (1993) Dissimilatory sulphite reductase from Archaeoglobus fulgidus: physico-

chemical properties of the enzyme and cloning, sequencing and analysis of the reductase genes. *J Gen Microbiol* **139**: 1817-1828.

Denkmann K, Grein F, Zigann R, Siemen A, Bergmann J, van Helmont S, Nicolai A, Pereira IAC & Dahl C (2012) Thiosulfate dehydrogenase: a widespread unusual acidophilic c-type cytochrome. *Environmental Microbiology* **14**: 2673-2688.

Deppenmeier U (2004) The Membrane-Bound Electron Transport System of Methanosarcina Species. *J Bioenerg Biomembr* **36**: 55-64.

Dhillon A, Goswami S, Riley M, Teske A & Sogin M (2005) Domain evolution and functional diversification of sulfite reductases. *Astrobiology* **5**: 18-29.

Dolla A, Donald M, Kurtz J, Teixeira M & Voordouw G (2007) *Biochemical, proteomic and genetic characterization of oxygen survival mechanisms in sulphate-reducing bacteria of the genus Desulfovibrio*. Cambridge University Press, Sulphate-reducing Bacteria.

Drake HL & Akagi JM (1977) Bisulfite reductase of Desulfovibrio vulgaris: explanation for product formation. *J Bacteriol* **132**: 139-143.

Ehrlich HL & Newman DK (2008) Geomicrobiology of Sulfur. *Geomicrobiology, Fifth Edition,* p.^pp. 439-489. CRC Press.

Fauque G, Peck HD, Jr., Moura JJ*, et al.* (1988) The three classes of hydrogenases from sulfate-reducing bacteria of the genus Desulfovibrio. *FEMS Microbiol Rev* **4**: 299-344.

Frigaard N-U & Dahl C (2009) Sulfur Metabolism in Phototrophic Sulfur Bacteria. *Advances in Microbial Physiology, Vol 54,* Vol. 54 (Poole RK, ed.) p.^pp. 103-200.

Gibson GR, Cummings JH & Macfarlane GT (1988) Competition for hydrogen between sulphate-reducing bacteria and methanogenic bacteria from the human large intestine. *J Appl Bacteriol* **65**: 241-247.

Grein F, Pereira IAC & Dahl C (2010) Biochemical Characterization of Individual Components of the Allochromatium vinosum DsrMKJOP Transmembrane Complex Aids Understanding of Complex Function In Vivo. *J Bacteriol* **192**: 6369-6377.

Grein F, Ramos AR, Venceslau SS & Pereira IA (2013) Unifying concepts in anaerobic respiration: insights from dissimilatory sulfur metabolism. *Biochim Biophys Acta* **1827**: 145-160.

Grein F, Venceslau SS, Schneider L, Hildebrandt P, Todorovic S, Pereira IAC & Dahl C (2010) DsrJ, an Essential Part of the DsrMKJOP Transmembrane Complex in the Purple Sulfur Bacterium Allochromatium vinosum, Is an Unusual Triheme Cytochrome c. *Biochemistry* **49**: 8290-8299.

Grimm F, Dobler N & Dahl C (2010) Regulation of dsr genes encoding proteins responsible for the oxidation of stored sulfur in Allochromatium vinosum. *Microbiol-Sgm* **156**: 764-773.

Hansel CM, Fendorf S, Jardine PM & Francis CA (2008) Changes in Bacterial and Archaeal Community Structure and Functional Diversity along a Geochemically Variable Soil Profile. *Appl Environ Microb* **74**: 1620-1633.

Harrison AG & Thode HG (1958) Mechanism of the bacterial reduction of sulphate from isotope fractionation studies. *Transactions of the Faraday Society* **54**: 84-92.

Hedderich R, Hamann N & Bennati M (2005) Heterodisulfide reductase from methanogenic archaea: a new catalytic role for an iron-sulfur cluster. *Biol Chem* **386**: 961-970.

Heidelberg JF, Seshadri R, Haveman SA*, et al.* (2004) The genome sequence of the anaerobic, sulfate-reducing bacterium Desulfovibrio vulgaris Hildenborough. *Nat Biotech* **22**: 554-559.

Holland HD (2006) The oxygenation of the atmosphere and oceans. *Philos Trans R Soc Lond B Biol Sci* **361**: 903-915.

Hsieh YC, Liu MY, Wang VCC, Chiang YL, Liu EH, Wu WG, Chan SI & Chen CJ (2010) Structural insights into the enzyme catalysis from comparison of three forms of dissimilatory sulphite reductase from Desulfovibrio gigas. *Mol Microbiol* **78**: 1101-1116.

Huynh BH, Kang L, DerVartanian DV, Peck HD, Jr. & LeGall J (1984) Characterization of a sulfite reductase from Desulfovibrio vulgaris. Evidence for the presence of a low-spin siroheme and an exchange-coupled siroheme-[4Fe-4S] unit. *J Biol Chem* **259**: 15373-15376.

Ikeuchi Y, Shigi N, Kato J, Nishimura A & Suzuki T (2006) Mechanistic insights into multiple sulfur mediators sulfur relay by involved in thiouridine biosynthesis at tRNA wobble positions. *Mol Cell* **21**: 97-108.

Johnston DT (2011) Multiple sulfur isotopes and the evolution of Earth's surface sulfur cycle. *Earth-Sci Rev* **106**: 161-183.

Jones HE & Skyring GW (1975) Effect of enzymic assay conditions on sulfite reduction catalysed by desulfoviridin from Desulfovibrio gigas. *Biochim Biophys Acta* **377**: 52-60.

Jørgensen BB & Fenchel T (1974) Sulfur Cycle of a Marine Sediment Model System. *Mar Biol* **24**: 189-201.

Kaplan IR & Rittenberg SC (1964) Microbiological Fractionation of Sulphur Isotopes. *Microbiology* **34**: 195-212.

Karkhoff-schweizer RAR, Bruschi M & Voordouw G (1993) Expression of the Beta-Subunit Gene of Desulfoviridin-Type Dissimilatory Sulfite Reductase and of the Alpha-Subunit and Beta-Subunit Genes Is Not Coordinately Regulated. *European Journal of Biochemistry* **211**: 501-507.

Karkhoff-Schweizer RR, Bruschi M & Voordouw G (1993) Expression of the gamma-subunit gene of desulfoviridin-type dissimilatory sulfite reductase and of the alpha- and beta-subunit genes is not coordinately regulated. *Eur J Biochem* **211**: 501-507.

Karkhoff-schweizer RR, Huber DPW & Voordouw G (1995) Conservation of the genes for dissimilatory sulfite reductase from *Desulfovibrio vulgaris* and *Archaeoglobus fulgidus* allows their detection by PCR. *Appl Environ Microb* **61**: 290-296.

Kaster AK, Moll J, Parey K & Thauer RK (2011) Coupling of ferredoxin and heterodisulfide reduction via electron bifurcation in hydrogenotrophic methanogenic archaea. *P Natl Acad Sci USA* **108**: 2981-2986.

Kisker C, Hinrichs W, Tovar K, Hillen W & Saenger W (1995) The complex formed between Tet repressor and tetracycline-Mg2+ reveals mechanism of antibiotic resistance. *J Mol Biol* **247**: 260-280.

Klein M, Friedrich M, Roger AJ, Hugenholtz P, Fishbain S, Abicht H, Blackall LL, Stahl DA & Wagner M (2001) Multiple lateral transfers of

dissimilatory sulfite reductase genes between major lineages of sulfate-reducing prokaryotes. *J Bacteriol* **183**: 6028-6035.

Klenk HP, Clayton RA, Tomb JF*, et al.* (1997) The complete genome sequence of the hyperthermophilic, sulphate-reducing archaeon Archaeoglobus fulgidus. *Nature* **390**: 364-&.

Kobayash.K, Takahash.E & Ishimoto M (1972) Biochemical Studies on Sulfate-Reducing Bacteria .11. Purification and Some Properties of Sulfite Reductase, Desulfoviridin. *J Biochem-Tokyo* **72**: 879-&.

Kobayash.K, Seki Y & Ishimoto M (1974) Biochemical Studies on Sulfate-Reducing Bacteria .13. Sulfite Reductase from Desulfovibrio-Vulgaris - Mechanism of Trithionate, Thiosulfate, and Sulfide Formation and Enzymatic Properties. *J Biochem-Tokyo* **75**: 519-529.

Kreke B & Cypionka H (1994) Role of Sodium-Ions for Sulfate Transport and Energy-Metabolism in Desulfovibrio Salexigens. *Arch Microbiol* **161**: 55-61.

Kulkarni G, Kridelbaugh DM, Guss AM & Metcalf WW (2009) Hydrogen is a preferred intermediate in the energy-conserving electron transport chain of Methanosarcina barkeri. *Proc Natl Acad Sci U S A* **106**: 15915-15920.

La Scola B & Raoult D (1999) Third human isolate of a Desulfovibrio sp identical to the provisionally named Desulfovibrio fairfieldensis. *Journal of Clinical Microbiology* **37**: 3076-3077.

Langendijk PS, Hanssen JTJ & Van der Hoeven JS (2000) Sulfate-reducing bacteria in association with human periodontitis. *Journal of Clinical Periodontology* **27**: 943-950.

Larsen O, Lien T & Birkeland NK (1999) Dissimilatory sulfite reductase from Archaeoglobus profundus and Desulfotomaculum thermocisternum: phylogenetic and structural implications from gene sequences. *Extremophiles* **3**: 63-70.

Leavitt WD, Halevy I, Bradley AS & Johnston DT (2013) Influence of sulfate reduction rates on the Phanerozoic sulfur isotope record. *Proc Natl Acad Sci U S A* **110**: 11244-11249.

Lee JP & Peck HD (1971) Purification of the enzyme reducing bisulfite to trithionate from Desulfovibrio gigas and its identification as

desulfoviridin. *Biochemical and Biophysical Research Communications* **45**: 583-589.

Lee JP, LeGall J & Peck HD (1973) Isolation of Assimilatory- and Dissimilatory-Type Sulfite Reductases from Desulfovibrio vulgaris. *J Bacteriol* **115**: 529-542.

Lee JP, Yi CS, Legall J & Peck HD (1973) Isolation of a New Pigment, Desulforubidin, from Desulfovibrio-Desulfuricans (Norway-Strain) and Its Role in Sulfite Reduction. *J Bacteriol* **115**: 453-455.

Lipmann F (1958) Biological Sulfate Activation and Transfer. *Science* **128**: 575-580.

Lobo SAL, Warren MJ & Saraiva LM (2012) Chapter Seven - Sulfate-Reducing Bacteria Reveal a New Branch of Tetrapyrrole Metabolism. *Advances in Microbial Physiology,* Vol. Volume 61 (Robert KP, ed.) p.^pp. 267-295. Academic Press.

Lobo SAL, Melo AMP, Carita JN, Teixeira M & Saraiva LM (2007) The anaerobe Desulfovibrio desulfuricans ATCC 27774 grows at nearly atmospheric oxygen levels. *FEBS Letters* **581**: 433-436.

Loubinoux J, Mory F, Pereira IAC & Le Faou AE (2000) Bacteremia caused by a strain of Desulfovibrio related to the provisionally named Desulfovibrio fairfieldensis (vol 38, pg 931, 2000). *Journal of Clinical Microbiology* **38**: 1707-1707.

Loubinoux J, Bronowicki J-P, Pereira IAC, Mougenel J-L & Le Faou AE (2002) *Sulfate-reducing bacteria in human feces and their association with inflammatory bowel diseases*.

Loy A, Duller S & Wagner M (2008) Evolution and ecology of microbes dissimilating sulfur compounds: Insights from siroheme sulfite reductases. *Microbial Sulfur Metabolism* 46-59.

Loy A, Duller S & Wagner M (2008) Evolution and Ecology of Microbes Dissimilating Sulfur Compounds: Insights from Siroheme Sulfite Reductases. *Microbial Sulfur Metabolism,*(Dahl C & Friedrich C, eds.), p.^pp. 46-59. Springer Berlin Heidelberg.

Loy A, Duller S, Baranyi C, Mussmann M, Ott J, Sharon I, Beja O, Le Paslier D, Dahl C & Wagner M (2009) Reverse dissimilatory sulfite reductase as phylogenetic marker for a subgroup of sulfur-oxidizing prokaryotes. *Environmental Microbiology* **11**: 289-299.

Luptakova A (2007) Importance of Sulphate-Reducing Bacteria in Environment. *Nova Biotechnologica* **VII-I**: 17-22.

Lyons TW & Gill BC (2010) Ancient Sulfur Cycling and Oxygenation of the Early Biosphere. *Elements* **6**: 93-99.

Mander GJ, Pierik AJ, Huber H & Hedderich R (2004) Two distinct heterodisulfide reductase-like enzymes in the sulfate-reducing archaeon Archaeoglobus profundus. *Eur J Biochem* **271**: 1106-1116.

Mander GJ, Duin EC, Linder D, Stetter KO & Hedderich R (2002) Purification and characterization of a membrane-bound enzyme complex from the sulfate-reducing archaeon Archaeoglobus fulgidus related to heterodisulfide reductase from methanogenic archaea. *European Journal of Biochemistry* **269**: 1895-1904.

Mander GJ, Weiss MS, Hedderich R, Kahnt J, Ermler U & Warkentin E (2005) X-ray structure of the gamma-subunit of a dissimilatory sulfite reductase: fixed and flexible C-terminal arms. *FEBS Lett* **579**: 4600-4604.

Martins M, Faleiro ML, Barros RJ, Veríssimo AR, Barreiros MA & Costa MC (2009) Characterization and activity studies of highly heavy metal resistant sulphate-reducing bacteria to be used in acid mine drainage decontamination. *Journal of Hazardous Materials* **166**: 706-713.

Martins M, Santos ES, Faleiro ML, Chaves S, Tenreiro R, Barros RJ, Barreiros A & Costa MC (2011) Performance and bacterial community shifts during bioremediation of acid mine drainage from two Portuguese mines. *Int Biodeter Biodegr* **65**: 972-981.

McDougall R, Robson J, Paterson D & Tee W (1997) Bacteremia caused by a recently described novel Desulfovibrio species. *Journal of Clinical Microbiology* **35**: 1805-1808.

Meyer B & Kuever J (2007) Phylogeny of the alpha and beta subunits of the dissimilatory adenosine-5'-phosphosulfate (APS) reductase from sulfate-reducing prokaryotes - origin and evolution of the dissimilatory sulfate-reduction pathway. *Microbiol-Sgm* **153**: 2026-2044.

Meyer L (1864) Chemische Untersuchung der Thermen zu Landeck in der Grafschaft Glatz. *Journal für Praktische Chemie* **91**: 1-15.

Moura I, LeGall J, Lino AR, Peck HD, Fauque G, Xavier AV, DerVartanian DV, Moura JJG & Huynh BH (1988) Characterization of two dissimilatory sulfite reductases (desulforubidin and desulfoviridin) from the sulfate-reducing bacteria. Moessbauer and EPR studies. *J Am Chem Soc* **110**: 1075-1082.

Müller AL, Kjeldsen KU, Rattei T, Pester M & Loy A (2015) Phylogenetic and environmental diversity of DsrAB-type dissimilatory (bi) sulfite reductases. *Isme J* **9**: 1152-1165.

Muyzer G & Stams AJ (2008) The ecology and biotechnology of sulphate-reducing bacteria. *Nat Rev Microbiol* **6**: 441-454.

Nakao K, Tanaka K, Ichiishi S, Mikamo H, Shibata T & Watanabe K (2009) Susceptibilities of 23 Desulfovibrio Isolates from Humans. *Antimicrob Agents Ch* **53**: 5308-5311.

Nakayama M, Akashi T & Hase T (2000) Plant sulfite reductase: molecular structure, catalytic function and interaction with ferredoxin. *Journal of Inorganic Biochemistry* **82**: 27-32.

Nethejaenchen R & Thauer RK (1984) Growth Yields and Saturation Constant of Desulfovibrio-Vulgaris in Chemostat Culture. *Arch Microbiol* **137**: 236-240.

Oliveira TF, Vonrhein C, Matias PM, Venceslau SS, Pereira IAC & Archer M (2008) Purification, crystallization and preliminary crystallographic analysis of a dissimilatory DsrAB sulfite reductase in complex with DsrC. *Journal of Structural Biology* **164**: 236-239.

Oliveira TF, Vonrhein C, Matias PM, Venceslau SS, Pereira IA & Archer M (2008) The crystal structure of Desulfovibrio vulgaris dissimilatory sulfite reductase bound to DsrC provides novel insights into the mechanism of sulfate respiration. *J Biol Chem* **283**: 34141-34149.

Oliveira TF, Franklin E, Afonso JP, Khan AR, Oldham NJ, Pereira IAC & Archer M (2011) Structural insights into dissimilatory sulfite reductases: structure of desulforubidin from Desulfomicrobium norvegicum. *Frontiers in Microbiology* **2**.

Oyaizu Y, Yang D, Oyaizu H & Woese CR (1985) 16s-Like Ribosomal-Rna Comparison between Bacteria and Wheat Mitochondria. *Jpn J Genet* **60**: 623-623.

Parey K, Warkentin E, Kroneck PM & Ermler U (2010) Reaction cycle of the dissimilatory sulfite reductase from Archaeoglobus fulgidus. *Biochemistry* **49**: 8912-8921.

Peck HD, Legall J & Vanbeeumen J (1982) Biochemistry of Dissimilatory Sulfate Reduction. *Philos T Roy Soc B* **298**: 443-466.

Pelsh AD (1936) About new autotrophic hydrogenthiobacteria (in Russian). *Trudy Solyanoi Laboratorii* **vypusk, M.-L., Izdatelstvo AN SSSR 5**: 109-126.

Pereira IA, Ramos AR, Grein F, Marques MC, da Silva SM & Venceslau SS (2011) A comparative genomic analysis of energy metabolism in sulfate reducing bacteria and archaea. *Front Microbiol* **2**: 69.

Pereira IAC (2008) Respiratory membrane complexes of Desulfovibrio. *Microbial Sulfur Metabolism* 24-35.

Pierik AJ, Duyvis MG, van Helvoort JMLM, Wolbert RBG & Hagen WR (1992) The third subunit of desulfoviridin-type dissimilatory sulfite reductases. *European Journal of Biochemistry* **205**: 111-115.

Pilsyk S & Paszewski A (2009) Sulfate permeasesphylogenetic diversity of sulfate transport. *Acta biochimica Polonica* **56**: 375-384.

Pires RH, Venceslau SS, Morais F, Teixeira M, Xavier AV & Pereira IA (2006) Characterization of the Desulfovibrio desulfuricans ATCC 27774 DsrMKJOP complex--a membrane-bound redox complex involved in the sulfate respiratory pathway. *Biochemistry* **45**: 249-262.

Postgate JR (1956) Cytochrome c3 and desulphoviridin; pigments of the anaerobe Desulphovibrio desulphuricans. *J Gen Microbiol* **14**: 545-572.

Postgate JR & Kent HM (1985) Diazotrophy within Desulfovibrio. *Microbiology* **131**: 2119-2122.

Pott AS & Dahl C (1998) Sirohaem sulfite reductase and other proteins encoded by genes at the dsr locus of Chromatium vinosum are involved in the oxidation of intracellular sulfur. *Microbiol-Uk* **144**: 1881-1894.

Rabus R, Hansen TA & Widdle F (2006) Dissimilatory Sulfate- and Sulfur-Reducing Prokaryotes. *The Prokaryotes,*(Stanley Falkow ER,

Karl-Heinz Schleifer,Erko Stackebrandt, ed.) p.^pp. 659–768. Springer, Singapore.

Rabus R, Venceslau SS, Wohlbrand L, Voordouw G, Wall JD & Pereira IA (2015) A Post-Genomic View of the Ecophysiology, Catabolism and Biotechnological Relevance of Sulphate-Reducing Prokaryotes. *Adv Microb Physiol* **66**: 55-321.

Ramos AR, Keller KL, Wall JD & Pereira IAC (2012) The membrane QmoABC complex interacts directly with the dissimilatory adenosine 5 '-phosphosulfate reductase sulfate reducing bacteria. *Frontiers in Microbiology* **3**.

Reijerse EJ, Sommerhalter M, Hellwig P, Quentmeier A, Rother D, Laurich C, Bothe E, Lubitz W & Friedrich CG (2007) The Unusal Redox Centers of SoxXA, a Novel c-Type Heme-Enzyme Essential for Chemotrophic Sulfur-Oxidation of Paracoccus pantotrophus†. *Biochemistry* **46**: 7804-7810.

Rieder R, Cammack R & Hall DO (1984) Purification and Properties of the Soluble Hydrogenase from Desulfovibrio-Desulfuricans (Strain Norway-4). *European Journal of Biochemistry* **145**: 637-643.

Sánchez-Andrea I, Rodríguez N, Amils R & Sanz JL (2011) Microbial Diversity in Anaerobic Sediments at Río Tinto, a Naturally Acidic Environment with a High Heavy Metal Content. *Appl Environ Microb* **77**: 6085-6093.

Sánchez-Andrea I, Sanz JL, Bijmans MFM & Stams AJM (2014) Sulfate reduction at low pH to remediate acid mine drainage. *Journal of Hazardous Materials* **269**: 98-109.

Sander J, Engels-Schwarzlose S & Dahl C (2006) Importance of the DsrMKJOP complex for sulfur oxidation in Allochromatium vinosum and phylogenetic analysis of related complexes in other prokaryotes. *Arch Microbiol* **186**: 357-366.

Schiffer A, Parey K, Warkentin E, Diederichs K, Huber H, Stetter KO, Kroneck PMH & Ermler U (2008) Structure of the dissimilatory sulfite reductase from the hyperthermophilic archaeon Archaeoglobus fulgidus. *J Mol Biol* **379**: 1063-1074.

Shen YA, Buick R & Canfield DE (2001) Isotopic evidence for microbial sulphate reduction in the early Archaean era. *Nature* **410**: 77-81.

Shigi N (2014) Biosynthesis and functions of sulfur modifications in tRNA. *Frontiers in Genetics* **5**.

Siegel LM, Davis PS & Kamin H (1974) Reduced Nicotinamide Adenine-Dinucleotide Phosphate-Sulfite Reductase of Enterobacteria .3. Escherichia-Coli Hemoflavoprotein - Catalytic Parameters and Sequence of Electron Flow. *Journal of Biological Chemistry* **249**: 1572-1586.

Simon J & Kroneck PMH (2013) Microbial Sulfite Respiration. *Advances in Microbial Physiology, Vol 62,* Vol. 62 (Poole RK, ed.) p.^pp. 45-117.

Skyring GW & Donnelly TH (1982) Precambrian Sulfur Isotopes and a Possible Role for Sulfite in the Evolution of Biological Sulfate Reduction. *Precambrian Res* **17**: 41-61.

Smith KW & Stroupe ME (2012) Mutational analysis of sulfite reductase hemoprotein reveals the mechanism for coordinated electron and proton transfer. *Biochemistry* **51**: 9857-9868.

Stahl DA, Fishbain S, Klein M, Baker BJ & Wagner M (2002) Origins and diversification of sulfate-respiring microorganisms. *Anton Leeuw Int J G* **81**: 189-195.

Stockdreher Y, Venceslau SS, Josten M, Sahl HG, Pereira IA & Dahl C (2012) Cytoplasmic sulfurtransferases in the purple sulfur bacterium Allochromatium vinosum: evidence for sulfur transfer from DsrEFH to DsrC. *Plos One* **7**: e40785.

Stroupe ME & Getzoff E (2009) The Role of Siroheme in Sulfite and Nitrite Reductases. *Tetrapyrroles,*p.^pp. 375-389. Springer New York.

Tan J & Cowan JA (1991) Enzymatic Redox Chemistry - a Proposed Reaction Pathway for the 6-Electron Reduction of So32- to S2- by the Assimilatory-Type Sulfite Reductase from Desulfovibrio-Vulgaris (Hildenborough). *Biochemistry* **30**: 8910-8917.

Tang K, Baskaran V & Nemati M (2009) Bacteria of the sulphur cycle: An overview of microbiology, biokinetics and their role in petroleum and mining industries. *Biochem Eng J* **44**: 73-94.

Tee W, DyallSmith M, Woods W & Eisen D (1996) Probable new species of Desulfovibrio isolated from a pyogenic liver abscess. *Journal of Clinical Microbiology* **34**: 1760-1764.

Thauer RK, Stackebrandt E & Hamilton WA (2007) *Energy metabolism and phylogenetic diversity of sulphate-reducing bacteria*. Cambridge University Press, Sulphate-reducing Bacteria.

Thauer RK, Kaster AK, Seedorf H, Buckel W & Hedderich R (2008) Methanogenic archaea: ecologically relevant differences in energy conservation. *Nature Reviews Microbiology* **6**: 579-591.

Thode H., Kleerekoper H. & D. M (1951) Isotope fractionation in the bacterial reduction of sulphate. *Research* 581–582.

Trudinge.Pa (1970) Carbon Monoxide-Reacting Pigment from Desulfotomaculum-Nigrificans and Its Possible Relevance to Sulfite Reduction. *J Bacteriol* **104**: 158-&.

Ullrich TC, Blaesse M & Huber R (2001) Crystal structure of ATP sulfurylase from Saccharomyces cerevisiae, a key enzyme in sulfate activation. *Embo Journal* **20**: 316-329.

Vairavamurthy MA, Orr WL & Manowitz B (1995) Geochemical transformations of sedimentary sulfur: An introduction. *Acs Sym Ser* **612**: 1-14.

Venceslau SS, Stockdreher Y, Dahl C & Pereira IA (2014) The "bacterial heterodisulfide" DsrC is a key protein in dissimilatory sulfur metabolism. *Biochim Biophys Acta* **1837**: 1148-1164.

Venceslau SS, Cort JR, Baker ES, Chu RK, Robinson EW, Dahl C, Saraiva LM & Pereira IA (2013) Redox states of Desulfovibrio vulgaris DsrC, a key protein in dissimilatory sulfite reduction. *Biochem Biophys Res Commun*.

Verstreken I, Laleman W, Wauters G & Verhaegen J (2012) Desulfovibrio desulfuricans Bacteremia in an Immunocompromised Host with a Liver Graft and Ulcerative Colitis. *Journal of Clinical Microbiology* **50**: 199-201.

Voordouw G (2011) Production-related petroleum microbiology: progress and prospects. *Curr Opin Biotech* **22**: 401-405.

Wagner M, Roger AJ, Flax JL, Brusseau GA & Stahl DA (1998) Phylogeny of dissimilatory sulfite reductases supports an early origin of sulfate respiration. *J Bacteriol* **180**: 2975-2982.

Wagner M, Loy A, Klein M, Lee N, Ramsing NB, Stahl DA & Friedrich MW (2005) Functional marker genes for identification of sulfate-reducing prokaryotes. *Environmental Microbiology* **397**: 469-489.

Wall JD, Arkin AP, Balci NC & Rapp-Giles B (2008) Genetics and genomics of sulfate respiration in Desulfovibrio. *Microbial Sulfur Metabolism* 1-12.

Weston B, Fogal B, Cook D & Dhurjati P (2015) An agent-based modeling framework for evaluating hypotheses on risks for developing autism: Effects of the gut microbial environment. *Med Hypotheses* **84**: 395-401.

Wing BA & Halevy I (2014) Intracellular metabolite levels shape sulfur isotope fractionation during microbial sulfate respiration. *Proceedings of the National Academy of Sciences* **111**: 18116-18125.

Zane GM, Yen HCB & Wall JD (2010) Effect of the Deletion of qmoABC and the Promoter-Distal Gene Encoding a Hypothetical Protein on Sulfate Reduction in Desulfovibrio vulgaris Hildenborough. *Appl Environ Microb* **76**: 5500-5509.

Zverlov V, Klein M, Lucker S, Friedrich MW, Kellermann J, Stahl DA, Loy A & Wagner M (2005) Lateral gene transfer of dissimilatory (bi)sulfite reductase revisited. *J Bacteriol* **187**: 2203-2208.

Chapter 2

Dissimilatory sulfite reductase and DsrC: isolation and analytic assays

Table of contents

2.1. Introduction

As referred in the previous chapter, there has been a lot of debate concerning the last step of dissimilatory sulfate reduction, the six electron reduction of sulfite to sulfite. There are two mechanisms proposed: i) the trithionate pathway, in which the DsrAB reduces sulfite to trithionate, thiosulfate and sulfide, and ii) the DsrAB/DsrC pathway, in which DsrC cooperates with DsrAB in the reduction of sulfite. This last mechanism was proposed by Oliveira et al. (Oliveira *et al.*, 2008), and implies the reduction of sulfite to an S^0 intermediate by DsrAB, which will interact with the Cys_A conserved cysteine of DsrC to release sulfide.

In this chapter we will describe the preparatory work required to set up the experiments described in Chapter 3, whose aim was to elucidate the mechanism of sulfite reduction by DsrAB and the role played by DsrC. For this two DsrABs were isolated, one from *D. vulgaris* and the other from *A. fulgidus*, and several recombinant DsrC mutants from *A. fulgidus* were prepared. The two DsrABs enzymes are structurally similar and evolutionarily related (Müller *et al.*, 2015) presenting the same quaternary structure, with only two main differences: i) the DsrAB from *D. vulgaris* has two non-catalytic sirohydrochlorines per each DsrA subunit instead of the two, also non-catalytic, sirohemes present in the DsrAs from *A. fulgidus* and ii) the DsrAB from *D. vulgaris* is always purified as a complex with none, one or two DsrC proteins ($\alpha_2\beta_2$ (minor), $\alpha_2\beta_2\gamma$ and $\alpha_2\beta_2\gamma_2$), while in the case of DsrAB from *A. fulgidus* the protein is purified without DsrC ($\alpha_2\beta_2$) (Oliveira *et al.*, 2008, Schiffer *et al.*, 2008, Oliveira *et al.*, 2011). Due to the fact that DsrAB from *D. vulgaris* cannot be purified without DsrC, the DsrAB from *A. fulgidus* was used to test the role of DsrC in the proposed mechanism by Oliveira et al. (Oliveira *et al.*, 2008), using also recombinant DsrC protein from the same organism.

Moreover, to identify the role of each conserved cysteine two DsrC variants with mutations in these cysteines were generated.

2.2. Materials and Methods

Purification of DsrABs

To study the dissimilatory reduction of sulfite to sulfide by the DsrAB, two dissimilatory sulfite reductases were purified: DsrAB from *D. vulgaris* str. Hildenborough (DSM 644) and *A. fulgidus* VC16 (4304).

DsrAB from D. vulgaris. *D. vulgaris* Hildenborough (DSM 644) cells were grown at 37 °C in a 300 L batch culture in a modified lactate/sulfate medium (Oliveira *et al.*, 2008). The soluble cell fraction was obtained as previously described (Oliveira *et al.*, 2008). All purification procedures were performed under aerobic atmosphere at 4 °C using an AKTA FPLC (Amersham Biotech Pharmacia) with two buffers, (A) 20 mM TrisHCl and (B) 50 mM TrisHCl with 1 M NaCl (both pH 7.6 and containing 10% glycerol). Buffer (A) was used to equilibrate the columns and buffer (B) to generate the ionic strength gradient. The soluble cell fraction was loaded in a Q-Sepharose fast-flow (XK50/30) column, and a stepwise salt gradient applied, with the DsrAB-containing fraction eluting at 300 mM NaCl. The characteristic *D. vulgaris* DsrAB absorption peak at 630 nm was used to track the protein, as previously described (Wolfe *et al.*, 1994, Marritt & Hagen, 1996). DsrAB-containing fractions were then loaded in a Q-Sepharose fast-flow (2.6 cm × 10.0 cm, Amersham Pharmacia Biotech) column and eluted in 250 mM NaCl. To verify enzyme purity, the final DsrAB-containing sample was analyzed by 12% SDS-PAGE gel electrophoresis. DsrC is present in the DsrAB

preparation from *D. vulgaris*, but remains functionally inactive during *in vitro* assays as previously described (Oliveira *et al.*, 2008).

DsrAB from A. fulgidus. *A. fulgidus* VC16 was kindly supplied by Doctor Luís Gafeira at Cell physiology and NMR laboratory coordinated by Professor Helena Santos at ITQB. *A. fulgidus* VC-16 (DSM 4304) was grown in sulfate/thiosulfate-lactate medium in a 300 L fermenter at 83 °C, as previously described (Stetter *et al.*, 1987), with some changes: the yeast extract was 0.05% (w/v), growth temperature was 83 °C, the medium was buffered with 20 mM PIPES sodium salt from sigma and 0.5 mM of sodium sulfide was used as initial reductant. Frozen cells were resuspended in 20 mM potassium phosphate (KPi) buffer pH 7 (buffer A), homogenized and disrupted in a French Press in the presence of DNase. The lysate was centrifuged at 58545 × *g* for 20 min, followed by ultracentrifugation at 100000 × *g* for 2 h. The supernatant was loaded in a Q-Sepharose high performance column (2.6 cm × 10.0 cm, Amersham Pharmacia Biotech) equilibrated with buffer A. DsrAB was eluted at 0.4 M KCl using a stepwise gradient (0-1 M KCl). This fraction was concentrated and desalted by ultrafiltration (10 kDa cutoff, Amicon, Millipore) with subsequent dilution with buffer A. The desalted protein was applied to a Resource-Q column (1.6 cm × 3.0 cm, Amersham Pharmacia Biotech) and eluted at 0.25 M KCl using a stepwise gradient (0-1 M KCl). This fraction was concentrated and desalted by ultrafiltration with buffer A containing 5% (v/v) glycerol. This two-step purification protocol was performed according to (Schiffer *et al.*, 2008). Protein was quantified by the extinction coefficient at 593 nm of 60 $mM^{-1}cm^{-1}$ (Dahl *et al.*, 1993).

DsrAB activity assays

Warburg activity assays. The enzymatic activity of sulfite reduction was initially measured in a Warburg equipment with 50 mM KPi pH 7 at room temperature (with *D. vulgaris* DsrAB) using 1 mM of methyl viologen (Mv) reduced with the *Desulfovibrio gigas* [NiFe] hydrogenase (purified as described (Romão *et al.*, 1997)) as electron donor, in the presence of hydrogen, 430 nM of DsrAB and sodium sulfite (up to 1 mM). The Warburg flasks were equipped with manometers filled with Krebs fluid (428 mM NaBr + 0.465 mM Triton X-100 + 0.512 mM acid fuchsin). The enzymatic assays were stopped by the addition of 2 M of sulfuric acid. The Warburg flasks have two side arms and one main reservoir (where the reaction takes place). The buffer, Mv and hydrogenase are placed in the main reservoir, while the stopping reagent and the sulfite reductase were in each side arm. The flask was capped and the atmosphere was flushed with hydrogen until the Mv was completely reduced (intense blue), after which the system was closed and the initial value at the manometer was annotated. The reaction started by adding the enzyme in the side arm. The activity was measured by the decrease in hydrogen pressure inside the closed system. To calculate the amount (µL) of hydrogen consumed in the Warburg flask the following formulas were used:

$$\mu L_{H_2} = h \times k \qquad (1)$$

$$k = \frac{V_g \times \frac{273}{T} + V_f \times \alpha_{H_2}}{P_0} \quad (\mu L/mm) \quad (2)$$

In equation (1), *h* is the value of the volume of the Krebs fluid in the manometer and k the constant calculated by equation (2), in which V_g is the gas volume of the empty flask and the V_f is the volume of the reaction. The $\alpha_{H2\ at\ 23\ °C}$ = 0,0177 (solubility of hydrogen at 23 °C) an P_0 = 10000

mm (Hg pressure expressed in terms of manometric fluid) were used for our experiments.

Anaerobic chamber assays. Another assay for enzymatic reduction of sulfite, thiosulfate and trithionate was performed inside an anaerobic chamber (95% Ar, 5% H_2) at 60 °C (*A. fulgidus*) or 37 °C (*D. vulgaris*) using reduced methyl viologen (Mv) as electron donor. The assays consisted of 50 mM KPi pH 7, 1 mM methyl viologen previously reduced with zinc granules, 430 nM of DsrAB, sodium sulfite (up to 0.5 mM) and, when added, recombinant DsrC (7.5 to 500 µM, WT or variants). The reaction started by addition of sulfite. Methyl viologen oxidation was monitored at 732 nm (ε=3.15 $mM^{-1}.cm^{-1}$) in a spectrophotometer (Shimadzu UV-1800). In all experiments where DsrC was used, it was previously reduced with 4 mM dithiothreitol (DTT) during 30 min at 37 °C, and the excess reductant was removed with a HiTrap Desalting column (GE Healthcare). Reduced DsrC was concentrated and kept under anaerobic conditions.

Anaerobic vials experiments. All solutions were prepared in an anaerobic chamber in previously boiled water, cooled under oxygen free N_2. *In vitro* reactions were carried out in 10 mL acid-washed, autoclave-sterilized, glass vials sealed with rubber septa. Each vial contained 50% buffer and 50% gaseous headspace. The reaction solution contained 50 mM KPi buffer (pH 7), varying sodium sulfite concentrations, 1 mM methyl viologen, 430 nM of DsrAB from *D. vulgaris* or *A. fulgidus*, and 8.25 nM [NiFe]-hydrogenase (297 U/mg). After removing the capped reaction vials from the chamber, the headspace was exchanged to 100% H_2 to initiate the experiments. Periodically samples were removed for sulfur compound analysis by HPLC.

Cloning, expression and purification of *A. fulgidus* DsrC

The *A. fulgidus* VC16 *dsrC* gene (AF2228) was amplified by PCR using genomic DNA and primers (#1/ #2 in Table 2.2) with EcoRI and HindIII restriction sites, respectively. The digested PCR product was cloned into pPR-IBA-2 (IBA, Germany), which allows insertion of a *Strep*-tag® II at the N-terminus, yielding plasmid IBAAFDsrC. The *dsrC Strep*-tag-encoding region was subcloned into the pET-22b(+) vector (Novagen) using *Nde*I and *Hin*dIII resulting in pET22AFDsrC. Site-directed mutagenesis was performed using the NZYMutagenesis kit (NZYTech) to replace two structural Cys (C77 and C85) for Ala, generating DsrCC77A/C85A (rDsrC2) with #3/#4 primers. The DsrCC77A/C85A/C114A (Cys_AAla variant) and DsrCC77A/C85A/C103A (Cys_BAla variant) variants were constructed using the template vector for DsrCC77A/C85A. DsrC variants were amplified using #5/#6 primers for DsrCC77A/C85A/C114A, and #7/#8 primers for DsrCC77A/C85A/C103A. All cloned vectors were verified by sequencing.

The recombinant plasmids were transformed in *E. coli* BL21 Gold (DE3) cells (Stratagene) containing the pRARE2 vector (for codons rarely used in *E. coli)* and were grown at 37 °C in LB medium supplied with ampicilin (100 µg/mL) and chloramphenicol (30 µg/mL) until an OD_{600} of 0.4. At this stage 500 µM of isopropyl-β-D-thiogalactopyranoside (IPTG) was added and growth was continued for another 3 h. Cells were then collect by centrifugation at 6000 × *g* for 10 min and stored at -20 °C for short periods or -80 °C for long time preservation.

E. coli cells were resuspended in 100 mM TrisHCl pH 8 with 150 mM NaCl (buffer W) and disrupted in a French Press in the presence of

DNase and a protease inhibitor cocktail (Roche Diagnostics). The extract was centrifuged for 20 min at 58545 × *g* and the supernatant was subjected to a heat shock at 70 °C for 10 min followed by centrifugation for 5 min at 58545 × *g* to remove precipitated proteins. The supernatant was loaded into a Strep-Tactin affinity column (IBA) equilibrated with buffer W. DsrC was eluted with buffer W containing 2.5 mM desthiobiotin, and was concentrated and dialyzed to 50 mM potassium phosphate pH 7.

Table. 2.1. List of strains and plasmids used in this study.

Strain or plasmid	Genotype or relevant characteristics	Source or reference
***E. coli* strains**		
***E. coli* α-Select**	F- *deoR endA1 relA1 gyrA96 hsdR*17 (r_{K}^{-} m_{K}^{+}) *supE*44 *thi*-1 Δ(*lacZYA-argFV*169) φ80δ*lacZ*ΔM15 *λ*-	Bioline
E. coli BL21 Gold (DE3)	F- *dcm*+ The *ompT hsdS* (r_{B}^{-} m_{B}^{-}) *gal* λ (DE3) *endA* Tet^{R}	Stratagene
***A. fulgidus* strain**		
DSM 4304	WT *A. fulgidus* VC-16	DSMZ
***D. vulgaris* strain**		
ATCC 29579	WT *D. vulgaris* Hildenborough	ATCC
Plasmids		
pPR-IBA2	*E. coli* expression plasmid; T7 promoter; Amp^{R}	IBA BioTAGnology
IBAAFDsrC	*Eco*RI – *Hin*dIII fragment of PCR-amplified *dsrC* from *A. fulgidus* in pPR-IBA2; intermediate plasmid encoding DsrC with N-terminal *Strep*-Tag II; Amp^{R}	This study
pET22b(+)	*E. coli* expression plasmid; T7 promoter; Amp^{R}	Novagen
pET22-AFDsrC	*Nde*I – *Hin*dIII fragment from IBAAFDsrC in pET22b(+); encoding DsrC with N-terminal *Strep*-Tag II; Amp^{R}	This study
pET22-AFDsrCC77A/C85A	pET22-AFDsrC encoding DsrC with N-terminal *Strep*-tag II and C77A and C85A substitutions; Amp^{R}	This study
pET22-AFDsrCC77A/C85A/C103A	pET22-AFDsrCC77A/C85A encoding DsrC with N-terminal *Strep*-tag II and C77A, C85A and C103A substitutions; Amp^{R}	This study
pET22-AFDsrCC77A/C85A/C114A	pET22-AFDsrCC77A/C85A encoding DsrC with N-terminal *Strep*-tag II and C77A, C85A and C114A substitutions; Amp^{R}	This study

Table. 2.2. List of primers used for plasmids construction.

Primer	Primer sequence (5'→3')
#1 DsrCAF-f	AGGGAATTCCATGCCAGAGTTAGAGG
#2 DsrCAF-r	AATAAGCTTAGACACAGCCAGTTGG
#3 DsrCC77AC85A-f	GTAAAGCACGCGAAGAAAGAGGTCAGGCCAGACGCGAA CCTGCAG
#4 DsrCC77AC85A-r	CTGCAGGTTCGCGTCTGGCCTGACCTCTTTCTTCGCGTG CTTTAC
#5 DsrCC77AC85AC114A-f	CTTCCAAAGCCAACTGGCGCGGTCTAAGCTTGCGGC
#6 DsrCC77AC85AC114A-r	GCCGCAAGCTTAGACCGCGCCAGTTGGCTTTGGAAG
#7 DsrCC77AC85AC103A-f	GCTGCTAGAATTGCTGGTCTTCCAAAG
#8 DsrCC77AC85AC103A-r	CAATTCTAGCAGCGTCCTTTGCAGGTC

Determination of sulfur compounds

Colorimetric detection methods. To quantify sulfite colorimetrically we used the 'Fuschin' assay adapted from Grant (Grant, 1947). Standards of sodium sulfite (Na_2SO_3 anhydrous, analytical grade) were prepared immediately before the assay with deoxygenated water (boiled and degassed with N_2) or KPi buffer (prepared anaerobically). The reaction mixture is composed of 0.04% w/v Pararosaniline-HCl (analytical grade) in 10% H_2SO_4 (analytical grade) v/v, stored in an aluminum-foil wrapped tube or amber-glass bottle at 4°C; and 3.7% formaldehyde prepared fresh each day by diluting 37% (stock) formaldehyde 1:10 water. The reaction was performed on the bench working under N_2 flow, or in an anaerobic chamber. A detailed step-by-step protocol is available in (Leavitt, 2014).

Trithionate and thiosulfate were measured by a modified cyanolysis protocol (Kelly and Wood, 1994; Kelly et al., 1969; Sörbo, 1957). The

method was adapted from the method of Kelly and Wood (Kelly and Wood, 1994) in the following: the reaction volumes were reduced to 10 mL (in volumetric flasks) and with nitric acid as it was used in the original version of this method (Sörbo, 1957). Samples were added to the reaction buffer to fit within the range of ferric thiocyanate standards (prepared from potassium thiocyanate as a simple standard and thiosulfate as a reaction standard) from 5 to 25 µM (final concentration in the 10 mL reaction), as well as 'blanks' prepared from the *in vitro* assay reaction buffer (50 mM potassium phosphate buffer at pH 7). This was typically 400 µL of *in vitro* solution added to the 10 mL cyanolysis reaction, in duplicate per method (2X thiosulfate determinations and 2X trithionate determinations). A detailed step-by-step protocol is available in (Leavitt, 2014).

For sulfide quantifications, we preserved samples in zinc acetate (2% w/v) from each closed system reaction, using a modified Cline (Cline, 1969) method. Analytical grade sodium sulfide (>98.9% Na_2S*9H_2O) was used as the standard, and prepared in deoxygenated (boiled and N_2-sparged) *in vitro* reaction buffer, by precipitating the sulfide with excess zinc acetate (anhydrous), mimicking our sampling protocol. A detailed step-by-step protocol is available in (Leavitt, 2014).

HPLC analysis. Thiol compounds were analyzed by HPLC after derivatization with Monobromobimane (mBbr). mBbr (Life Technologies) was diluted in HPLC ultra-pure acetonitrile to a final concentration of 50 mM. For the derivatization protocol, described in (Fahey & Newton, 1987), 10 µL of sample from the enzymatic reaction were derivatized with two fold excess of mBbr versus the initial concentration of sulfite substrate, in 20 mM HEPES buffer pH 8, in a final volume of 86 µL. The reactions were performed in the dark during 10 min, after which 4 µL of methanosulfonic acid 5 M were added to stop the reaction.

Derivatized sulfur compounds (sulfite, thiosulfate and sulfide) were analyzed by HPLC (Waters Alliance 2695) equipped with a fluorescence detector (Waters 486) with an excitation wavelength of 380 nm and emission wavelength of 480 nm, using a reverse phase ultrasphere C18 column (4.6 mm × 25 cm, 5 µm, Beckman Coulter) at 35 °C. Derivatized samples were diluted with 10 mM methanosulfonic acid. The gradient was performed with 0.25% acetic acid pH 4 in MilliQ water (solvent A) and 100% methanol (solvent B), at 1.20 $mL.min^{-1}$. The elution protocol was the following (% of solvent B): 0 min, 20%; 5 min, 20%; 13 min, 50%; 16 min, 52%; 20 min, 100%; 24 min, 100%; 26 min 20% and 31 min, 20%. The retention times were: 3.44, 5.6 and 15.12 min for sulfite, thiosulfate and sulfide, respectively. Calibration curves were performed with sodium thiosulfate, sodium sulfite and sodium sulfide nonahydrate, using freshly prepared solutions at pH 7.

Trithionate does not react with mBbr and was determined according to Jeffrey and coworkers (Jeffrey & Brunt, 2007), also using HLPC (Waters Alliance 2695) equipped with a UV-visible detector (Waters 2487) at the wavelength of 192 nm using a Dionex IonPac AS16 RIFC column (4 mm × 25 cm) coupled to a Dionex IonPac AG16 RIFC pre-column (4 mm × 5 cm), at 35 °C. An isocratic gradient was performed with 150 mM of sodium perchlorate in MilliQ water at 1 $mL.min^{-1}$. The retention time of sodium trithionate is 5.6 min. The calibration curve was performed with sodium trithionate standard, kindly synthesized by A. Masterson from Professor David Johnston's Laboratory at Harvard University, diluted in the enzymatic reaction mixture.

MalPEG gel-shift assays (GSA)

The MalPEG gel-shift assay was used to monitor the redox state of DsrC cysteines as described (Venceslau *et al.*, 2013). Briefly, at different time points during the enzymatic sulfite reduction assay a sample of reaction mixture corresponding to 5 µg of DsrC were removed and immediately mixed with 1 mM MalPEG (methoxy-polyethylene glycol maleimide, MW 5000 $g.mol^{-1}$, Fluka) for 15 min at 37 °C inside the anaerobic chamber. The reaction was terminated by adding an equal volume of 2xSDS loading buffer (38 mM TrisHCl buffer pH 6.8 with 10% glycerol, 6% SDS, 0.05% bromophenol blue) and the sample was analyzed by 10% Tricine-SDS-PAGE without boiling, under non-reducing conditions, followed by staining with Coomassie Blue.

2.3. Results and discussion

Growth and purifications

There was no previous experience in the lab of growing *A. fulgidus*. Our first approach was to optimize the growth conditions of *A. fulgidus* VC16. When we started growing this organism the maximum optic density at 600 nm (OD_{600}) after 24 h was ~0.300. After several attempts with more thiosulfate, sulfate and both, the growth of *A. fulgidus* was never higher than OD_{600} 0.350. A significant improvement was achieved by the removal of sodium dithionite as a reducing agent and the increase of the PIPES buffer concentration from 8.23 mM to 20 mM, resulting in a maximum OD_{600} after 24 h of ~0.500. With this protocol a 300 L fermenter was performed, with a yield of 0.38 g/L in a total of ~112 g of wet cells of *A. fulgidus*.

The main difference between the two DsrAB (*D. vulgaris* Vs *A. fulgidus*) is the presence/absence of DsrC. In a native gel the DsrAB from *D. vulgaris* always appears in two bands (corresponding to DsrAB bound to one (named Fast form) or two (named slow form) DsrC proteins) (Figure 2.1 A), whereas the DsrAB from *A. fulgidus* displays only one band (Figure 2.1 B) (Dahl *et al.*, 1993, Oliveira *et al.*, 2008). Both proteins were purified with a ratio 280/391 nm of 2.9 for DsrAB from *D. vulgaris* and 2.4 for DsrAB from *A. fulgidus*.

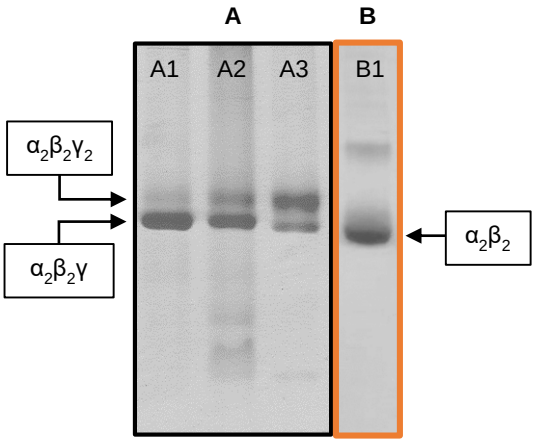

Figure. 2.1. Native polyacrylamide gel of the purification of DsrAB from D. vulgaris (A) and from A. fulgidus (B) using the Q-Sepharose resin, staining with coomassie. A1) fraction of the elution with 300 mM NaCl, A2) fraction of the final part of the elution with 300 mM NaCl, A3) elution with 350 mM NaCl, B1) elution with 250 mM KCl

Activity assays

DsrAB from *D. vulgaris.* The activities for sulfite reduction by DsrAB from *D. vulgaris* were measured with two different methodologies: Warburg method and sulfite consumption analysis by HPLC.

Our first approach was the use of the Warburg equipment. This methodology measures the hydrogen pressure in a closed system. In this system *D. gigas* [NiFe] hydrogenase was used to reduce the Mv, which was used as the artificial electron donor for DsrAB to reduce sulfite. Through the consumption of the hydrogen by the hydrogenase we can indirectly measure the activity of the DsrAB.

In the conditions used for this assays, the Warburg method was shown to have low reproducibility for the analysis of sulfite reduction. A high variation between replicates was observed and could be attributed to several features: gas leaking from the Warburg flasks, differences in

bath temperature over time or differences in the activation of the hydrogenase. Due to these differences in the replicates, we decided to use a different method to evaluate the activity of sulfite reduction by DsrAB from *D. vulgaris.*

The second approach used was the determination of sulfite consumption. In these experiments closed anaerobic vials were used to harbor the reaction for sulfite reductase by DsrAB with Mv as electron donor reduced with Hase, under a H_2 atmosphere. Due to the slow activity of DsrAB alone its kinetic performance of sulfite reduction was analyzed after two hours of activity. At this time 10 µL sample was removed and analyzed by HPLC (Figure 2.2).

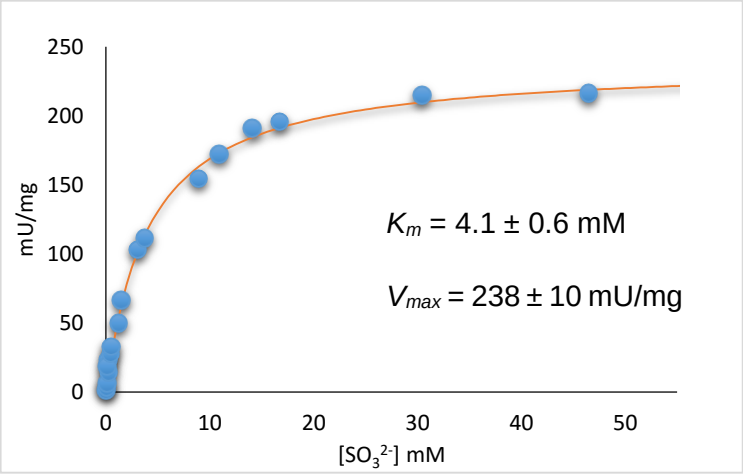

Figure. 2.2. Activity assays with D. vulgaris DsrAB at 37 °C. One unit (U) is defined as the quantity of enzyme that catalyzes the conversion of one µmol of substrate per minute.

With this assay a K_m of 4.1 mM and a V_{max} of 238 mU/mg was determined for *D. vulgaris* DsrAB. This experiment also showed that there was no substrate inhibition of the activity of sulfite reduction by DsrAB of *D. vulgaris* at initial concentrations of sulfite as high as 50 mM.

DsrAB from *A. fulgidus.* The activity measurements for sulfite reduction by DsrAB of *A. fulgidus* were performed in the anaerobic chamber with the UV-visible spectrophotometer and with zinc reduced methyl viologen as the artificial electron donor. These assays were performed at 60 °C, even though the optimal temperature for sulfite reduction of this DsrAB is 80 °C. We did not perform the activity assays at the optimal temperature to avoid overheating of the chamber. To test the activity of DsrAB and to compare it to DsrAB of *D. vulgaris* the Kpi buffer was prepared at pH 7 instead of the optimal pH 6 (Parey *et al.*, 2010).

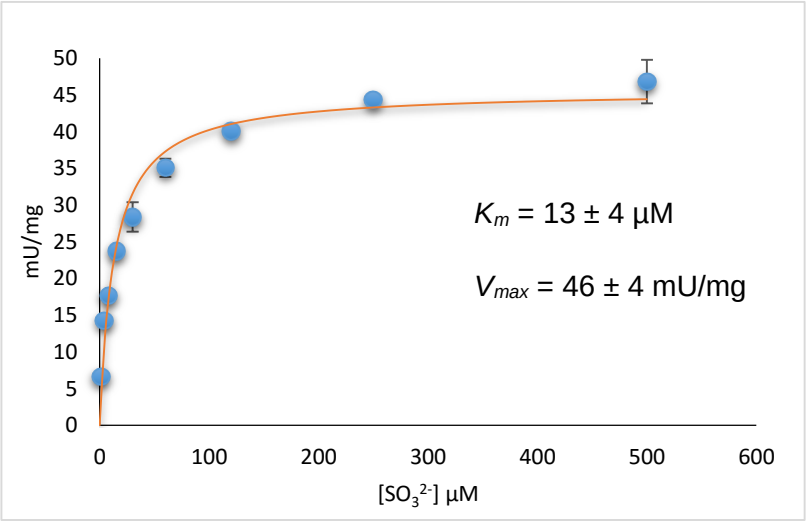

Figure. 2.3. Activity assays with A. fulgidus DsrAB at 60 °C. One unit (U) is defined as the quantity of enzyme that catalyzes the conversion of one µmol of substrate per minute.

These experiments (Figure 2.3) with DsrAB from *A. fulgidus* showed a K_m of 13 µM and a V_{max} of 46 mU/mg (similar to the value reported in (Parey *et al.*, 2010)). We also tested the activity with different substrates (sulfite, thiosulfate and trithionate) with DsrAB in the same conditions (Figure 2.4). In the conditions in which we performed these assays

(pH 7), the same catalytic activity was observed for all three substrates. These results did not agree with the previous work of Parey and coworkers (Parey *et al.*, 2010) that verified that at pH 7 the DsrAB from *A. fulgidus* had a higher activity with thiosulfate than with sulfite or trithionate.

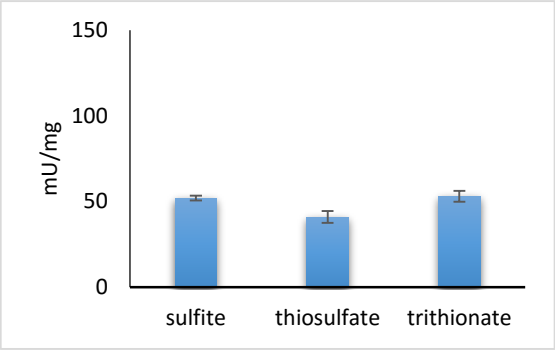

Figure. 2.4. Activity measured for sulfite/thiosulfate/trithionate (500 µM) with DsrAB and methyl viologen as artificial electron donor.

Recombinant DsrC from *A. fulgidus.* DsrC has been an intriguing protein since it was first discovered, associated with DsrAB (Pierik *et al.*, 1992). In 2008, the crystal structure of DsrAB from *D. vulgaris* Hildenborough showed how DsrC interacts with DsrAB. Oliveira and coworkers proposed that DsrC is a partner of DsrAB required for sulfite reduction (Oliveira *et al.*, 2008).

To study the role of DsrC in DsrAB activity (discussed in chapter 3) we produced heterologous recombinant DsrC in *E. coli.* First the *dsrC* gene from *A. fulgidus* was cloned and inserted in pPR-IBA2 vector that inserts a strep-tag II in the N-terminal of the rDsrC, producing the vector IBAAFDsrC. The N-terminal was selected to avoid disturbing the strictly conserved C-terminal that interacts with DsrAB. This vector was transformed in *E. coli* BL21 (DE3) Gold with the pRARE2 vector to

produce the rDsrC protein. However, even after several growth optimizations (temperature, oxygen, and IPTG concentration) we never obtained yields of the rDsrC protein higher than 1 mg/L of culture. As so, a different approach was used, here we removed the *dsrC* gene along with the Strep-tag II from the IBAAFDsrC vector and cloned it in pET22b(+), without the 6-His tag present in this original vector. With this change the pET22-AFDsrC was generated. This vector was transformed in *E. coli* BL21 (DE3) Gold with the pRARE2 vector. As the DsrC protein belongs to an extremophile that grows at 83 °C we used temperature heat shock (70 °C) as the first purification step. This changes led to a 10 fold increase in the rDsrC protein yield.

The analysis of the interaction of DsrAB and rDsrC in the presence of sulfite and methyl viologen (Mv) as the artificial electron donor confirm what has suggested by Oliveira and coworkers, DsrC is indeed a partner of DsrAB increasing the sulfite activity by DsrAB at 60 °C (see chapter 3).

For analysis of the redox state of DsrC upon reaction with DsrAB we used the gel shift assay (GSA), set up by Venceslau et al. (Venceslau 2014). This assay uses the thiol-binding reagent MalPEG to induce a shift in the molecular mass of the protein that corresponds to the number of cysteines labelled.

With the GSA we realized that the two structural cysteines of DsrC would also bind the reagent (MalPEG). To simplify the GSA results we decided to generate a new rDsrC, in which the two structural cysteines (Cys 77 and Cys 85) were substituted by alanines. This new vector, pET22-AFDsrCC77A/C85A, was generated using the pET22-AFDsrC along with the primers #3 and #4. This vector was then transformed in *E. coli* BL21 (DE3) Gold with the pRARE2 vector, which led to the

production of the rDsrC2 protein. The final yield of 15 mg/L of culture was in the same range of rDsrC.

The two cysteines (Cys 77 and Cys 85) were considered structural residues for the stabilization of the protein at high temperature (Mander *et al.*, 2005) (Figure 2.5). For this reason, we decided to do measure the stability of the new rDsrC2 variant, by comparing the temperature melting

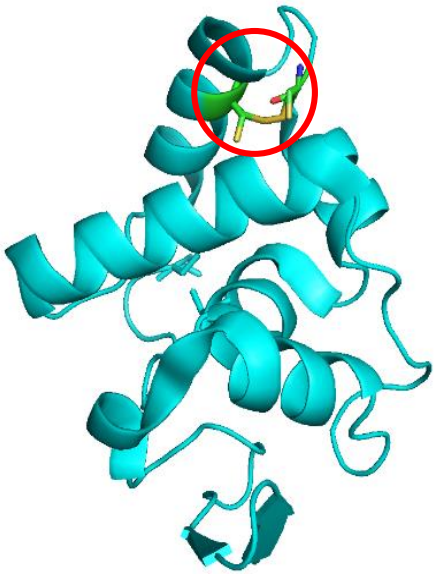

Figure. 2.5. Schematic representation of the DsrC from A. fulgidus. The red circle highlights the two cysteines (77 and 85) bounded by a disulfide bridge (yellow). The Pymol program was used to generate the cartoon (pdb 2A5W)

curve of the two proteins, rDsrC and rDsrC2, by Circular Dichroism. According to this experiment both proteins behaved equally showing that the absence of these cysteines in rDsrC2 did not reduce its stability to high temperature. Moreover, the kinetic behavior of rDsrC2 with DsrAB was similar to that of rDsrC.

Also to test the importance of DsrC in DsrAB sulfite reduction it is essential to understand the role of each cysteine. For this, two variants were generated from the pET22-AFDsrCC77A/C85A: the $Cys_{A}Ala$

(mutation on the Cys 114) variant was generated using the primers #5 and #6, the Cys_BAla (mutation on the Cys 103) variant was generated using the primers #7 and #8. These two variants were also transformed in *E. coli* BL21 (DE3) Gold with the pRARE2 vector and being the total yield similar to rDsrC2.

Substrate and products detection. We first followed substrate (sulfite) consumption and detection of products using colorimetric methods such as Fuchsin (sulfite), Cyanolysis III and II (Thiosulfate and trithionate, respectively) and Cline (sulfide). These methods proved to be time consuming (for a large set of samples) and sample demanding (which required a large volume of enzymatic reaction). As so, HPLC measurement seemed a better option. To do so we optimized two HPLC methods to quantify the products that could be formed during DsrAB sulfite reduction: 1) the derivatization of the free thiols with monobromobimane (mBbr) for sulfite, thiosulfate and sulfide, and 2) a method for the detection of trithionate (without derivatization).

The mBbr method was based on the Fahey method (Fahey & Newton, 1987). We were able to reduce 49 min in the total run, and still accurately detect sulfite, thiosulfate and sulfide (Figure 2.6). This was achieved by increasing the temperature to 35 °C and the pH 4.

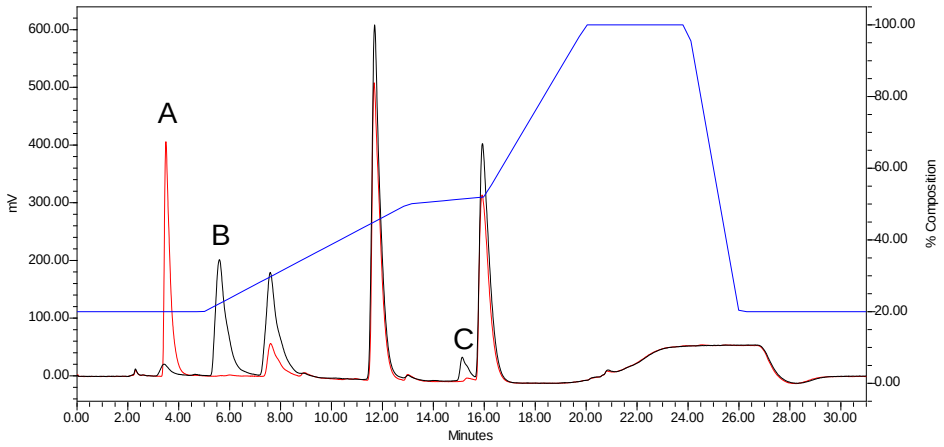

Figure. 2.6. Overlapped HPLC chromatograms of the standards: sulfite (A), thiosulfate (B) and sulfide (C).

The trithionate detection method had to be implemented in our laboratory. The problem behind the detection of trithionate by HPLC using the UV-visible detector was the absorbance of the mobile phase in the 190-200 nm region (Miura & Kawaoi, 2000). The use of sodium perchlorate as a mobile phase and an anion exchange column solved this problem (Jeffrey & Brunt, 2007). According to the trithionate UV-visible spectrum, the best absorbance region to detect this compound is at 192 nm. This method proved to be very good for the quantification of trithionate (Figure 2.7).

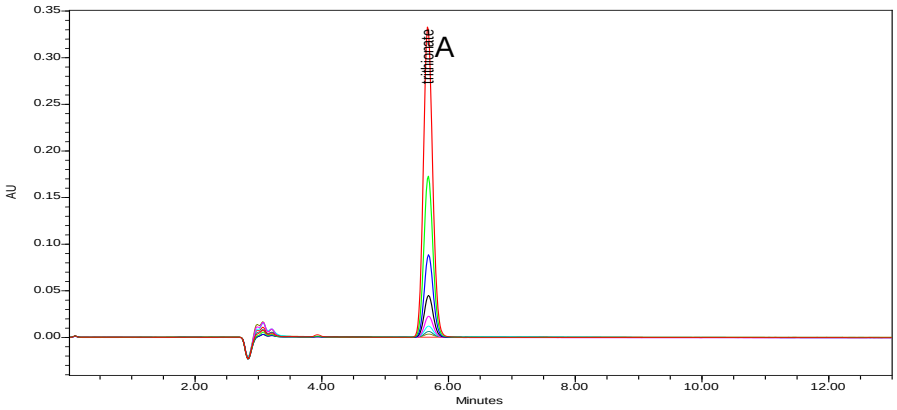

Figure. 2.7. HPLC overlapped chromatograms of the standard trithionate (A).

2.4. Conclusions

This preparatory work was necessary to allow the analysis of sulfite reduction by DsrAB in the presence of its physiological partner, DsrC, described in the next chapter. We were able to purify DsrAB from *A. fulgidus* without the presence of the DsrC protein, contrary to what happens when purifying DsrAB from *D. vulgaris.* Also, the generation of the three recombinant DsrC variants (rDsrC2, Cys_BAla and Cys_AAla) enabled the understanding of the role of each cysteine for the reduction of sulfite by DsrAB (see chapter 3). The implementation of the two HPLC methods contributed for a fast analysis of the substrate and the products as well as to low the detection limit for all the chemical compounds analyzed.

References

Dahl C, Kredich NM, Deutzmann R & Truper HG (1993) Dissimilatory sulphite reductase from Archaeoglobus fulgidus: physico-chemical properties of the enzyme and cloning, sequencing and analysis of the reductase genes. *J Gen Microbiol* **139**: 1817-1828.

Fahey RC & Newton GL (1987) Determination of low-molecular-weight thiols using monobromobimane fluorescent labeling and high-performance liquid-chromatography. *Meth Enzymol* **143**: 85-96.

Fahey RC & Newton GL (1987) Determination of Low-Molecular-Weight Thiols Using Monobromobimane Fluorescent Labeling and High-Performance Liquid-Chromatography. *Methods in Enzymology* **143**: 85-96.

Jeffrey MI & Brunt SD (2007) The quantification of thiosulfate and polythionates in gold leach solutions and on anion exchange resins. *Hydrometallurgy* **89**: 52-60.

Jeffrey MI & Brunt S (2007) Loading and elution of gold thiosulfate from anion exchange resins. *Australas I Min Met* 239-243.

Mander GJ, Weiss MS, Hedderich R, Kahnt J, Ermler U & Warkentin E (2005) X-ray structure of the gamma-subunit of a dissimilatory sulfite reductase: fixed and flexible C-terminal arms. *FEBS Lett* **579**: 4600-4604.

Marritt SJ & Hagen WR (1996) Dissimilatory sulfite reductase revisited - The desulfoviridin molecule does contain 20 iron ions, extensively demetallated sirohaem, and an S=9/2 iron-sulfur cluster. *European Journal of Biochemistry* **238**: 724-727.

Miura Y & Kawaoi A (2000) Determination of thiosulfate, thiocyanate and polythionates in a mixture by ion-pair chromatography with ultraviolet absorbance detection. *Journal of chromatography A* **884**: 81-87.

Müller AL, Kjeldsen KU, Rattei T, Pester M & Loy A (2015) Phylogenetic and environmental diversity of DsrAB-type dissimilatory (bi) sulfite reductases. *Isme J* **9**: 1152-1165.

Oliveira TF, Vonrhein C, Matias PM, Venceslau SS, Pereira IA & Archer M (2008) The crystal structure of Desulfovibrio vulgaris dissimilatory sulfite reductase bound to DsrC provides novel insights into the mechanism of sulfate respiration. *J Biol Chem* **283**: 34141-34149.

Oliveira TF, Vonrhein C, Matias PM, Venceslau SS, Pereira IAC & Archer M (2008) Purification, crystallization and preliminary crystallographic analysis of a dissimilatory DsrAB sulfite reductase in complex with DsrC. *Journal of Structural Biology* **164**: 236-239.

Oliveira TF, Franklin E, Afonso JP, Khan AR, Oldham NJ, Pereira IAC & Archer M (2011) Structural insights into dissimilatory sulfite reductases: structure of desulforubidin from Desulfomicrobium norvegicum. *Frontiers in Microbiology* **2**.

Parey K, Warkentin E, Kroneck PM & Ermler U (2010) Reaction cycle of the dissimilatory sulfite reductase from Archaeoglobus fulgidus. *Biochemistry* **49**: 8912-8921.

Pierik AJ, Duyvis MG, Vanhelvoort J, Wolbert BG & Hagen WR (1992) The 3rd subunit of Desulfoviridintype dissimilatory sulfite reductases. *European Journal of Biochemistry* **205**: 111-115.

Romão CV, Pereira IA, Xavier AV, LeGall J & Teixeira M (1997) Characterization of the [NiFe] hydrogenase from the sulfate reducer Desulfovibrio vulgaris Hildenborough. *Biochem Biophys Res Commun* **240**: 75-79.

Schiffer A, Parey K, Warkentin E, Diederichs K, Huber H, Stetter KO, Kroneck PMH & Ermler U (2008) Structure of the dissimilatory sulfite reductase from the hyperthermophilic archaeon Archaeoglobus fulgidus. *J Mol Biol* **379**: 1063-1074.

Schiffer A, Parey K, Warkentin E, Diederichs K, Huber H, Stetter KO, Kroneck PMH & Ermler U (2008) Structure of the dissimilatory sulfite reductase from the hyperthermophilic archaeon *Archaeoglobus fulgidus*. *J Mol Biol* **379**: 1063-1074.

Stetter KO, Lauerer G, Thomm M & Neuner A (1987) Isolation of extremely thermophilic sulfate reducers: evidence for a novel branch of Archaebacteria. *Science* **236**: 822-824.

Venceslau SS, Cort JR, Baker ES, Chu RK, Robinson EW, Dahl C, Saraiva LM & Pereira IAC (2013) Redox states of *Desulfovibrio vulgaris*

DsrC, a key protein in dissimilatory sulfite reduction. *Biochem Biophy Res Commun* **441**: 732-736.

Wolfe BM, Lui SM & Cowan JA (1994) Desulfoviridin, a Multimeric-Dissimilatory Sulfite Reductase from Desulfovibrio-Vulgaris (Hildenborough) - Purification, Characterization, Kinetics and Epr Studies. *European Journal of Biochemistry* **223**: 79-89.

Chapter 3

A DsrC trisulfide links dissimilatory sulfate reduction to energy conservation

André A. Santos[1†], Sofia S. Venceslau[1†], Fabian Grein[1‡], William D. Leavitt[2§], Christiane Dahl[3], David T. Johnston[2] and Inês A. C. Pereira[1*]

Affiliations:

[1]Instituto de Tecnologia Química e Biológica António Xavier, Universidade Nova de Lisboa, Oeiras, Portugal.

[2]Department of Earth & Planetary Science, Harvard University, Cambridge, MA, USA.

[3]Institut für Mikrobiologie & Biotechnologie, Rheinische Friedrich-Wilhelms-Universität Bonn, Germany

†Authors contributed equally, where André A. Santos produced the recombinant DsrC variants, purified all proteins, performed the kinetic enzymatic assays and sulfur product analyses

[‡]Current address: Institute for Pharmaceutical Microbiology, Rheinische Friedrich-Wilhelms-Universität Bonn, Germany

[§]Current address: Department of Earth & Planetary Sciences, Washington University in St. Louis, MO, USA

Table of contents

One Sentence Summary: The physiological product of sulfite reduction, which governs the global sulfur cycle, is an intramolecular trisulfide in the protein DsrC, the reduction of which is coupled to energy conservation

Abstract

Dissimilatory sulfate reduction is a microbially mediated process that has governed the Earth's biogeochemical sulfur cycle for the last 2 billion years. Marine sulfate is the Earth's largest mobile sulfur reservoir, representing a global sink for electrons. Over geological timescales, microbial sulfate reduction mediates the Earth's net oxidation state. In biogeochemistry, it has been used for decades as a proxy for atmospheric oxygenation, due to its strong signature in sulfur isotope discrimination. Yet the enzymatic mechanisms that generate the isotope effects in sulfate reduction are unknown. The key step in microbial sulfate reduction is the reduction of adenosine 5´-phosphosulfate to sulfite by ApsAB. Its biochemistry has been elusive. Here we show that the product of sulfite reduction by DsrAB is a Cys-S-S-S-Cys trisulfide between two conserved cysteines of the DsrC protein, which we show to be a physiological reaction substrate. Dissimilatory sulfate reduction couples the 4-electron reduction of the DsrC trisulfide to energy conservation.

3.1. Introduction

Sulfur is a versatile element with extremely rich chemistry, and the breadth of its biological forms and mechanisms of action is still being unraveled. On a global scale the sulfur biogeochemical cycle is driven by microbial processes, most importantly marine sulfate (SO_4^{2-}) reduction. Sulfate reduction impacts the redox balance of the planet, over geological timescales, due to the burial of reduced sulfides. The pool of marine sulfate corresponds to an oxidant capacity 10-fold larger than that of atmospheric oxygen (Hayes & Waldbauer, 2006). Microbial sulfate reduction has a strong signature in sulfur isotope discrimination, used to trace sulfur cycling and the Earth's redox environment in both ancient and modern settings (Berner & Canfield, 1989, Canfield, 1998, Farquhar *et al.*, 2010, Halevy *et al.*, 2012). This microbial process has a dissimilatory (respiratory) nature, and is performed by a specific group of organisms (sulfate reducing bacteria and archaea), in contrast to assimilatory sulfate reduction performed by many prokaryotic and eukaryotic organisms.

Both assimilatory and dissimilatory pathways of sulfate reduction (Figure 3.1) involve activation to adenosine 5´-phosphosulfate (APS) and subsequent reduction to sulfite (SO_3^{2-}). The sulfite reductases, responsible for the reduction of sulfite to sulfide in both pathways, have a siroheme coupled to a [4Fe-4S] cluster as catalytic cofactor (Crane & Getzoff, 1996, Simon & Kroneck, 2013). The assimilatory sulfite reductases (aSiRs) are NADH- or ferredoxin-dependent enzymes present in plants, fungi, bacteria and archaea, where they are responsible for the direct reduction of sulfite to sulfide (S^{2-}). This is further converted to cysteine, the precursor of other sulfur-containing

biomolecules. The dissimilatory sulfite reductases (dSiRs) are present in sulfate reducers (Grein *et al.*, 2013), where dSiR operates to reduce sulfite, and in other microorganisms that use sulfur compounds for their energy metabolism. These include phototrophic and chemotrophic sulfur

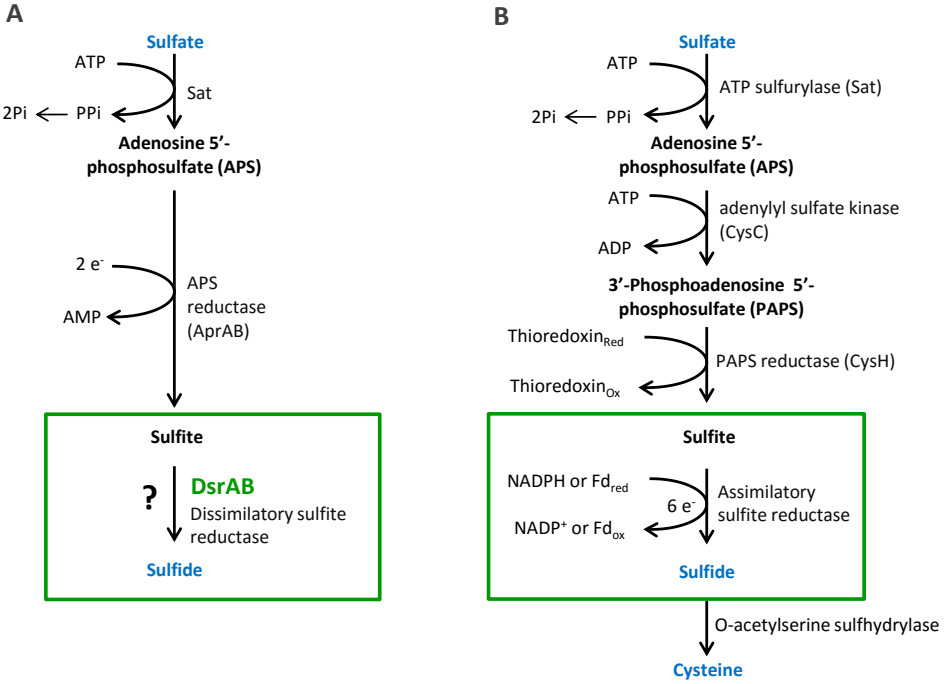

Figure. 3.1. ***Comparison of the dissimilatory and assimilatory sulfate reduction pathways. (A)*** *Dissimilatory pathway used by sulfate reducing bacteria to respire sulfate, with production of sulfide.* ***(B)*** *Assimilatory pathway as operational in E. coli, producing cysteine, the precursor of other sulfur-containing biomolecules. In many bacteria and in plants, sulfite is also generated by direct reduction of APS*

oxidizing bacteria where dSiR presumably operates in reverse (Frigaard & Dahl, 2009), and many microorganisms that can reduce sulfite, thiosulfate ($S_2O_3^{2-}$) and organosulfonates (R-SO_3) or disproportionate sulfur compounds (Simon & Kroneck, 2013, Müller *et al.*, 2015).

The most widespread dSiR is DsrAB, a key enzyme in prokaryotic sulfur metabolism (Grein *et al.*, 2013). DsrAB is closely related to aSiR

and both proteins diverged from a common ancestor that was present in ancient organisms preceding the separation of the Archaea and Bacteria domains (Crane *et al.*, 1995, Wagner *et al.*, 1998). An unrelated heme *c*-containing dSiR was recently described (Hermann *et al.*, 2015), but is present in only a few proteobacteria. Through its operation in sulfate reducers, DsrAB is believed to be a major player in determining sulfur isotope fractionations preserved in geological records and used to reconstruct the redox history of the Earth's surface (Bradley *et al.*, 2011).

Despite their close phylogenetic and structural relationship, a few fundamental differences distinguish DsrAB from aSiR. The latter carries out the direct six-electron reduction of sulfite to sulfide, whereas *in vitro* DsrAB produces a mixture of products ranging from trithionate and thiosulfate to fully reduced sulfide (Lee & Peck, 1971). This observation forms the basis for the long unresolved issue of whether dissimilatory sulfate reduction involves a direct reduction of sulfite to sulfide by DsrAB or whether trithionate and thiosulfate are necessary intermediates (Figure 3.2) (Peck *et al.*, 1982, Brunner & Bernasconi, 2005).

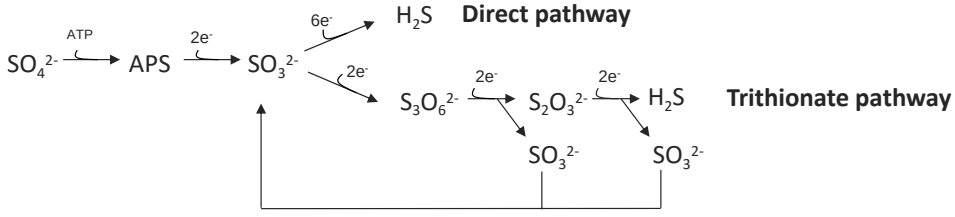

Figure. 3.2. ***The two previously proposed pathways for dissimilatory sulfate reduction.*** *The direct pathway involves the six-electron reduction of sulfite to sulfide by DsrAB. The trithionate pathway invokes the necessary production of trithionate and thiosulfate as intermediates in sequential two-electron reductions, and implies the actions of thiosulfate and trithionate reductases.*

This is a key question that shapes both biochemical and geochemical models of S cycling (Brunner & Bernasconi, 2005, Bradley *et al.*, 2011). Another important difference between DsrAB and aSiR is that while aSiR processes small quantities of sulfite for assimilation, DsrAB must turn over large sulfite pools for respiration. In this light, it is surprising that the *in vitro* catalytic activity of DsrAB is much lower than that of aSiRs (Crane & Getzoff, 1996), hinting at a need for activating proteins. Finally, dissimilatory sulfite reduction must somehow be coupled to chemiosmotic energy transduction in order to conserve the free energy resulting from reduction of sulfite to sulfide ($\Delta G^{o'}$ = -172 kJ/mol for HSO_3^-/HS^- with H_2 as electron donor). Since DsrAB is a soluble protein not associated to the membrane (like aSiR), how energy is conserved during sulfite reduction is a critically important, yet unresolved question.

The crystal structure of DsrAB from the sulfate reducing bacterium *Desulfovibrio vulgaris* provided crucial insight into the process of sulfite reduction by showing the close and likely functional association to DsrC (Oliveira *et al.*, 2008). DsrC is a small protein with a highly conserved C-terminal arm containing two strictly conserved cysteines: the penultimate residue, which we name Cys_A, and another found eleven residues before, which we name Cys_B (Figure 3.3) (Venceslau *et al.*, 2014).

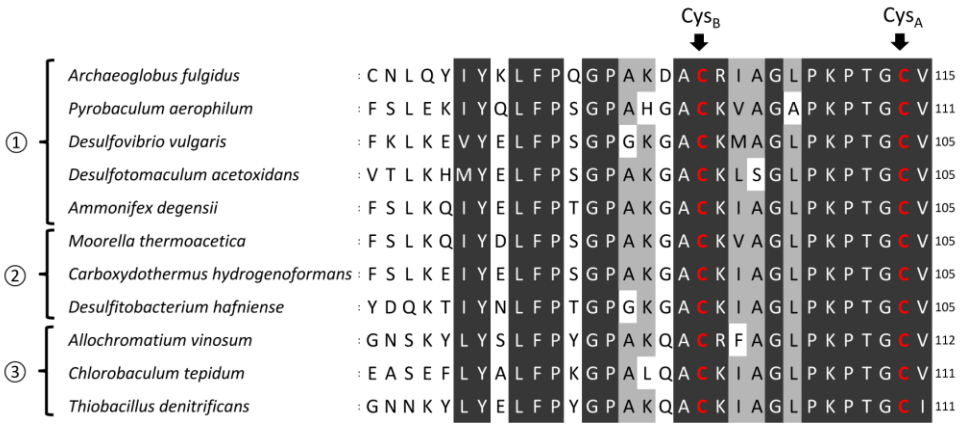

Figure. 3.3. ***Alignment of the DsrC C-terminal arm.*** *DsrC from sulfate reducing organisms (1), organisms that reduce sulfite/thiosulfate (2) and sulfur oxidizing bacteria (3) are included. Strictly conserved residues are in black. The key DsrC Cys$_A$ and Cys$_B$ are highlighted in red.*

In the crystal structure of the *D. vulgaris* DsrAB-DsrC complex, this C-terminal arm inserts into a channel present between DsrA and DsrB such that Cys$_A$ is positioned directly next to the substrate-binding site, suggesting a role in catalysis (Oliveira *et al.*, 2008). A central role of DsrC in dissimilatory sulfite reduction is further supported by the observation that all genomes containing the *dsrAB* genes also encode *dsrC* (Venceslau *et al.*, 2014), with the latter being one of the most highly expressed energy metabolism genes. This is true in both isolated organisms (Haveman *et al.*, 2003, Keller *et al.*, 2014) and in metatranscriptomic studies (Canfield *et al.*, 2010, Stewart *et al.*, 2011). DsrC is also part of a larger family of proteins that include TusE, a sulfur trafficking protein known to perform thiomodification of tRNAs via a persulfide relay system (Ikeuchi *et al.*, 2006), and RspA, thought to have a regulatory role (Venceslau *et al.*, 2014). While the two C-terminal cysteines in DsrC are always conserved, only Cys$_A$ is conserved in TusE and neither Cys is in fact conserved in RspA (Venceslau *et al.*, 2014).

3.2. Materials and Methods

Purification of *A. fulgidus* DsrAB.

The purification protocol is detailed in chapter 2.

Cloning, expression and purification of *A. fulgidus* DsrC

The cloning, expression and purification protocols for the recombinant DsrC from *A. fulgidus* are detailed in chapter 2.

DsrAB activity assays

The protocol for the sulfite activities of DsrAB and rDsrC are detailed in chapter 2. To assess the importance of DsrC Cys on the enzymatic activity of DsrAB, the two cysteines were either alkylated or oxidized to form a disulfide bond. Alkylation was performed by incubating DsrC with 50 mM iodoacetamide (Sigma) in 50 mM ammonium bicarbonate pH 7.8 during 30 min at 55 °C. The intramolecular oxidation of DsrC Cys was obtained by incubation with 1 M L-arginine (Sigma) for 2 h at 30 °C, as standard oxidizing conditions lead to formation of the dimer (Venceslau *et al.*, 2013). Excess of iodoacetamide or arginine was removed by centrifugal gel filtration (Micro Bio-Spin 6, Bio-Rad).

Determination of sulfur compounds by HPLC

The determination of the sulfur compounds by HPLC are detailed in chapter 2.

MalPEG gel-shift assays

The MalPEG gel-shift assays are detailed in chapter 2.

Determination of DsrC thiol content by DTNB

DsrC was subject to DTNB analysis to quantify the number of sulfhydryl groups present before and after the enzymatic assay with DsrAB. A sample of reduced DsrC (0.8 – 3 nmol) used for the enzymatic assay, was incubated in 100 mM potassium phosphate pH 8, 1 mM EDTA, and 200 µM DTNB (Sigma) for 15 min at room temperature. The production of 2-nitro-5-thiobenzoate anion (TNB^{2-}) was quantified by measuring the absorbance at 412 nm using the extinction coefficient of 14150 $M^{-1}cm^{-1}$ (Riddles *et al.*, 1983). To measure the number of DsrC sulfhydryl groups after the enzymatic reaction with DsrAB and sulfite, this was extracted from the reaction mixture using a Strep-Tactin affinity column. After protein concentration, the same protocol as described above was performed.

Mass spectrometry

DsrC wt and variants were analyzed for intact mass and peptide mass fingerprinting by MALDI-TOF-TOF. The proteins were analyzed before addition to the sulfite reductase assay, i.e., in the reduced form, and at the end of the enzymatic assay.

***Intact mass*.** The protein buffer was exchanged to 20 mM ammonium acetate pH 7.2 before analysis using a centrifugal gel filtration column (Micro Bio-Spin 6, Bio-Rad). To quantify the number of reduced cysteines, samples were incubated with 50 mM iodoacetamide

(Sigma) in 50mM ammonium bicarbonate pH 7.8 during 30 min at 55 °C still under anaerobic conditions. After DsrC alkylation the buffer was exchanged to 20 mM ammonium acetate pH 7.2. Samples (0.4 µL) were spotted directly onto the MALDI plate and were mixed in a 1:1 ratio with 10 mg/ml of matrix sinapinic acid dissolved in 50% (v/v) acetonitrile and 5% (v/v) formic acid, and allowed to air dry.

Peptide mass fingerprinting. Samples were first alkylated with iodoacetamide, as the described above, and run in a 10% Tricine-SDS-PAGE under non-reducing conditions. Gel slices containing DsrC were cut and digested with Asp-N (Roche, 20 ng/µl) overnight at 37 °C. This protease was chosen to generate a peptide containing both conserved C-terminal Cys: ^{101}DA**C**RIAGLPKPTG**C**V^{115}, with 1500.8 Da. The digested peptides were desalted and concentrated using a POROS R2 column (Applied Biosystems) and eluted directly onto the MALDI plate using 0.6 µL of 5mg/ml alpha-cyano-4-hydroxycinnamic acid (Sigma) in 50% (v/v) acetonitrile and 5% (v/v) formic acid and air dried.

The data was acquired in linear MS mode using a 4800*plus* MALDI-TOF-TOF (AB Sciex) mass spectrometer and the 4000 Series Explorer Software v.3.5.5 (Applied Biosystems). External calibration was performed using Promix1 and Pepmix1 (Laser BioLabs) for intact mass and peptide mass fingerprinting techniques, respectively. The precursor ions of interest from the MS spectra were selected for MS/MS analysis. MS data was obtained by the Mass Spectrometry Unit (UniMS), ITQB/iBET, Oeiras, Portugal.

Generation of *dsrC* complementation and deletion strains in *D. vulgaris*

To try to generate a deletion mutant for the chromosomal *dsrC* gene, plasmid pMOΔ*dsrC* was created to delete this gene by double homologous recombination in *D. vulgaris* Hildenborough. This plasmid was obtained by sequence ligation independent cloning (SLIC; (Li & Elledge, 2007)) fusing four different fragments that were obtained by PCR amplification. The fragments corresponded to the upstream and downstream regions of the chromosomal *dsrC* (primers #9/ #10 and #11/ #12), the kanamycin resistance gene and pUC origin/ Spec gene (primers #13/ #14 and #15/ #16) from pSC27 (Keller *et al.*, 2011); were then added to the pMO719 background via SLIC. Products from the amplification were inserted into *E. coli* α-select Silver Efficiency (Bioline®) and successful transformants were isolated on LB medium containing spectinomycin (100µg/ml) (Zane *et al.*, 2010). Correct isolates were identified by the expected PCR amplicons from the plasmids constructs and also by sequencing. *D. vulgaris* cells grown either on lactate-sulfate medium or on pyruvate medium (fermentative conditions) were electroporated with pMOΔ*dsrC,* according to (Zane *et al.*, 2010, Keller *et al.*, 2011). Despite numerous attempts, clones could never be obtained from the respective plates containing G418 (a kanamycin analogue to which the *kan* gene also confers resistance (Zane *et al.*, 2010)). Negative and positive controls were done simultaneously to exclude problems with the electroporation itself.

To overcome the inability to create a Δ*dsrC* deletion strain in *D. vulgaris*, a second approach was followed to allow manipulation of the *dsrC* gene by first introducing in the cell a plasmid for expression of *dsrC*,

then allowing the deletion of the chromosomal copy of *dsrC*, using pMOΔ*dsrC*. The pMOIPHisDsrC plasmid was created for the production of His-tagged DsrC. Initially, *dsrC* was amplified from chromosomal DNA of *D. vulgaris* using primers #17 and #18 which fuse a 6xHis-tag to the N-terminus of the protein. The resulting fragment was digested with *NdeI* and *EcoRI* and ligated into pPR-IBA-2 (IBA, Germany) that has been digested with the same restriction enzymes. The *dsrC His*-tag fused fragment was subcloned into pMOIP5 (Ramos *et al.*, 2012), giving rise to pMOIPHisDsrC plasmid, whose expression is under control of the constitutive *aph*II promoter (Zane *et al.*, 2010). The pMOIPHisDsrC plasmid was inserted into *D. vulgaris* by electroporation, originating strain IPFG06. Subsequently, the pMOΔ*dsrC* deletion plasmid was inserted into IPFG06 strain and transformants were selected on pyruvate plates containing geneticin and spectinomycin, resulting in IPFG07 strain. Two additional plasmids encoding DsrC with cysteine to alanine point mutations were created: pMOIPHisDsrCC26A/C93A (Cys_BAla variant; primers #19/ #20 and #21/ #22) and pMOIPHisDsrCC26A/C104A (Cys_AAla variant; primers #19/ #20 and #23/ #24), where Cys26 a non-conserved cysteine was mutated to Ala. Plasmids pMOIPHisDsrCC26A/C93A and pMOIPHisDsrCC26A/C104A were inserted into *D. vulgaris* resulting in IPFG08 and IPFG10 strains, respectively, both containing the chromosomal and plasmid copies of *dsrC*. Subsequently, the pMOΔ*dsrC* deletion plasmid was inserted successfully into IPFG08 originating IPFG09 after selection. However, this procedure was not successful for the IPFG10 strain, despite multiple attempts. The pMOIPHisDsrC-like plasmids were sequenced before and after insertion into *D. vulgaris*. The *dsrC* gene deletion in strains IPFG07 and IPFG09 *versus* WT and IPFG06 were confirmed by PCR using primers #25/#26 and Southern blot.

Growth experiments

D. vulgaris Hildenborough WT and variant strains (IPFG06, IPFG07 and IPFG09) were grown anaerobically at 37 ºC in 100 mL flasks with 50ml of MOY medium (Zane *et al.*, 2010) with lactate-sulfate (30-30 mM). All cultures were inoculated with 2% (v/v) freshly grown cells grown in pyruvate fermentation medium, which consists in MOY medium with pyruvate (60 mM) supplemented with a small amount of sulfate (2 mM). Antibiotics were added as follows: G418 at 400 µg/ml for IPFG07 and IPFG09, and spectinomycin at 100 µg/ml for all variants. For the growth curves only spectinomycin was maintained due to the presence of pMOIPHisDsrC-like plasmids. Growth was monitored by optical density (600 nm) with a spectrophotometer Shimadzu UV-1603. All optical density measurements are the mean of triplicates. The results for maximum OD and doubling times were statistically analyzed with SigmaStat 3.0, using the ANOVA method and pairwise multiple comparison procedures (Holm-Sidak test). The differences obtained between strains for both parameters were statistically significant (p- value ≤ 0.001).

For confirmation that the genotype was maintained, at the end of growth in lactate-sulfate medium cells were collected for DNA extraction (DNA Purification kit, Promega) and PCR was performed using primers #25/#26.

Western blot analysis of DsrC expression

Cells of *D. vulgaris* WT and variants grown in lactate-sulfate were collected at the end of exponential phase, and centrifuged for 12 min at 3000 × *g*. Cells were disrupted using the BugBuster® Protein Extraction Reagent (Novagen) for 20 min at room temperature and centrifuged at 16000 × *g* for 20 min at 4 ºC. Crude extracts (40µg) were resolved on 10% Tricine-SDS-PAGE gels under reducing and denaturing conditions prior to transfer to PVDF membranes (transfer buffer: 48 mM Tris and 39 mM Glycine pH 9.2) using a Mini Trans-Blot® electrophoretic transfer cell (BioRad) during 8 min at 100 V and 350 mA. After blocking in 5% skim milk, the blot was probed with rabbit anti-DsrC from *D. vulgaris* followed by incubation with AP-conjugated anti-rabbit IgG (1:15,000; Sigma), as described in (Venceslau *et al.*, 2013).

3.3. Results and discussion

We report both *in vitro* and *in vivo* studies showing that DsrC is a substrate for DsrAB and that the product of dissimilatory sulfite reduction by DsrAB is a DsrC trisulfide formed between the two conserved Cys of its C-terminal arm. First we tested the effect of DsrC on the activity of sulfite reduction by DsrAB *in vitro*, looking at the oxidation of reduced methyl viologen (Mv) as artificial electron donor (Figure 3.4A).

For these studies we used DsrAB and DsrC from the thermophilic

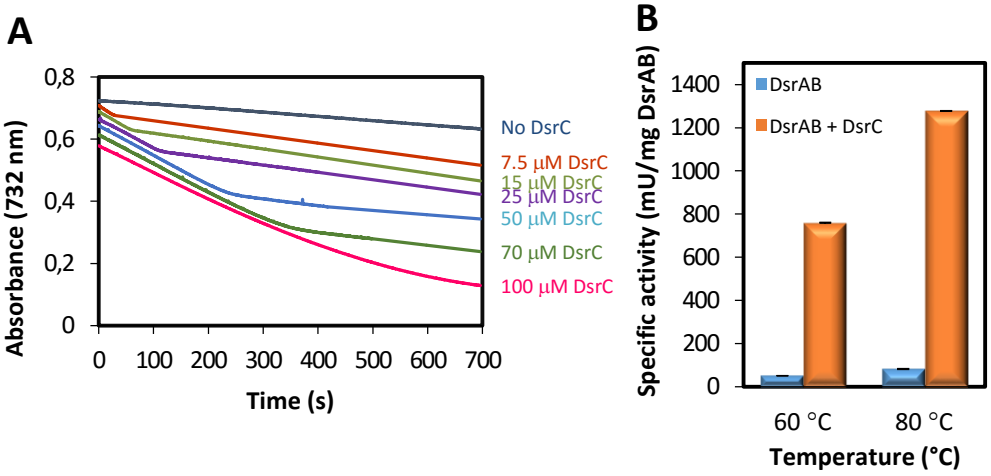

Figure. 3.4. ***Effect of DsrC on sulfite reduction by DsrAB. (A)*** *Sulfite reduction activity of DsrAB in the presence of different DsrC concentrations. Activity is monitored by oxidation of Mv followed at 732 nm. Representative traces are shown.* ***(B)*** *Specific activity of DsrAB in the presence/ absence of DsrC (7.5 µM). Data points are mean ±SD, N=3.*

archaeon *Archaeoglobus fulgidus*, as DsrAB can be isolated from this organism separate from DsrC (Schiffer *et al.*, 2008) (in contrast to *Desulfovibrio* organisms where the two proteins form a tight complex). The presence of reduced DsrC induced an initial fast rate of reaction, which then slows to a rate similar to that in experiments where DsrC is

absent. The duration of the fast phase is directly proportional to the amount of DsrC added (Figure 3.5).

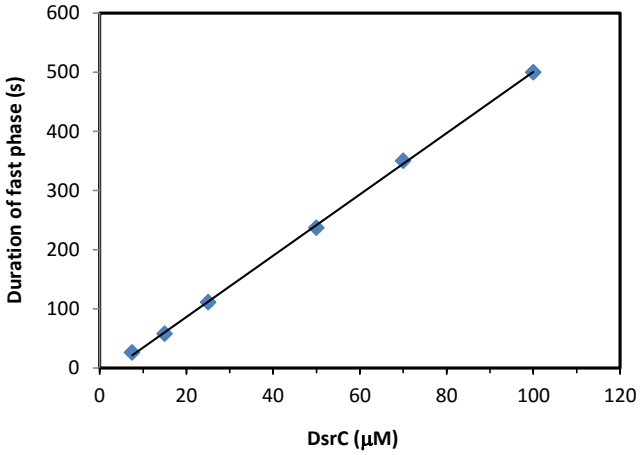

Figure. 3.5. ***Variation of the length of the fast phase of sulfite reduction by DsrAB with DsrC concentration.***

During the fast phase, the sulfite reduction rate is increased by 15-fold over the slow phase at 60 ºC (the temperature routinely used for the assay), and this effect is even more evident at 80 ºC, the optimum temperature for this enzyme (Figure 3.4B). Thus, reduced DsrC induces a strong increase in the specific activity of sulfite reduction by DsrAB, while the K_m for sulfite is not affected (11±4 µM in the absence of DsrC and 12±3 µM in its presence).

When the DsrC cysteines are previously alkylated or when DsrC is added in the oxidized disulfide state (Venceslau *et al.*, 2013), then no effect on the reaction rate of DsrAB is observed. This indicates that the rate increase is strictly dependent on the presence of reduced Cys_A and Cys_B on DsrC. The fact that duration of the fast phase is dependent on the concentration of DsrC (Figure 3.5) suggests that it is being consumed (i.e. oxidized) in the reaction. To further test this we performed a

sequential addition experiment where more DsrC was added after reaching the slow phase (Figure 3.6). Upon each addition of DsrC, another fast reaction phase occurred, where the duration was again

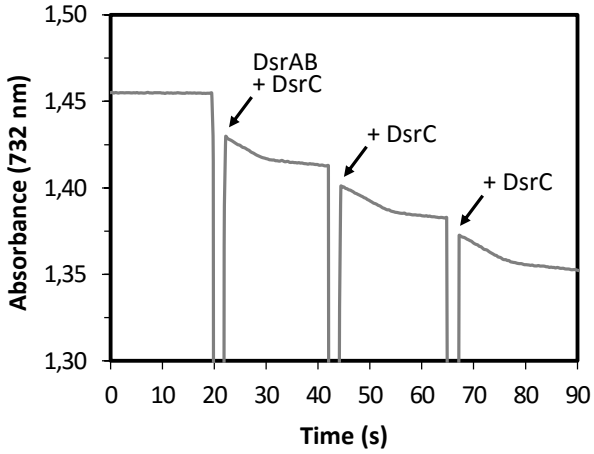

Figure. 3.6. ***Effect of DsrC on sulfite reduction by DsrAB.*** *Sulfite reduction activity by DsrAB upon successive additions of DsrC. The reaction mixture contained reduced Mv and sulfite and at 20 s DsrAB (430 nM) and DsrC (7.5 µM) were added. After reaching the slow phase, two additions of DsrC were performed (at 43 s and 65 s).*

proportional to the amount of DsrC added. This further confirms that the transition to the slow phase is induced by the DsrC-concentration dependence of sulfite reduction kinetics. Tracking sulfite consumption during the fast phase (upon addition of different DsrC concentrations), a clear one to one relationship (Figure 3.7) reveals that DsrC is being used as a substrate by DsrAB. We further quantified how much Mv is oxidized in the fast and slow phases relative to the concentration of sulfite consumed in the same period. This relationship is 1.8±0.3 µmol Mv/µmol SO_3^{2-} in the fast phase and 4.1±1.2 µmol MV/µmol SO_3^{2-} in the slow phase. Since Mv is a one-electron donor, this indicates that two electrons are being used to reduce sulfite in the presence of DsrC. In the absence of DsrC the number of electrons is higher and more variable, which

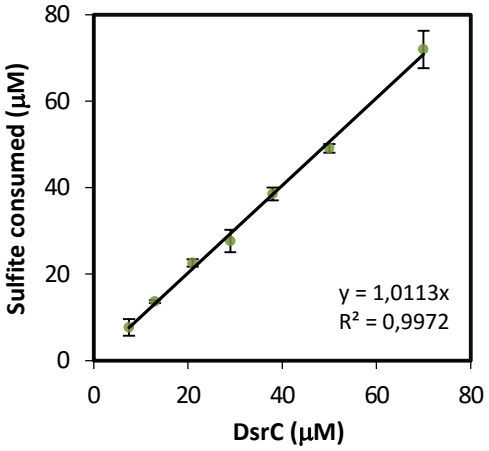

Figure. 3.7. ***Effect of DsrC on sulfite reduction by DsrAB.*** *Sulfite consumed in the fast phase versus the concentration of DsrC present in the assay. A sample of the reaction mixture was taken at the beginning and end of the fast phase for sulfite quantification by HPLC (all data points are mean ± SD, N=3).*

agrees with the reported mixture of products being formed (trithionate, thiosulfate and sulfide), corresponding to different degrees of reduction. DsrAB can also reduce thiosulfate or trithionate (Parey *et al.*, 2010), so we tested if DsrC has an effect on the rate of reduction of these two compounds. No effect was observed (Figure 3.8), suggesting these are not physiological substrates of DsrAB. Taken together, these results

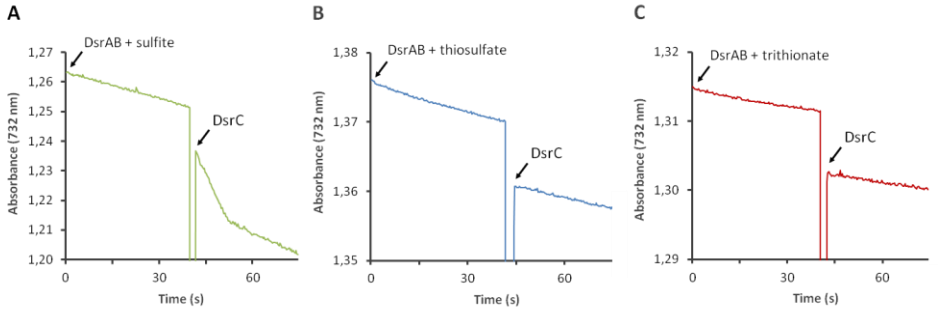

Figure. 3.8. ***Effect of DsrC on the reduction rate of different substrates with DsrAB.*** ***(A)*** *reduction of sulfite;* ***(B)*** *reduction of thiosulfate;* ***(C)*** *reduction of trithionate. Oxidation of MV was monitored at 732 nm using 7.5 µM wild-type DsrC and 250 µM of substrate*

indicate that DsrC is a requisite substrate in physiological sulfite reduction and key to the dissimilatory sulfate/sulfite reduction pathway.

In order to identify the sulfur products formed during sulfite reduction by DsrAB in the absence / presence of DsrC, we tracked sulfide and thiosulfate (as fluorescent bromobimane derivatives) from the reaction mixture across both fast and slow phases. In the absence of DsrC, sulfide and thiosulfate are produced right from the start of the reaction (Figure 3.9A), whereas in the presence of DsrC (50 µM) no sulfur products are detected until the reaction enters the slow phase (Figure 3.9B). Similar results were observed for trithionate in experiments using

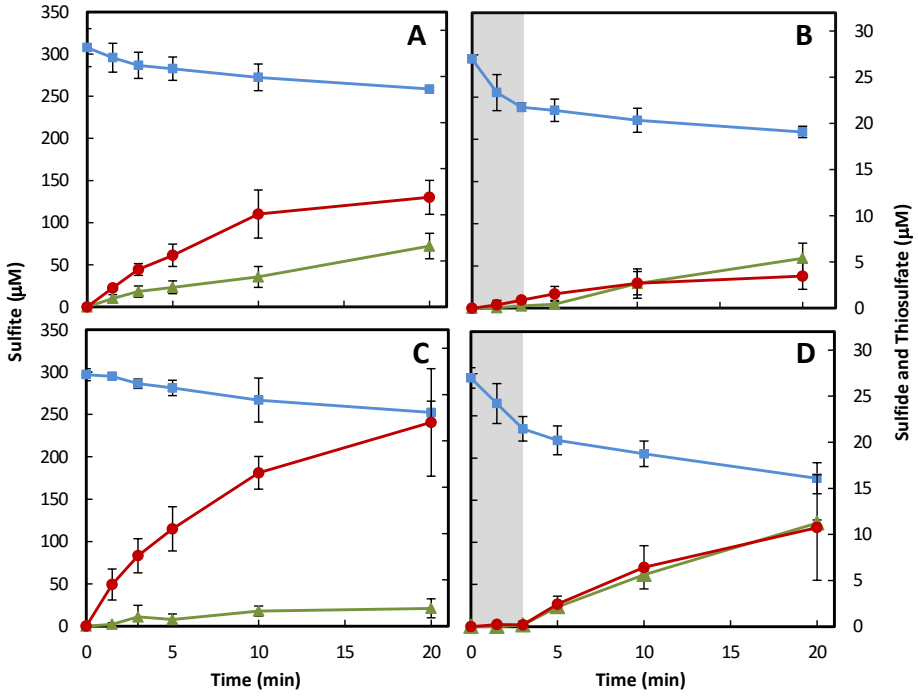

Figure. 3.9 ***Sulfite consumption and thiosulfate and sulfide production by DsrAB.*** *Sulfite, thiosulfate and sulfide were measured by HPLC after mbbr labelling from samples taken at different time points from the enzymatic assays.* ***(A)*** *Assay in the absence of DsrC;* ***(B)*** *Assay in the presence of 50 µM wild-type DsrC;* ***(C)*** *Assay in the presence of 50 µM DsrC Cys_AAla variant;* ***(D)*** *Assay in the presence of 50 µM DsrC Cys_BAla variant. (All data points are mean ±SD, N=3). The grey areas highlight the fast phase in the presence of WT and Cys_BAla DsrC.*

a higher concentration of DsrC (100 µM). In parallel, the redox state of DsrC was analyzed during the fast and slow phases with a gel-shift assay using the cysteine-labelling reagent MalPEG, which increases the mass of the protein by about 10kDa per reduced Cys (Venceslau *et al.*, 2013). Two parallel experiments were carried out with different concentrations of DsrC (50 and 100 µM) (Figure 3.10A). At time zero, DsrC is in a reduced state as revealed by the shift for one (Cys_A) and

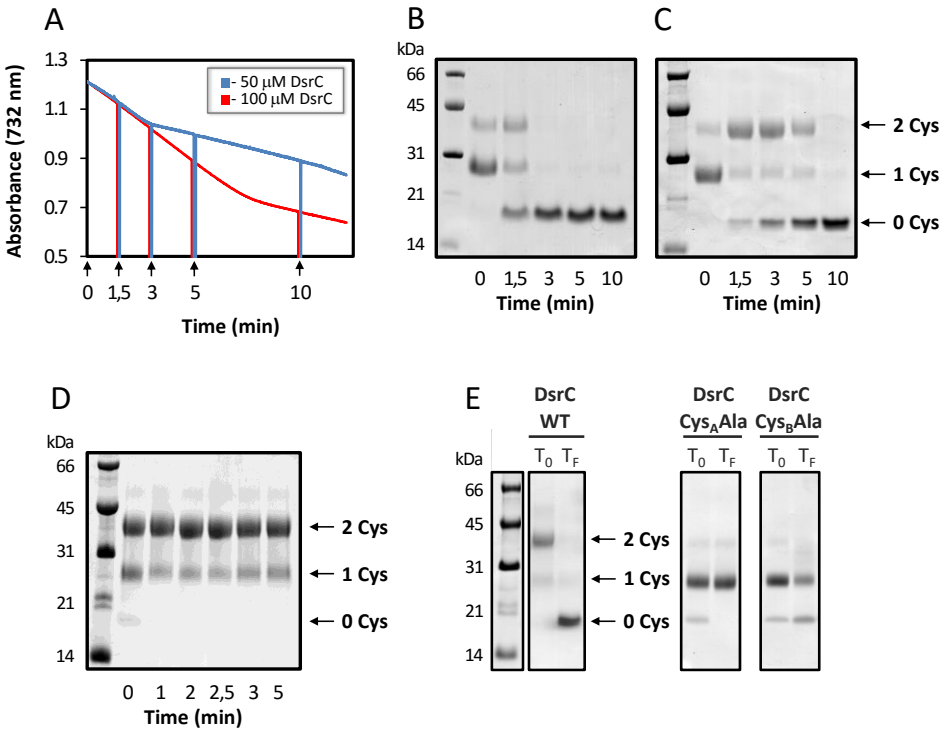

Figure. 3.10. ***Redox state of DsrC upon reaction with DsrAB and sulfite. (A)*** *Kinetic trace of Mv oxidation in two enzymatic assays with different DsrC concentrations: 50 µM (blue) and 100 µM (red). Samples were taken at the time points indicated for analysis of DsrC redox state.* ***(B)*** *Gel shift analysis of MalPEG-labelled DsrC taken from the 50 µM assay at different time points. Shifts for one and two Cys labelled are observed in the reduced state as Cys_A is more accessible for labelling than Cys_B. At the end of the fast phase all DsrC is converted to a form where no Cys is labelled (no shift).* ***(C)*** *Gel shift analysis of MalPEG-labelled DsrC taken from the 100 µM assay at different time points. Complete oxidation of DsrC is observed at 10 min versus 3 min in (B).* ***(D)*** *Gel shift analysis of MalPEG-labelled DsrC taken from a control assay where DsrAB is omitted.* ***(E)*** *Gel shift analysis of MalPEG-labelled DsrC taken from enzymatic assays with wild-type DsrC (WT), Cys_AAla and Cys_BAla variants. Samples were taken after reaching the slow phase.*

two cysteines (Cys_A and Cys_B) labelled, but during the reaction an oxidized form is produced, as evidenced by no observed shift (Figure 3.10B and 3.10C). In both experiments, at the end of the fast phase all DsrC is converted to this oxidized form where the two Cys no longer react with MalPEG. In a control experiment where DsrAB is absent, DsrC remains reduced (Figure 3.10D).

Mass spectrometry analysis of intact DsrC recovered after the end of the fast phase (1530.7 Da), showed a distinct mass increase of 32 Da, relative to the value measured at the start of the experiment (1498.7 Da), indicating that one sulfur atom is bound to DsrC after reaction with DsrAB and sulfite. For increased mass accuracy, we performed peptide mass fingerprinting of DsrC recovered from the reaction, with and without alkylation, focusing on the C-terminal peptide (residues 101 to 115) (Table 3.1 and Figure 3.11). At time zero alkylation with iodoacetamide or DTNB confirmed the presence of two reduced Cys on DsrC (Figure 3.11A and 3.11C). After the fast phase, the mass of the DsrC C-terminal peptide shows a precise mass increase of 32 Da (Figure 3.11B), and no reactivity with the alkylating reagents (Figure 3.11D), indicating that Cys_A and Cys_B are no longer reduced. In control experiments where DsrAB is absent, the C-terminal peptide is not altered (Figure 3.12A and 3.12B), with two free Cys present before and after the incubation (Figure 3.12C and 3.12D). These results allow us to discount our prior model where we predicted a DsrC persulfide as the product of sulfite reduction by DsrAB (Oliveira *et al.*, 2008, Venceslau *et al.*, 2014); this is because a persulfide would react with both the alkylating and gel shift reagents, which is clearly not occurring. Moreover, chemical oxidation of a persulfide product is also highly unlikely under the strictly anaerobic conditions of the experiment. These results reveal the nature of the product of sulfite

reduction by DsrAB/DsrC as a DsrC-bound trisulfide species, where a single sulfur originating from sulfite is bound to the two DsrC cysteines (Cys_A and Cys_B).

Table. 3.1. ***Mass spectrometry data of the DsrC C-terminal peptide.*** *The mass (Da) of the ^{101}DACRIAGLPKPTGCV^{115} peptide was measured from digested DsrC (WT, Cys_AAla and Cys_BAla variants) recovered from the reaction mixture at time zero (T_0) and at the end of the assay (T_F). Before digestion the recovered DsrC was alkylated with iodoacetamide (+IA) or not (-IA). Nº Cys refers to the number of free Cys present in the sample as derived from the mass increase after reaction with iodoacetamide. The mass difference refers to the difference between the C-terminal peptide mass at the end of the assay and at time zero (without alkylation). In the control experiment DsrAB was omitted from the assay mixture.*

	T_0 - IA	T_0 + IA	T_F - IA	T_F + IA	Mass difference
WT DsrC	1498,7	1614,8	1530,7	1530,7	+32
Nº Cys		2		0	
Control	1498,7	1614,8	1498,7	1614,8	0
Nº Cys		2		2	
Cys_AAla DsrC	1468,8	1525,8	1468,8	1525,8	0
Nº Cys		1		1	
Cys_BAla DsrC	1468,8	1525,8	1468,8	1525,8	0
			1500,8		+32
Nº Cys		1		1	

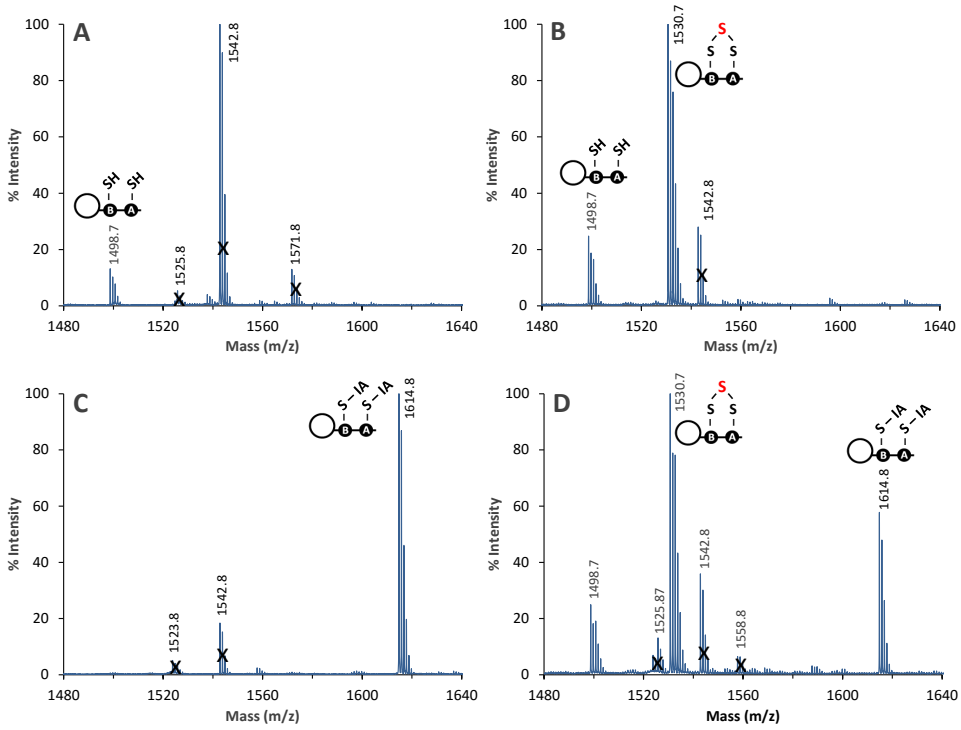

Figure. 3. 11. ***MALDI-TOF spectra of wild-type DsrC peptides before and after reaction with DsrAB and sulfite.*** *The DsrC C-terminal peptide (*^{101}*DA**C**RIAGLPKPTG**C**V*^{115} *with 1498.7 Da) before the reaction (A) shows a mass increase of 32 Da after the enzymatic reaction (B). A small amount of unreacted DsrC is detected. The number of free cysteines in DsrC before* ***(C)*** *and after* ***(D)*** *enzymatic sulfite reduction was assessed by alkylation with iodoacetamide, which adds 57 Da per each reduced cysteine. This shows that the 1530.7 peptide is not alkylated (D). Other peptides of no interest are marked with X*

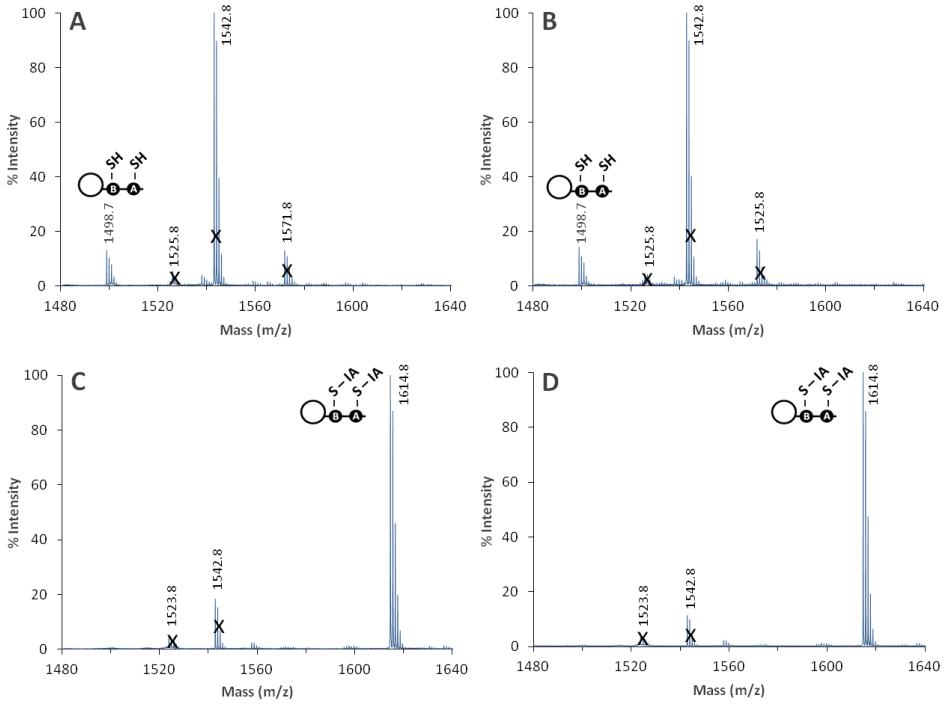

Figure. 3.12. ***MALDI-TOF spectra of wild-type DsrC peptides in a control experiment without DsrAB.*** *The DsrC C-terminal peptide (^{101}DA**C**RIAGLPKPTG**C**V^{115} with 1498.7Da) before the reaction (A), shows no change after a control experiment with sulfite and reduced MV, but no DsrAB (B). The number of free cysteines in DsrC before* ***(C)*** *and after* ***(D)*** *the experiment was assessed by alkylation with iodoacetamide. The C-terminal peptide is not modified in this experiment. Other peptides of no interest are marked with X.*

To further investigate the role of each C-terminal Cys in the reaction mechanism, we produced two DsrC variants lacking each of these residues. The protein lacking Cys_A (Cys_AAla variant) did not increase the rate of DsrAB-catalyzed sulfite reduction, but had a significant effect on the product composition; here sulfide is the major product with negligible production of thiosulfate or trithionate (Figure 3.9C). In contrast, the protein lacking Cys_B (Cys_BAla variant) had a similar effect on DsrAB activity as the wild-type DsrC, both in terms of rate and absence of free sulfur products in the fast phase (Figure 3.9D). In the gel shift assay the

Cys_AAla variant showed a shift corresponding to one free Cys after the reaction (Figure 3.10E). Alkylation also confirmed one free Cys at the start and end of the experiment, and no mass increase was observed either by intact mass or peptide mass fingerprinting (Table 3.1 and Figure 3.13). In the gel shift assay the Cys_BAla variant showed a mixture of two products, one with no shift corresponding to an oxidized form and one with one free Cys (Figure 3.10E). Intact mass analysis of this variant showed a mass increase of 52Da, which is not alkylated, and agrees with a persulfide sulfenate (SOH) derivative of Cys_A. Peptide mass fingerprinting revealed the presence of two products, a major one with no mass increase, and a minor one with additional 32Da (Table 3.1 and Figure 2.14B). Alkylation revealed the presence of one free Cys at the start and end of the experiment (Table 3.1 and Figure 3.14D).

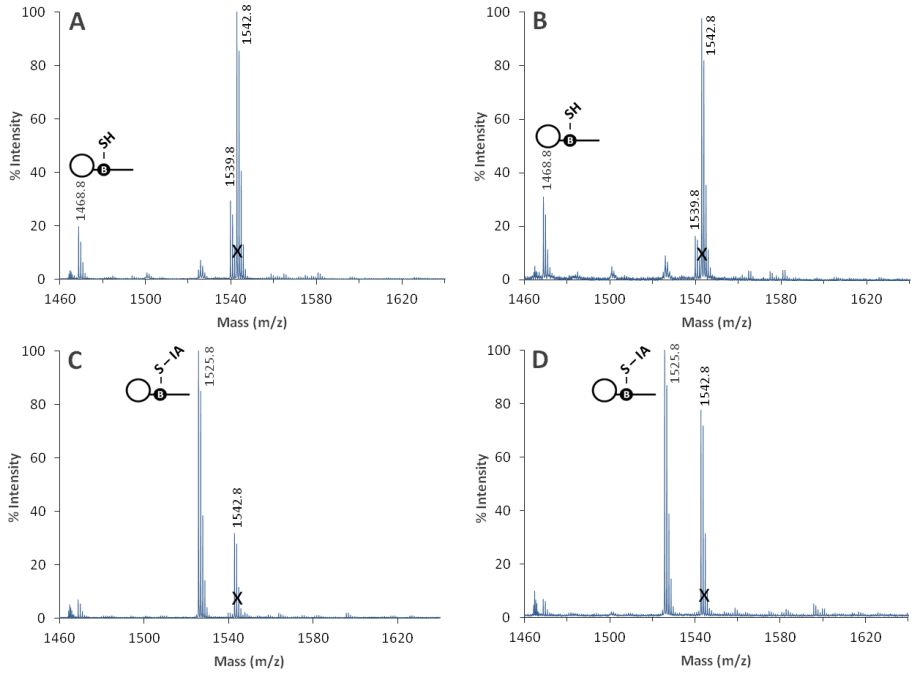

Figure. 3.13. ***MALDI-TOF spectra of DsrC Cys$_A$Ala variant peptides before and after sulfite reduction by DsrAB.*** *The Cys$_A$Ala DsrC C-terminal peptide (^{101}DA**C**RIAGLPKPTG**A**V^{115} with 1468.8Da) (A), is not altered in the enzymatic reaction (B). The number of free cysteines in Cys$_A$Ala DsrC before* ***(C)*** *and after* ***(D)*** *enzymatic sulfite reduction was assessed by alkylation with iodoacetamide. Other peptides of no interest are marked with X.*

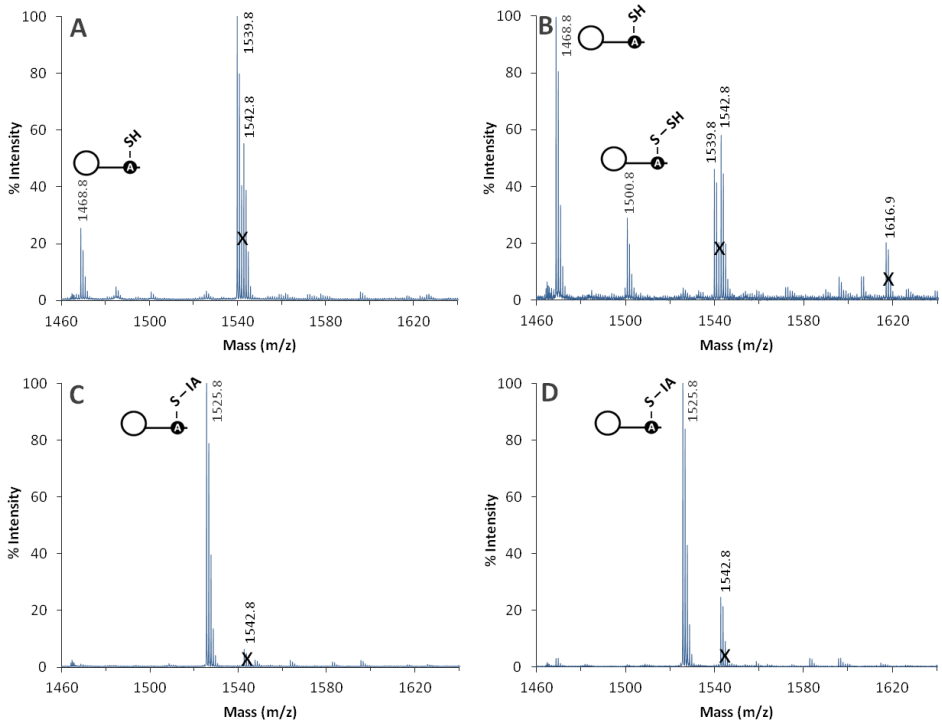

Figure. 3. 14. ***MALDI-TOF spectra of DsrC Cys$_B$Ala variant peptides before and after reaction with DsrAB and sulfite.*** *The Cys$_B$Ala DsrC C-terminal peptide (^{101}DA**A**RIAGLPKPTG**C**V^{115} with 1468.8Da) before the reaction (A) presents two forms after the enzymatic reaction, an unaltered form and a persulfide form (1500.8Da corresponding to a +32Da increase). The number of free cysteines in Cys$_B$Ala DsrC before **(C)** and after **(D)** enzymatic sulfite reduction was assessed by alkylation with iodoacetamide. Other peptides of no interest are marked with X*

Taken together these results suggest a mechanism for the DsrAB/DsrC reduction of sulfite (Figure 3.15). Oxidized DsrAB takes up two electrons from a physiological electron donor reducing the siroheme Fe and its coupled [4Fe-4S] cluster (step 1). Following binding of bisulfite (the most likely substrate at physiological pH), a subsequent two-electron reduction and dehydration takes place to produce an S^{II} intermediate (steps 2 and 3) (Crane *et al.*, 1997, Parey *et al.*, 2010). This

is then reduced by DsrC Cys_A concomitant with release of H_2O to form an S^I intermediate bound to DsrC (step 4). Structural rearrangement of the DsrC C-terminal arm, such that the two Cys come together, then

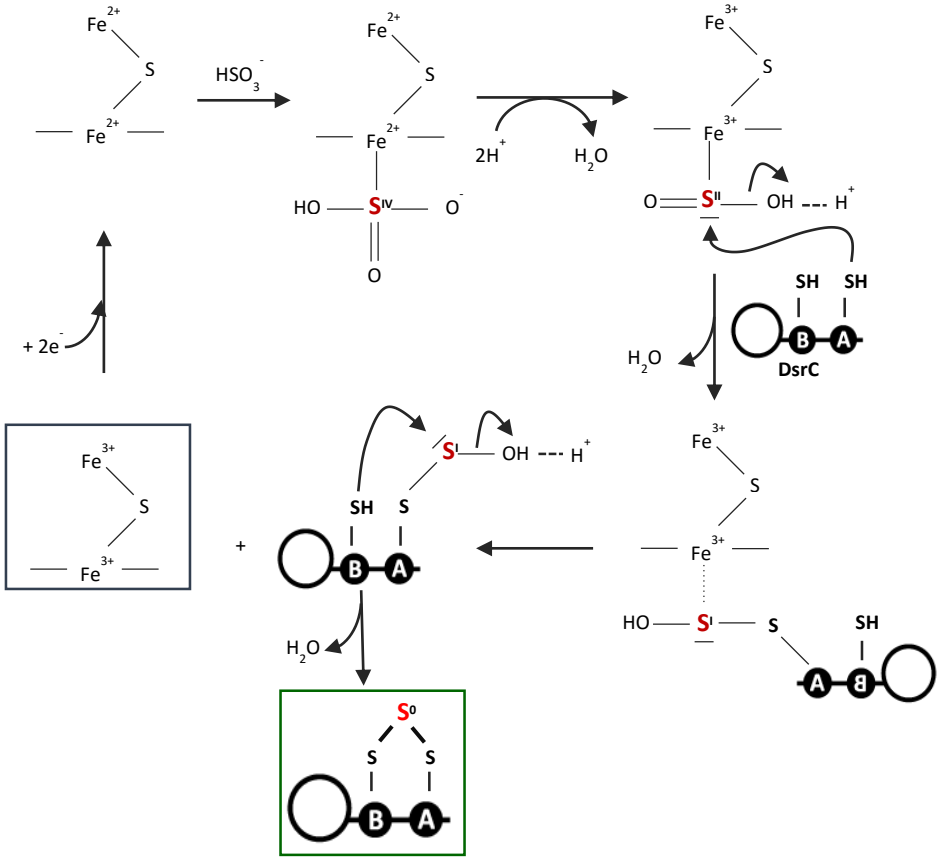

Figure. 3.15. ***Physiological role of DsrC in sulfite reduction by DsrAB. (A)*** *Proposed mechanism for reduction of sulfite by DsrAB with involvement of DsrC. The reaction is assumed to start with the two-electron reduction of the heme and [4Fe-4S] cluster of oxidized DsrAB (in blue) by a redox partner (step 1), followed by binding of bisulfite (step 2). These two steps may occur in the reverse order. A two-electron reduction of the substrate followed by dehydration leads to a S^{II} intermediate (step 3). Reaction of this intermediate with DsrC Cys_A and dehydration leads to the S^I intermediate (step 4). We postulate that this intermediate is released from the heme Fe coordination, and that the DsrC C-terminal arm adopts the retracted conformation where the two Cys are in short distance from each other (step 5). This allows the reaction of Cys_B with the S^I intermediate, leading to production of the trisulfide product (in green, step 6).*

allows internal reduction by DsrC Cys_B, with H_2O release, yielding the S^0 trisulfide product (steps 5 and 6). Our proposed mechanism is supported by the observation that the DsrC C-terminal arm can adopt a retracted conformation while still bound to DsrAB (Hsieh *et al.*, 2010), where the two Cys are in closer proximity to one another, allowing for the attack of Cys_B on the S^I intermediate. Notably, a direct disulfide bond between the two DsrC Cys has never been observed in the crystal structures reporting this retracted conformation of the DsrC C-terminal arm (Mander *et al.*, 2005, Hsieh *et al.*, 2010). Such a disulfide bond is likely sterically hindered, as supported by the difficulty in generating the internal Cys_A-Cys_B disulfide *in vitro*. In oxidizing conditions, a DsrC dimer connected by a Cys_A-Cys_A bond is produced instead (Venceslau *et al.*, 2013).

This novel mechanism clearly explains the results obtained with the DsrC variants. In the absence of DsrC Cys_A, which is the first key Cys to

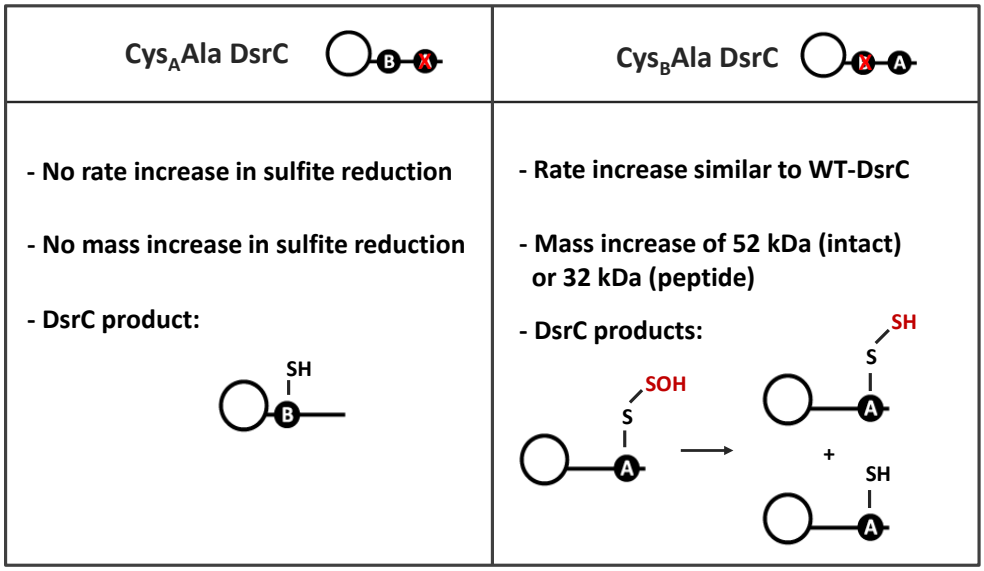

Figure. 3.16. ***Products of sulfite reduction by DsrAB and DsrC variants.*** *The Cys_AAla variant has no effect on sulfite reduction and is not modified. The Cys_BAla variant has a similar effect as WT DsrC, but the products formed are unstable.*

react, there is no effect on the reaction rate and DsrC is not modified (Figure 3.16).

In the absence of Cys_B, the S^I intermediate with a persulfide sulfenate group is produced, which cannot react further and can be released as a product (corresponding to the detected mass increase of 52 Da). This is likely an unstable product and decomposes to a mixture of the persulfurated (+32 Da) and the unmodified protein, as detected by peptide mass fingerprinting and alkylation (Figure 3.14).

The *in vitro* production of thionates ($S_3O_6^{2-}$ and $S_2O_3^{2-}$) by DsrAB in the absence of reduced DsrC, can be explained by further reaction of the partially reduced S^{II} and S^0 intermediates with more sulfite, yielding trithionate and thiosulfate, respectively (Figure 3.17).

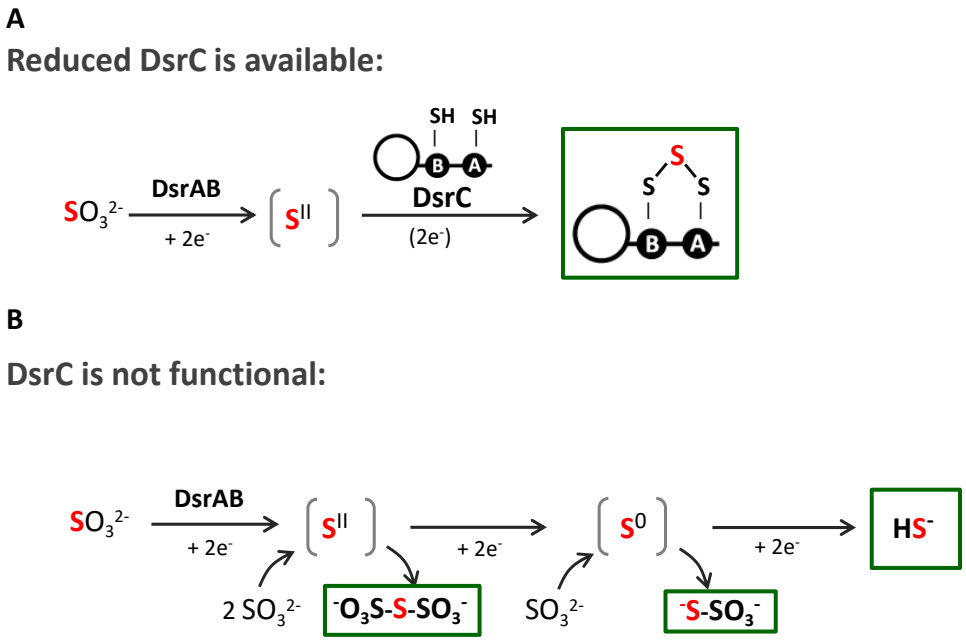

Figure. 3.17. ***Products of DsrAB sulfite reduction in the presence or absence of functional DsrC. (A)*** *If reduced DsrC is available DsrAB receives two electrons from a physiological partner and two other electrons are supplied by DsrC to form the trisulfide product.* ***(B)*** *If DsrC is not functional the S^{II} intermediate can react with additional sulfite to form trithionate, or it can be further reduced to give a S^0 intermediate, which can also react with further sulfite to produce thiosulfate or be reduced further to give sulfide.*

It should be noted that in the absence of DsrC the siroheme active site of DsrAB is directly accessible through a wide channel where the DsrC C-terminal arm usually binds. This channel is distinct from the much narrower substrate access channel, where sulfite must diffuse in when DsrC is docked to DsrAB (Oliveira *et al.*, 2008). This different substrate accessibility in the presence and absence of DsrC explains the product composition observed for the $Cys_{A}Ala$ DsrC variant (Figure 3.9C). With this variant the C-terminal arm inserts into the DsrAB structure blocking the DsrC channel (though not participating in the reaction due to the $Cys_{A}Ala$ mutation), with access of sulfite now occurring exclusively through the narrower substrate channel. This likely restricts or slows down the reaction of additional sulfite with the semi-reduced intermediates, allowing for its complete reduction and the observed production of sulfide as the main product (Figure 3.9C). Therefore, previous reports of thiosulfate and trithionate production as *in vitro* products of DsrAB (Lee & Peck, 1971, Peck *et al.*, 1982) are the result of *in vitro* experimental parameters that do not represent physiological (*in vivo*) conditions – e.g., the absence of reduced DsrC and high concentrations of (bi)sulfite.

To complement these results we did *in vivo* studies on the physiological role of DsrC, using *D. vulgaris*, a model sulfate reducing deltaproteobacterium for which genetic tools are available. Multiple attempts to produce a *dsrC* deletion mutant proved unsuccessful, as also observed by others (J. D. Wall, personal communication), revealing that DsrC is an essential protein in this organism. We took a different approach for genetic studies of *dsrC* in *D. vulgaris* and provided a second copy of the *dsrC* gene *in trans* on a plasmid, resulting in strain IPFG06 (Figure 3.18).

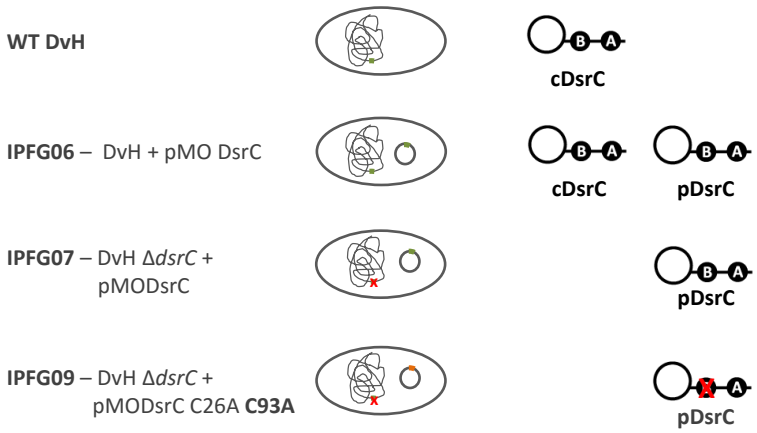

Figure. 3. 18. ***Schematic representation of the different*** **D. vulgaris** ***strains produced.*** *The wild-type* D. vulgaris *(DvH) contains only the chromosomal copy of the* dsrC *gene (cDsrC). IPFG06 contains both the chromosomal and a plasmid copy of* dsrC *(pDsrC). IPFG07 contains only the plasmid-copy of* dsrC*. IPFG09 contains only the plasmid copy of* dsrC*, containing the Cys_BAla mutation and a C26A mutation in one structural cysteine.*

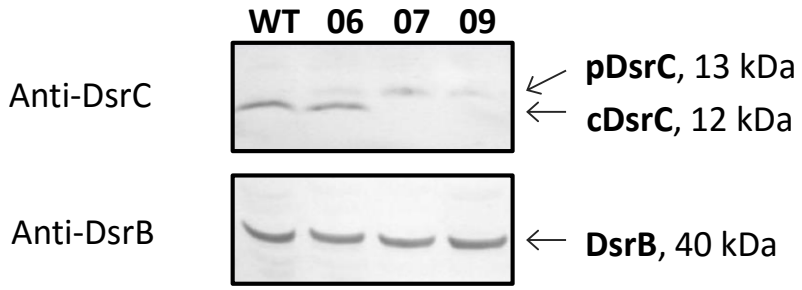

Figure. 3. 19. ***Western blot of DsrC in the different D. vulgaris strains.*** *The plasmid-encoded DsrC (pDsrC) has a higher mass than the chromosome-encoded DsrC (cDsrC) due to the presence of a His-tag. The Western blot for DsrB in the same samples is shown as internal control*

This strain produces native chromosomally encoded DsrC (c-DsrC) plus a minor amount of plasmid encoded DsrC (p-DsrC) (Figure 3.19). The chromosomal *dsrC* gene was deleted in strain IPFG06 to generate strain IPFG07 containing only the plasmid *dsrC* copy transcribed from a weaker promoter (p-DsrC). The same strategy was applied to generate strain IPFG09 where only a plasmid *dsrC* copy encoding a Cys_B to alanine exchange is present (p-Cys_BAla-DsrC). Western blot revealed

reduced levels of DsrC in strains IPFG07 and IPFG09, as expected (Figure 3.19). In the case of DsrC lacking Cys_A we generated the *D. vulgaris* strain with the intact chromosomal copy of *dsrC* and Cys_AAla-

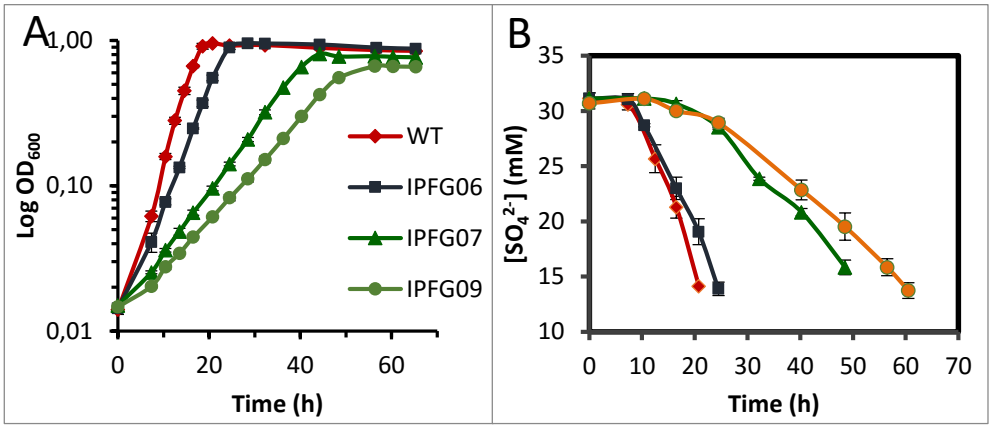

Figure. 3.20. ***(A) Growth profile of* D. vulgaris *wild-type (WT) and IPFG06, IPFG07 and IPFG09 strains on lactate/sulfate medium.*** *The corresponding doubling times and maximal optical density are shown below. Data are mean ±SD, N=3. All differences are statistically significant (*p-*value≤0.001).* ***(B) Sulfate consumption of the different* D. vulgaris *strains.*** *Sulfate measurements were performed from growth experiments in (A) (30mM lactate/30mM sulfate). Data are mean ±SD, N=3.*

dsrC in trans but, despite numerous attempts, it was not possible to delete the chromosomal copy and generate the strain with only Cys_AAla-*dsrC*, even with selection under pyruvate fermentation conditions. This strongly indicates that Cys_A is necessary for functional DsrC, and further, that Cys_A-containing DsrC is necessary for the growth of viable cells. We then compared the growth profiles of strains IPFG06, IPFG07 and IPFG09 during lactate/sulfate respiration to those of the wild-type *D. vulgaris* (Figure 3.20A). Strain IPFG06 showed a small increase in doubling time relative to the wild-type and reached similar cell densities (Figure 3.20A). In contrast, the strain containing only p-DsrC (IPFG07) had a significant increase in doubling time and reached a lower cell density. This effect was even more pronounced for the strain containing p-Cys_BAla-DsrC (IPFG09) (Figure 3.20A). The differences in growth rate

were also reflected in sulfate consumption rates (Figure 3.20B). Overall, these *in vivo* studies showed that DsrC and specifically its Cys_A are essential for sulfate reduction, as well as cell viability. Furthermore, it is clear that Cys_B, though not strictly essential, plays an important role in sulfite reduction. Moreover, the overall expression level of DsrC is a limiting factor in sulfate respiration, as revealed by the reduced growth rate of strain IPFG07.

3.4. Conclusion

Overall, our *in vitro* and *in vivo* results provide evidence that DsrC is an essential protein for sulfite reduction by DsrAB and thus for sulfate/sulfite respiration. DsrC is in fact a substrate for DsrAB and, along with sulfite, is converted to the trisulfide form over the course of the reaction. Protein polysulfides and persulfides have recently emerged as the cellular currency for an activated form of sulfur that is involved in key cellular functions, such as H_2S signaling, biosynthesis of sulfur-containing cofactors, and modulation of enzyme activities and redox homeostasis (Paul & Snyder, 2012, Ida *et al.*, 2014, Toohey & Cooper, 2014). Our data expand the physiological role of these sulfur species by showing that a protein trisulfide is a key metabolite in the dissimilatory sulfate reduction pathway. Protein trisulfides have also been reported in proteins involved in tRNA sulfuration (Liu *et al.*, 2012, Liu *et al.*, 2012), in sulfide:quinone oxidoreductase (Cherney *et al.*, 2012) and in several antibodies (Nielsen *et al.*, 2011). The finding of a trisulfide contrasts with our previous proposal that DsrC persulfide and disulfide forms would be involved in sulfite reduction (Oliveira *et al.*, 2008, Venceslau *et al.*, 2014), but is actually a superior solution, both in chemical and biological terms. Our new mechanism indicates that upon (bi)sulfite reduction by DsrAB only two electrons are taken up by DsrAB from an, as yet unidentified,

physiological electron donor. The other two electrons necessary to produce the trisulfide originate from Cys_A and Cys_B on reduced DsrC. Critically, the DsrC trisulfide will be reduced in a fourth step to produce the final product sulfide and recycle DsrC. This new step in the sulfate reduction pathway is most likely carried out by the membrane DsrMKJOP complex (Figure 3.21), which includes the DsrK subunit whose characteristic EPR signature indicates a [4Fe-4S] cluster known to perform disulfide reductions (Pires *et al.*, 2006, Grein *et al.*, 2013, Venceslau *et al.*, 2014) . DsrK is closely related to the HdrD heterodisulfide reductase of methanogens (Hedderich *et al.*, 2005), and has been shown to interact with DsrC (Grein *et al.*, 2010, Venceslau *et al.*, 2014).

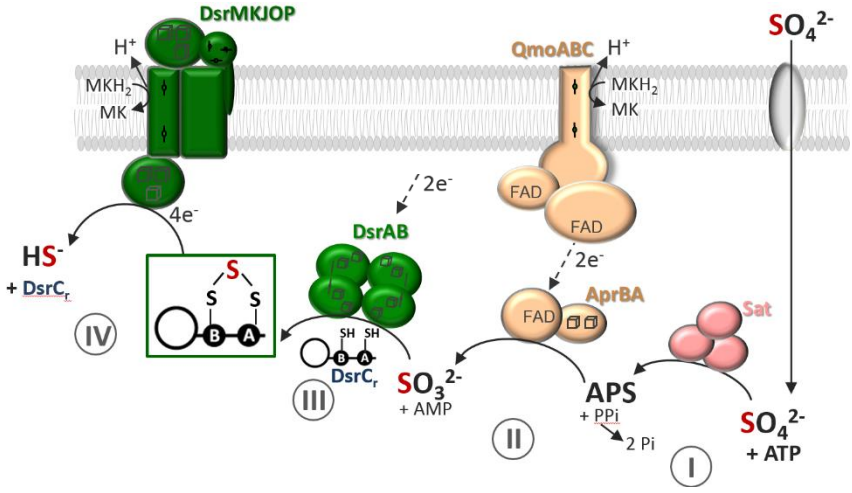

Figure. 3.21. ***Schematic representation of the sulfate respiratory pathway****, involving import of sulfate into the cell, its activation by sulfate adenylyl transferase (Sat) to adenosine 5'-phosphosulfate (APS) (I), reduction of APS to sulfite by the APS reductase (II), reduction of sulfite to the DsrC trisulfide by DsrAB/DsrC (III), and finally reduction of the DsrC trisulfide to sulfide and reduced DsrC by the DsrMKJOP membrane complex (IV).*

The existence of a fourth step in the dissimilatory sulfate reduction pathway has far reaching implications for the bioenergetics of this anaerobic respiratory process. It means that four of the six electrons for (bi)sulfite reduction originate from the reduced menaquinone pool, coupling the generation of a ΔpH across the membrane directly to sulfite reduction and energy conservation. Therefore, the production of a DsrC trisulfide, and subsequent reduction by DsrK, allows for the soluble process at DsrAB to be coupled to energy conservation at the membrane level (DsrMKJOP). These insights into the mechanism of biological sulfate reduction carry significant and unexplored consequences for interpreting reaction rates and isotope effects in sulfur metabolism and improve our understanding of the sulfur cycle, both in modern and in ancient times.

Acknowledgments: We thank R. Soares for the MS measurements, C. Leitão for HPLC technical support and H. Santos and L. Gafeira for providing *Archaeoglobus fulgidus*. We also thank J. Wall for plasmids for genetic manipulation of *D. vulgaris*, A. Ramos for technical assistance, A. Masterson for synthesis of the trithionate standard, A. Bradley for detailed discussions, and W. Martin for critical reading of the manuscript. This work was funded by grants from NSF (1225980) and from FCT, Portugal (UID/Multi/04551/2013, PTDC/QUI-BIQ/100591/2008 and PTDC/BBB-BQB/0684/2012). AS and SSV are recipients of FCT fellowships (SFRH/BD/77940/2011 and SFRH/BPD/79823/2011). WDL acknowledges support by an NSF-GRFP and the Fossett Fellowship from Washington University in St. Louis. The data reported in this paper are provided in the supplementary materials.

References

Berner RA & Canfield DE (1989) A new model for atmospheric oxygen over Phanerozoic time. *Am J Sci* **289**: 333-361.

Bradley AS, Leavitt WD & Johnston DT (2011) Revisiting the dissimilatory sulfate reduction pathway. *Geobiology* **9**: 446-457.

Brunner B & Bernasconi SM (2005) A revised isotope fractionation model for dissimilatory sulfate reduction in sulfate reducing bacteria. *Geochimica Et Cosmochimica Acta* **69**: 4759-4771.

Canfield DE (1998) A new model for Proterozoic ocean chemistry. *Nature* **396**: 450-453.

Canfield DE, Stewart FJ, Thamdrup B, De Brabandere L, Dalsgaard T, Delong EF, Revsbech NP & Ulloa O (2010) A Cryptic Sulfur Cycle in Oxygen-Minimum-Zone Waters off the Chilean Coast. *Science* **330**: 1375-1378.

Cherney MM, Zhang YF, James MNG & Weiner JH (2012) Structure-activity characterization of sulfide:quinone oxidoreductase variants. *Journal of Structural Biology* **178**: 319-328.

Crane BR & Getzoff ED (1996) The relationship between structure and function for the sulfite reductases. *Curr Opin Struc Biol* **6**: 744-756.

Crane BR, Siegel LM & Getzoff ED (1995) Sulfite reductase structure at 1.6 A - Evolution and catalysis for reduction of inorganic anions. *Science* **270**: 59-67.

Crane BR, Siegel LM & Getzoff ED (1997) Probing the catalytic mechanism of sulfite reductase by x-ray crystallography: Structures of the Escherichia coli hemoprotein in complex with substrates, inhibitors, intermediates, and products. *Biochemistry* **36**: 12120-12137.

Fahey RC & Newton GL (1987) Determination of low-molecular-weight thiols using monobromobimane fluorescent labeling and high-performance liquid-chromatography. *Meth Enzymol* **143**: 85-96.

Farquhar J, Wu NP, Canfield DE & Oduro H (2010) Connections between Sulfur Cycle Evolution, Sulfur Isotopes, Sediments, and Base Metal Sulfide Deposits. *Econ Geol* **105**: 509-533.

Frigaard NU & Dahl C (2009) Sulfur metabolism in phototrophic sulfur bacteria. *Advances in Microbial Physiology* **54**: 103-200.

Grein F, Pereira IAC & Dahl C (2010) Biochemical Characterization of Individual Components of the Allochromatium vinosum DsrMKJOP Transmembrane Complex Aids Understanding of Complex Function In Vivo. *J Bacteriol* **192**: 6369-6377.

Grein F, Ramos AR, Venceslau SS & Pereira IA (2013) Unifying concepts in anaerobic respiration: Insights from dissimilatory sulfur metabolism. *Biochimica Et Biophysica Acta-Bioenergetics* **1827**: 145-160.

Grein F, Ramos AR, Venceslau SS & Pereira IA (2013) Unifying concepts in anaerobic respiration: insights from dissimilatory sulfur metabolism. *Biochim Biophys Acta* **1827**: 145-160.

Halevy I, Peters SE & Fischer WW (2012) Sulfate Burial Constraints on the Phanerozoic Sulfur Cycle. *Science* **337**: 331-334.

Haveman SA, Brunelle V, Voordouw JK, Voordouw G, Heidelberg JF & Rabus R (2003) Gene expression analysis of energy metabolism mutants of Desulfovibrio vulgaris Hildenborough indicates an important role for alcohol dehydrogenase. *J Bacteriol* **185**: 4345-4353.

Hayes JM & Waldbauer JR (2006) The carbon cycle and associated redox processes through time. *Philosophical Transactions of the Royal Society B: Biological Sciences* **361**: 931-950.

Hedderich R, Hamann N & Bennati M (2005) Heterodisulfide reductase from methanogenic archaea: a new catalytic role for an iron-sulfur cluster. *Biol Chem* **386**: 961-970.

Hermann B, Kern M, La Pietra L, Simon J & Einsle O (2015) The octahaem MccA is a haem c-copper sulfite reductase. *Nature* **520**: 706-U318.

Hsieh YC, Liu MY, Wang VCC, Chiang YL, Liu EH, Wu WG, Chan SI & Chen CJ (2010) Structural insights into the enzyme catalysis from comparison of three forms of dissimilatory sulphite reductase from Desulfovibrio gigas. *Mol Microbiol* **78**: 1101-1116.

Ida T, Sawa T, Ihara H*, et al.* (2014) Reactive cysteine persulfides and S-polythiolation regulate oxidative stress and redox signaling. *P Natl Acad Sci USA* **111**: 7606-7611.

Ikeuchi Y, Shigi N, Kato J, Nishimura A & Suzuki T (2006) Mechanistic insights into multiple sulfur mediators sulfur relay by involved in thiouridine biosynthesis at tRNA wobble positions. *Mol Cell* **21**: 97-108.

Jeffrey MI & Brunt SD (2007) The quantification of thiosulfate and polythionates in gold leach solutions and on anion exchange resins. *Hydrometallurgy* **89**: 52-60.

Keller KL, Wall JD & Chhabra S (2011) Methods for engineering sulfate reducing bacteria of the genus *Desulfovibrio*. *Meth Enzymol* **497**: 503-517.

Keller KL, Rapp-Giles BJ, Semkiw ES, Porat I, Brown SD & Wall JD (2014) New model for electron flow for sulfate reduction in *Desulfovibrio alaskensis* G20. *Applied and Environmental Microbiology* **80**: 855-868.

Lee JP & Peck HD (1971) Purification of the enzyme reducing bisulfite to trithionate from Desulfovibrio gigas and its identification as desulfoviridin. *Biochemical and Biophysical Research Communications* **45**: 583-589.

Li MZ & Elledge SJ (2007) Harnessing homologous recombination *in vitro* to generate recombinant DNA via SLIC. *Nat Methods* **4**: 251-256.

Liu YC, Zhu X, Nakamura A, Orlando R, Soll D & Whitman WB (2012) Biosynthesis of 4-Thiouridine in tRNA in the Methanogenic Archaeon Methanococcus maripaludis. *Journal of Biological Chemistry* **287**: 36683-36692.

Liu YC, Dos Santos PC, Zhu X, Orlando R, Dean DR, Soll D & Yuan J (2012) Catalytic Mechanism of Sep-tRNA:Cys-tRNA Synthase SULFUR TRANSFER IS MEDIATED BY DISULFIDE AND PERSULFIDE. *Journal of Biological Chemistry* **287**: 5426-5433.

Mander GJ, Weiss MS, Hedderich R, Kahnt J, Ermler U & Warkentin E (2005) X-ray structure of the gamma-subunit of a dissimilatory sulfite reductase: fixed and flexible C-terminal arms. *FEBS Letters* **579**: 4600-4604.

Müller AL, Kjeldsen KU, Rattei T, Pester M & Loy A (2015) Phylogenetic and environmental diversity of DsrAB-type dissimilatory (bi)sulfite reductases. *ISME J* **9**: 1152-1165.

Nielsen RW, Tachibana C, Hansen NE & Winther JR (2011) Trisulfides in Proteins. *Antioxidants & Redox Signaling* **15**: 67-75.

Oliveira TF, Vonrhein C, Matias PM, Venceslau SS, Pereira IAC & Archer M (2008) The crystal structure of *Desulfovibrio vulgaris* dissimilatory sulfite reductase bound to DsrC provides novel insights into the mechanism of sulfate respiration. *The Journal of Biological Chemistry* **283**: 34141-34149.

Parey K, Warkentin E, Kroneck PMH & Ermler U (2010) Reaction cycle of the dissimilatory sulfite reductase from *Archaeoglobus fulgidus*. *Biochemistry* **49**: 8912-8921.

Paul BD & Snyder SH (2012) H2S signalling through protein sulfhydration and beyond. *Nature Reviews Molecular Cell Biology* **13**: 499-507.

Peck HD, Jr., LeGall J & VanBeeumen J (1982) Biochemistry of dissimilatory sulphate reduction. *Philosophical Transactions of the Royal Society B: Biological Sciences* **298**: 443-466.

Pires RH, Venceslau SS, Morais F, Teixeira M, Xavier AV & Pereira IA (2006) Characterization of the Desulfovibrio desulfuricans ATCC 27774 DsrMKJOP complex--a membrane-bound redox complex involved in the sulfate respiratory pathway. *Biochemistry* **45**: 249-262.

Ramos AR, Keller KL, Wall JD & Pereira IAC (2012) The membrane QmoABC complex interacts directly with the dissimilatory adenosine 5 '-phosphosulfate reductase sulfate reducing bacteria. *Front Microbiol* **3**: 137.

Riddles PW, Blakeley RL & Zerner B (1983) Reassessment of Ellman's reagent. *Meth Enzymol* **91**: 49-60.

Schiffer A, Parey K, Warkentin E, Diederichs K, Huber H, Stetter KO, Kroneck PMH & Ermler U (2008) Structure of the dissimilatory sulfite reductase from the hyperthermophilic archaeon *Archaeoglobus fulgidus*. *J Mol Biol* **379**: 1063-1074.

Schiffer A, Parey K, Warkentin E, Diederichs K, Huber H, Stetter KO, Kroneck PM & Ermler U (2008) Structure of the dissimilatory sulfite

reductase from the hyperthermophilic archaeon *Archaeoglobus fulgidus*. *Journal of Molecular Biology* **379**: 1063-1074.

Simon J & Kroneck PMH (2013) Microbial Sulfite Respiration. *Advances in Microbial Physiology* **62**: 45-117.

Stetter KO, Lauerer G, Thomm M & Neuner A (1987) Isolation of extremely thermophilic sulfate reducers: evidence for a novel branch of Archaebacteria. *Science* **236**: 822-824.

Stewart FJ, Dmytrenko O, Delong EF & Cavanaugh CM (2011) Metatranscriptomic analysis of sulfur oxidation genes in the endosymbiont of *Solemya velum*. *Frontiers in Microbiology* **2**: 134.

Toohey JI & Cooper AJL (2014) Thiosulfoxide (Sulfane) Sulfur: New Chemistry and New Regulatory Roles in Biology. *Molecules* **19**: 12789-12813.

Venceslau SS, Stockdreher Y, Dahl C & Pereira IAC (2014) The "bacterial heterodisulfide" DsrC is a key protein in dissimilatory sulfur metabolism. *Biochimica Et Biophysica Acta-Bioenergetics* **1837**: 1148-1164.

Venceslau SS, Cort JR, Baker ES, Chu RK, Robinson EW, Dahl C, Saraiva LM & Pereira IAC (2013) Redox states of *Desulfovibrio vulgaris* DsrC, a key protein in dissimilatory sulfite reduction. *Biochem Biophy Res Commun* **441**: 732-736.

Venceslau SS, Cort JR, Baker ES, Chu RK, Robinson EW, Dahl C, Saraiva LM & Pereira IA (2013) Redox states of *Desulfovibrio vulgaris* DsrC, a key protein in dissimilatory sulfite reduction. *Biochemical and Biophysical Research Communications* **441**: 732-736.

Wagner M, Roger AJ, Flax JL, Brusseau GA & Stahl DA (1998) Phylogeny of dissimilatory sulfite reductases supports an early origin of sulfate respiration. *J Bacteriol* **180**: 2975-2982.

Zane GM, Yen HCB & Wall JD (2010) Effect of the deletion of *qmoABC* and the promoter-distal gene encoding a hypothetical protein on sulfate reduction in *Desulfovibrio vulgaris* Hildenborough. *Appl Environ Microbiol* **76**: 5500-5509.

Chapter 4

Searching for the DsrAB physiological electron donor

Table of contents

4.1. Introduction

We showed in the previous chapter that four of the six electrons needed for sulfite reduction by DsrAB are donated by DsrC, but the physiological partner that donates the first two electrons has still not been identified.

The DsrAB protein contains two ferredoxin like domains per each αβ structure (in DsrB), each one containing an exposed [4Fe-4S] cluster that is suggested to receive electrons from an external donor and transfer them to the catalytic site (Figure 4.1) (Dahl *et al.*, 1993, Karkhoff-schweizer *et al.*, 1995, Oliveira *et al.*, 2008). Based on this information we reasoned that the physiological electron donor to DsrAB should be also a ferredoxin or a ferredoxin-reducing protein.

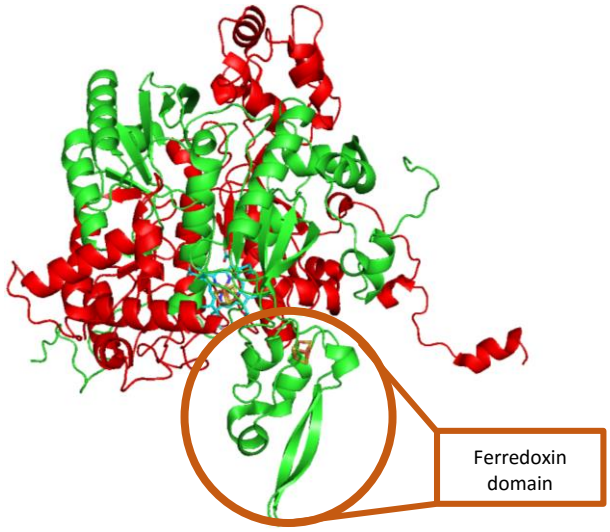

Figure. 4.1. Scheme of α (red) and β (green) subunits with the ferredoxin domain (cluster 2) of the β subunit in evidence by the brown circle. Cartoon designed by Pymol using the pdb 2V4J.

In 1999 Larsen *et* al identified a ferredoxin-like gene immediately upstream of *dsrA* gene in *Desulfotomaculum thermocisternum*. With a multiple alignment of 23 [4Fe-4S]–ferredoxins, they grouped this

ferredoxin from *D. thermocisternum* along with ferredoxin IV of *A fulgidus* and ferredoxin I from *D. vulgaris* (Larsen *et al.*, 1999). After, in 2011 Pereira and coworkers confirmed that all SRP have one or several copies of ferredoxin I, and that in three Gram-positive organisms and *Ammonifex degensii*, the *dsrMK-dsrC* gene cluster is preceded by a ferredoxin gene. Moreover, a ferredoxin gene was also found after de *dsrMKJOP* genes and in close proximity to *dsrAB* in three *Deltaproteobacteria* (Pereira *et al.*, 2011). These observations support the proposal that a ferredoxin is involved in the same metabolic pathway as DsrAB, and can possibly act as its physiological electron donor.

We analyzed the genome of several SPR looking for ferredoxin-reducing enzymes that would be present in all SRP. Three possible candidates were selected: the aldehyde oxidoreductase (AOR), the pyruvate ferredoxin-oxidoreductase (PFOR) and the carbon monoxide dehydrogenase (CODH).

Aldehyde oxidoreductase (AOR). Prokaryotic AORs are either mononuclear molybdenum-containing enzymes binding one pyranopterin from the xanthine oxidase family, or tungsten-containing enzymes that have a bis-pyranopterin cofactor and use ferredoxin as

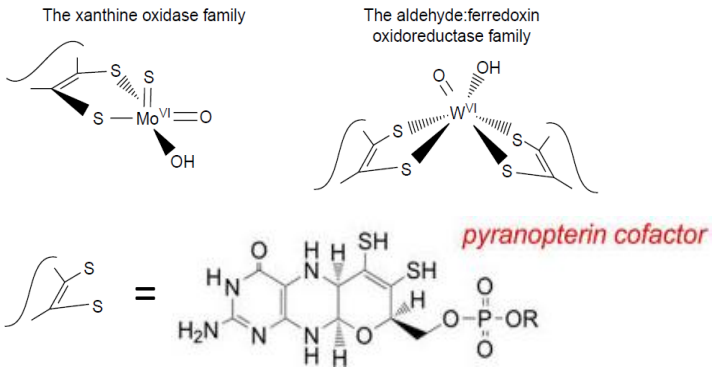

Figure. 4.2. Active-site structures of molybdenum- and tungsten-containing AORs and the structure of the pyranopterin cofactor common to molybdenum- and tungsten-containing AORs (Hille et al., 2014).

electron acceptor (aldehyde:ferredoxin oxidoreductase family) (equation 4.1) (Brondino *et al.*, 2006, Romao, 2009, Hille *et al.*, 2014, Correia *et al.*, 2015).

$$RCHO + H_2O + 2Fd_{ox} \rightarrow RCOOH + 2H^+ + 2Fd_{red} \quad (4.1)$$

All purified tungsten-containing AORs are highly sensitive to oxygen, losing activity immediately after contact with oxygen (Mukund & Adams, 1991, Hensgens *et al.*, 1995, Roy *et al.*, 2001, Rauh *et al.*, 2004, Bevers *et al.*, 2005), while the molybdenum-containing proteins are tolerant to oxygen (Barata *et al.*, 1993, Thapper *et al.*, 2006). Also, the tungsten-containing AORs have an aldehyde activity around one order of magnitude higher than the molybdenum-containing AORs. It was described by Hensgens and coworkers that *D. gigas* probably has both enzymes depending on the metal (Mo or W) used during growth (Hensgens *et al.*, 1994).

Pyruvate ferredoxin-oxidoreductase (PFOR). PFORs have a variable quaternary structure as they are mostly homodimeric but with examples of the heterodimeric form (such as in *Halobacterium* PFOR enzymes (Ragsdale, 2003) or octomeric form (*D. vulgaris* Hildenborough (Garczarek *et al.*, 2007)) . PFORs are thiamine pyrophosphate (TPP)-containing iron-sulfur proteins that catalyze the oxidative decarboxylation of pyruvate with coenzyme-A and with ferredoxin (or flavodoxin) as the electron acceptor (equation 4.2) (Uyeda & Rabinowitz, 1971):

$$C_3H_4O_3 + CoA + Fd_{ox} \rightarrow acetyl\text{-}CoA + Fd_{red} \quad (4.2)$$

Due to its very low redox potential (-540 mV), this reaction plays a crucial role in anaerobic microorganisms, as it can achieve the reduction of ferredoxin or flavodoxin. Even further, in strict anaerobes, PFOR allows for energy conservation by substrate-level phosphorylation through the phosphoroclastic reaction (equation 4.2-4.4) (Ragsdale, 2003).

$$acetyl\text{-}CoA + Pi \rightarrow CoA + acetyl\text{-}phosphate \quad (4.3)$$

$$acetyl\text{-}phosphate + ADP \rightarrow ATP + acetate \quad (4.4)$$

Carbon monoxide dehydrogenase (CODH). CODHs are proteins able to catalyze the (reversible) oxidation of CO with water to CO_2 (equation 4.5) (Jeoung *et al.*, 2014). CODHs proteins can fall into two classes: while in aerobic bacteria CODHs contain a copper and molybdenum active site, anaerobic bacteria and archaea use a nickel and iron-containing CODH (Jeoung *et al.*, 2014).

$$CO + H_2O \rightleftarrows CO_2 + 2H^+ + 2e^- \quad (4.5)$$

CODHs have multiple biological roles where they are associated with different physiological partners. CODHs can be associated with energy conservation as they can be coupled with membrane bound hydrogenases to generate a proton motive force by combining the oxidation of CO with the production of hydrogen (Soboh et al., 2002, Wu et al., 2005). Also, CODHs can be linked to the Wood-Ljungdahl pathway where a Ni,Fe-CODH forms a complex with acetyl-CoA synthase (ACS),

in which CO_2 is reduced to CO at the catalytic center of CODH and used by ACS coupling it with a methyl group to form acetyl-CoA (Ragsdale, 2004). Moreover, CODHs can be associated with oxidative stress response and with the generation of NADPH (Wu *et al.*, 2005).

NADH oxidoreductase. NADH oxidoreductases are able to (reversibly) oxidize NADH with an electron acceptor to NAD^+ and protons (equation 4.7).

$$NADH + e^- acceptor \rightleftarrows NAD^+ + H^+ \quad (4.7)$$

Membrane-bound NADH:quinone oxidoreductases can be divided in three different families: Complex I, Type II NAD(P)H dehydrogenase (NDH-2) and Na^+-translocating NADH:quinone oxidoreductase complex (Na^+-NQR) (Feng *et al.*, 2012). The respiratory Complex I, present in many aerobic organisms, couples the oxidation of NADH to the reduction of quinone or ubiquinone and exports protons to the periplasm creating a proton motive force crucial for the generation of ATP by ATP synthases (Sazanov, 2015). The NDH-2 can be found in prokaryotes, fungi and plants, and can catalyze the two-electron transfer from NAD(P)H to quinones, without the translocation of protons across the membrane (Melo *et al.*, 2004). The third family is the rarest, the Na^+-NQR, present in some bacteria, are able to couple the transport of Na^+ with the transfer of electrons from NADH to quinone/ubiquinone, generating a redox-driven transmembrane electrochemical Na^+ potential (Barquera, 2014, Reyes-Prieto *et al.*, 2014). Na^+-NQR is evolutionary related to Na^+-dependent NADH:ferredoxin oxidoreductase, Rnf complex, present in several anaerobes (Biegel & Muller, 2010),which links the oxidation of

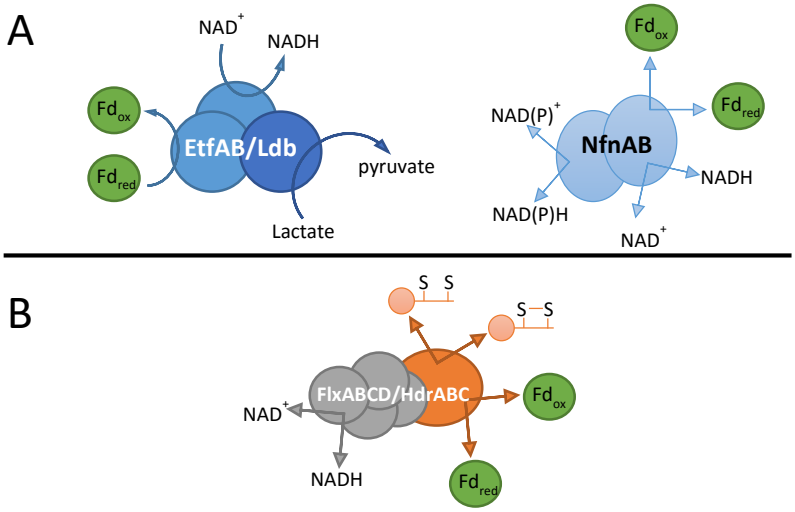

Figure. 4.3. Scheme of the mechanism of: electron bifurcation (A) of EtfAB/Ldb and NfnAB, and electron confurcation (B) of FlxABCD/HdrABC (Rabus et al., 2015)

NADH to the reduction of ferredoxin, importing Na^+/H^+ to the cytoplasm, or the reduction of NAD^+ to the oxidation of ferredoxin to translocate Na^+/H^+ across the cytoplasmic membrane generating a Na^+/H^+ gradient that can be used to produce ATP (Schmehl *et al.*, 1993, Biegel *et al.*, 2011). Other NADH oxidoreductases are also soluble proteins with the ability to interact with different partners. Some of these proteins can be involved in electron bifurcation/confurcation (Figure 4.3) such as: the NADH-dependent reduced ferredoxin:$NADP^+$ oxidoreductase (NfnAB), that uses NADH and reduced ferredoxin as electrons to reduce $NADP^+$ (Wang *et al.*, 2010, Huang *et al.*, 2012); the electron-transferring flavoprotein (EtfAB), which in anaerobic bacteria can, for example, be coupled with lactate dehydrogenase linking the reduction of NAD^+ with the oxidation of ferredoxin to reduce lactate to pyruvate (Weghoff *et al.*, 2015); and the Flavin oxidoreductase (FlxABCD) that was shown to be associated with the heterodisulfide reductase complex (HdrABC) (Pereira *et al.*, 2011) in which the reduction of a disulfide bridge and the reduction of a ferredoxin is linked to the oxidation of NADH (or the

reverse) (Ramos *et al.*, 2015). The NADH oxidoreductases can also be linked to oxygen scavenging mechanisms by rubredoxin:oxygen oxidoreductase (Roo). In this mechanism, the NADH-rubredoxin oxidoreductase oxidizes NADH and reduces rubredoxin, which will reduce Roo (a protein responsible for the reduction of oxygen to water without the formation of hydrogen peroxide (Chen *et al.*, 1993, Santos *et al.*, 1993)).

It is also known that NADH oxidases play an important role in sulfur oxidation and sulfite assimilation. According to Lübbe *et* al. when purifying the "reverse" DsrAB from *A. vinosum* another protein is always co-purified, a NAD^+ reductase – DsrL (Lubbe *et al.*, 2006). Furthermore, a mutant of *A. vinosum* containing a deletion in the *drsL* gene was completely unable to oxidize sulfur globules. This suggested a crucial role of DsrL in the oxidation of sulfur globules. Also, in the case of the aSiR, the electrons for sulfite reduction come from the flavoprotein subunit that has two flavin cofactors and accepts electrons from NADPH (Crane & Getzoff, 1996). These results led us to consider also an NADH oxidase as a possible electron donor for DsrAB for all SRP.

For these studies DsrAB from *D. vulgaris* and *A. fulgidus* were used. It must be noted that the pure fraction of DsrAB from *D. vulgaris* is always a mixture between $\alpha_2\beta_2$, $\alpha_2\beta_2\gamma$ and $\alpha_2\beta_2\gamma_2$. On the other hand, the pure DsrAB fraction from *A. fulgidus* is only $\alpha_2\beta_2$, having no DsrC protein covalently bound to DsrAB.

4.2. Materials and methods

Pyruvate ferredoxin-oxidoreductase (PFOR) from *A. fulgidus*

The cultivation of *A. fulgidus* VC16 (DSM 4304) was carried out as previously described (Stetter *et al.*, 1987) with some changes: the yeast extract was 0.05% (w/v), growth at 83 °C, the flasks were flushed only with argon, the medium was buffered with 20 mM PIPES sodium salt, and 0.5 mM of sodium sulfide was used as initial reductant. The frozen cells were resuspended anaerobically in 20 mM potassium phosphate (Kpi) buffer pH 7 (buffer A) with 10% glycerol and 2 mM dithiothreitol, homogenized and disrupted in a French Press. The lysate was centrifuged at 58545 × *g* for 20 minutes and the supernatant was centrifuged again at 100000 × *g* for 2 hours. The purifications where performed in an anaerobic chamber. The soluble fraction was applied to a Q-Sepharose Fast Flow (2.6 cm × 10.0 cm; Amersham Pharmacia Biotech) equilibrated with buffer A. PFOR was eluted using a stepwise gradient (0-1 M KCl) at 0.25 M KCl. This fraction was desalted by ultrafiltration (cutoff = 10 kDa; Amicon) with subsequent dilution with buffer A. The desalted protein was loaded on a second Q-Sepharose Fast Flow (2.6 cm ×10.0 cm; Amersham Pharmacia Biotech) equilibrated with buffer A and eluted by a stepwise gradient (0-1 M KCl) at 0.25 M KCl. This fraction was desalted by ultrafiltration (cutoff = 10 kDa; Amicon) with subsequent dilution with buffer A. Finally this fraction was loaded on a phenyl-sepharose column (1.6 cm × 10.0 cm; Amersham Pharmacia Biotech) equilibrated with buffer A with 1.1 M of ammonium sulfate (buffer C). The PFOR fraction was eluted at 35% buffer A. The protein was concentrated to 0.7 mg/ml and maintained anaerobic and on

ice during use. The PFOR activity was measured in the anaerobic chamber using a spectrophotometer at 578 nm in a quartz cuvette with stirring. For this, 50 mM of Kpi pH 7 with 0.1 mM of Coenzyme-A, 5 mM of sodium pyruvate, 1 mM Dithiothreitol and 100 µL of sample where used.

Aldehyde ferredoxin-oxidoreductase (AOR) from *D. gigas*

The cultivation of *D. gigas* was carried out as previously described (Barata *et al.*, 1993) with pyruvate and 1 µM molybdenum and absence of tungsten. The frozen cells were re-suspended aerobically in 20 mM TrisHCl buffer pH 7.5 (buffer A), homogenized and disrupted in a French Press. The lysate was centrifuged at 58545 × *g* for 20 minutes and the supernatant was centrifuged again at 100000 × *g* for 2 hours. The soluble fraction was applied to a Q- Sepharose Fast Flow (1.6 cm × 10.0 cm; Amersham Pharmacia Biotech) equilibrated with buffer A. Aor was eluted in a stepwise gradient (0–1.0 M NaCl) at 0.25 M NaCl. This fraction was desalted by ultrafiltration (cutoff = 10 kDa; Amicon) with subsequent dilution with buffer A. The desalted protein was loaded on a Resource-Q 6 mL (Amersham Pharmacia Biotech) equilibrated with buffer A and eluted by a stepwise gradient (0 – 1 M NaCl) at 0.2 M KCl. This fraction was desalted by ultrafiltration (cutoff = 10 kDa; Amicon) with subsequent dilution with buffer A. Protein was concentrated to 13 mg/ml and maintained anaerobic and on ice during use. The purification of Aor was followed by aldehyde oxidase activity. This activity was performed aerobically in a spectrophotometer at 600 nm in a quartz cuvette with stirring. For this, 50 mM of TrisHCl pH 7.5 with 35 µM of DCPIP, 500 µM of acetaldehyde and 2 µL of sample where used.

Carbon monoxide dehydrogenase (CODH) from *D. vulgaris*

This enzyme was kindly given to us by Doctor Sébastien Dementin Principal Investigator at CNRS - Centre National de la Recherche Scientifique. The enzyme was produced and purified by Jessica Hadj-said a PhD student at Doctor Sébastien Dementin laboratory. For the CODH activities measure we used the following protocol: the enzyme was incubated at room temperature for 20 min in 1.5 mL tubes containing 50 µL of 0.44 µM enzyme solution in 0.1 M TrisHCl pH 8 in the presence of 2.4 mM of Ni + 1.2 mM of sodium dithionite. The CO oxidation activity assays were performed in a glove box (under N_2 atmosphere) using a spectrophotometer. CO oxidation was assayed at 37 °C by monitoring the reduction of methyl viologen (Mv) at 732 nm (ε = 3.15 $mM^{-1}.cm^{-1}$) in a quartz cuvette of 1 cm of optical length. The reaction was initiated by injecting 10 µL of pre-incubated enzyme in a stirred 1 mL solution containing 0.1 M TrisHCl pH 10, 2.4 mM of Mv and 25 µM of CO (25 µL of a CO-saturated solution injected just before enzyme addition) (Hadj-Said *et al.*, 2015). This enzyme was always kept on ice inside an anaerobic flask next to a paper soaked in a sodium dithionite solution due to its immediate inactivation by oxygen.

Recombinant NADH oxidase (rNoxA-3) from *A. fulgidus*

The *A. fulgidus* VC16 *noxA-3* gene (AF0400) was amplified by PCR using genomic DNA and the following olinucleotides: 5'- ACC CCC ATA TGA ACG TTG TTG TAA TCG G -3' and 5'- TTA CTC GAG TCA AAA CCA GAA GGC CAT TC -3' with NdeI and XhoI restriction sites, respectively. The PCR product was cloned into pET22b(+) vector (Novagen), in which the native codon stop was maintained to remove the

strep tag. The recombinant plasmids were transformed in *E. coli* BL21 Gold (DE3) cells (Stratagene) containing the pRARE2 vector (for contains codons rarely used in *E. coli)* and the cells were grown at 37°C in LB medium (Roth Diagnostics) along with 6.3 µM Riboflavin, with ampicilin (100 µg/mL) and chloramphenicol (30 µg/mL) until an OD_{600} of 0.4. At this stage 500 µM of isopropyl-b-D-thiogalactopyranoside (IPTG) was added and growth was continued for another 3h. Cells were then collect by centrifugation at 6000 × *g* for 10 minutes and stored at -20 °C for short periods or -80 °C for long time preservation. Cells were re-suspended in 20 mM Kpi pH 7 (buffer A) and disrupted in a French Press in the presence of a protease inhibitor cocktail (Complete by Roche Diagnostics). The extract was centrifuged for 20 min at 58545 × *g*, followed by a protein precipitation step at 70 °C and centrifugation for 5 min at 58545 × *g*. The soluble fraction was filtered and loaded on a Resource-Q 6 mL (Amersham Pharmacia Biotech) equilibrated with buffer A and eluted by a stepwise gradient (0-1 M KCl) at 0.350 M KCl. This fraction was desalted by ultrafiltration (cutoff = 10 kDa; Amicon) with subsequent dilution with buffer A. The protein was concentrated to 33 mg/ml and maintained anaerobic and on ice during use. The rNoxA- 3 activity was followed by NADH oxidation. This activity was performed aerobically in a spectrophotometer at 340 nm in a quartz cuvette with stirring. For this, 50 mM of Kpi pH 7 with 100 µM of NADH, 5 µM of FAD and 2 µM of sample were used and the oxidation of NADH was monitored at 340 nm or at 600 nm, when DCPIP (80 µM) was used as the artificial electron acceptor.

Electron transfer assays and HPLC data analysis

The reactions of DsrAB with the possible electron donors were performed in an anaerobic chamber using 0.5 mL tubes at 37 °C for DsrAB from *D. vulgaris* and 60 °C for DsrAB from *A. fulgidus*. All activities were performed according to the electron donor reactions in the presence of DsrAB (0.430 µM) and sulfite (0.5 mM for DsrAB from *A. fulgidus* and 2.5 mM for DsrAB of *D. vulgaris*) as the electron acceptors. The decrease of sulfite was monitored by HPLC after derivatization with monobromobimane (mBbr). The mBbr stock was diluted in HPLC ultra-pure acetonitrile to a final concentration of 50 mM. For the derivatization protocol, at each desired time 10 µL of sample was derivatized with a twofold excess of mbbr versus the initial concentration of sulfite, in HEPES buffer 20 mM pH 8, in a final volume of 86 µL (example: to 10 µL of sample with 500 µM of sulfite 1 mM of mbbr (2 µL) and 84 µL HEPES were added). The reactions were performed in the dark during 10 min after which 4 µL of methanosulfonic acid 5 M were added to stop the reaction. For HPLC separations the derivatized samples were diluted to the desired final concentration in 10 mM methanosulfonic acid. The analysis were executed using an HPLC (Waters Alliance 2695) equipped with a fluorescence detector (Waters 486) with excitation at 380 nm and emission at 480 nm, using a Beckman Coulter reversed-phase-column ultrasphere C18 Beckman Coulter (4.6-25; 5 µm), at 35 °C. The gradient was performed with 0.25% acetic acid pH 4 in MilliQ water (A) and 100% Methanol (B). Flow-rate was 1.20 mL/min. The elution protocol was as follows: 0-5 min 20% B, 5-13 min 20%-50% B, 13-16 min 50%-52% B, 16- 20 min 52%-100% B, 20-24 min 100% B, 24-26 min 100%-20% B and 26-31 min 20% B. Calibration curves were performed with sodium sulfite

Surface plasmon resonance (SPR) analysis

To analyze *in vitro* protein-protein interactions we used surface plasmon resonance in a BIAcore 2000 system. For the immobilization of the proteins the CM5 chip (carboxymethylated dextran covalently attached to a gold surface) was used, to which proteins bind via amine, thiol, aldehyde or carboxyl groups. All assays were performed at 25 °C with the running buffer (RB) (10 mM HEPES, 150 mM NaCl, 50 µM EDTA, 0.005% Tween 20 pH 7.4). DsrAB from *D. vulgaris* and *A. fulgidus* were covalently immobilized to the CM5 sensor chip by the amine coupling protocol described by the manufacturer. The proteins DsrAB from *D. vulgaris* and *A. fulgidus* were immobilized in the flow cells 2 and 3 respectively, in order to achieve 600 Resonance Units (RU) per which protein. The kinetic experiments were performed immediately after immobilization. Flow cell 1 was used as control. 500 mM NaCl was used to dissociate the analyte and regenerate the chip after each interaction assay. In all experiments the analyte was injected at a flow rate of 10 µM/min for 2 min over the flow cells 1, 2 and 3. After 2 min regeneration with NaCl, RB was applied to restore the base line.

4.3. Results and discussion

Electron donor analysis

Pyruvate ferredoxin-oxidoreductase (PFOR)

In this work we first tried to purify PFOR from *A. fulgidus* due to its presumed stability to high temperatures and to test for the interaction with DsrAB from the same organism. However, this enzyme proved to be extremely unstable, and after the purification we had very little protein and the activity rapidly decreased to 19% of the initial value. This led us to use instead the PFOR from *D. africanus*, a more stable protein, which was already available in our laboratory (purified as described by Pieulle and coworkers (Pieulle *et al.*, 1995)). In the structure of *D. africanus* PFOR, the TPP and a proximal [4Fe-4S] cluster are buried within the protein and the two additional [4Fe-4S] are placed near the surface which allow the interaction with a partner such as ferredoxin (Chabriere *et al.*, 1999). The PFOR from *D. africanus* is one of the few examples of a PFOR stable in the presence of oxygen. According to Chabrière and coworkers, this PFOR has an additional domain (domain IV), absent in many PFORs, which protects the enzyme against oxygen damage. This is a homodimeric protein with 256 kDa and three [4Fe-4S] clusters per subunit. Through sequence analysis of the α (H585DRAFT_03763) and β subunits (H585DRAFT_03764) we verified that: for the α subunit the identities with PFOR from *D. vulgaris* and *A. fulgidus* VC16 are low (E value of $2e^{-25}$ for *D. vulgaris* Hildenborough PorA α subunit, Dvu1569 and $3e^{-21}$ for *A fulgidus* VC16 PFOR α subunit, AF0749); for the β subunit the E value is $4e^{-141}$ (PorB β subunit, Dvu1570) for *D. vulgaris* Hildenborough and $1e^{-22}$ (PFOR β subunit, AF0750). Although the PFOR from *D. africanus* only share high similarity with PorB

of *D. vulgaris*, this is still a good candidate to test due to its ability to reduce ferredoxin like subunits.

We analyze the PFOR from *D. africanus* with circular dichroism for its stability at 60 °C, the temperature used for the *A. fulgidus* DsrAB activity. This allowed us to conclude that the structure of PFOR from *D. africanus* was still stable at this high temperature. The specific activity of our PFOR was of 17 U/mg in accordance with previous studies (Pieulle *et al.*, 1995)

Aldehyde oxidoreductase (AOR)

As referred before, to select the Mo-AOR, *D. gigas* must be grown on molybdenum and absent of W. We did not try to isolate the tungsten AOR due to its reported extreme oxygen sensitivity. Therefore, we grew *D. gigas* only in the presence of Mo and purified the corresponding AOR protein aerobically.

Table.4.1. Sequence comparison between Aor genes of D. gigas and the homologues in D. vulgaris and A. fulgidus (analysis conducted in www.img.jgi.doe.gov)

	E value						
***D. gigas* loci**	*D. vulgaris* loci				*A. fulgidus* loci		
	DVU1559	DVU1179	DVU0687	DVU0687	AF2281	AF0023	AF0077
DGI_0902	0.0	-	-	-	-	-	-
DGI_1056	-	0.0	-	-	$7e^{-78}$	-	-
DGI_1447	-	-	$1e^{-08}$	-	-	$1e^{-17}$	-
DGI_3127	-	-	-	0.0	-	-	$3e^{-137}$

Until the present day, only one AOR from *D. gigas* was found be resistant to oxygen and to contain Mo as the metal cofactor in *D. gigas* (DGI_0902). Moreover, from the four AOR present in *D. gigas*

(Table 4.1) three have an approximated weight of 60 kDa and only one (DGI_0902) of 100 kDa. Due to the fact that our AOR is resistant to oxygen (its activity did not decreased with time in the presence of oxygen) and that according to the 12% SDS gel the purified AOR has ~100 kDa, we know that our purified AOR is the DGI_0902. To measure the activity of AOR we used acetaldehyde and DCPIP as electron donor. After optimization of the protocol for the activity, this protein revealed a turnover of 2.71 s^{-1}, which is about 2 times higher than the reported activity for the molybdenum AOR of *D. gigas* (Barata *et al.*, 1993).

Carbon monoxide dehydrogenase (CODH)

The Ni,Fe-CODH used in this work is the CooS from *D. vulgaris* and it is predicted to have four [4Fe- 4S] clusters and a mass of 67 kDa. The sequence comparison between the CODH of *D. vulgaris* and the CODH of *A. fulgidus* (AF_1849) shows a high similarity (E value $8e^{-125}$). After incubation with nickel and dithionite, the CODH has an activity of 163 U/mg.

Recombinant NoxA-3 from *A. fulgidus* VC16

To search for conserved NADH oxidases in the SRP group we used all six NADH oxidases present in *D. vulgaris* Hildenborough (Dvu1613, DVU1165, DVU1974, DVU3212, DVU3292 and DVU2680) and blasted them against the list of SRP (using IMG). The locus DVU3212 was present in all 97 genomes analyzed with extremely high similarity, the only exception being *Thermodesulfovibrio yellowstonii* (no gene similarity). Homologues to this gene are also present in sulfite reducers, sulfur reducers and in organisms related to sulfur respiration such as *Pyrococcus furiosus* (PF1186). As so, we compared the gene locus DVU3212 against all five NoxA loci for *A. fulgidus* and identified the gene

locus AF0400 with the highest E value (Table 4.2). From this, we decided to use the *noxA-3* gene to test as electron donor for DsrAB, as this is the most homologous protein to the widespread Nox in SRP. For this, the *noxA-3* gene (AF0400) was cloned into a pet22b vector (without the tag to avoid disturbing the folding of the native NoxA-3).

Table. 4.2. Analysis of the comparison of the DVU3212 gene locus from D. vulgaris with the five noxA gene loci present in A. fulgidus.

		E value
		***D. vulgaris* locus**
***A. fulgidus* loci**		**DVU3212**
NoxA-1	AF0254	$5e^{-61}$
NoxA-2	AF0395	$3e^{-74}$
NoxA-3	**AF0400**	**$8e^{-120}$**
NoxA-4	AF0951	$1e^{-39}$
NoxA-5	AF1858	$1e^{-41}$

This vector was inserted in BL21 (DE3) Gold cells along with the pRARE2 vector for the production of rNoxA-3 protein. To purify this, a heat-shock treatment was first used to remove most of the *E. coli* native proteins that precipitate at high temperature (70 °C). After two ionic exchange columns, high purity rNoxA-3 was obtained. Since this was the first time that this protein has been isolated we characterized its activity.

The NoxA-3 protein from *A. fulgidus* VC16 is predicted to belong to Pyridine nucleotide-disulfide oxidoreductase, NAD-binding domain (Pfam PF00070), Rhodanese-like domain (SUPERFAMILY SSF52821) and to have a FAD/NAD(P)-binding domain. In order to verify which flavins are preferably bound by rNoxA-3, FAD, FMN or both, we checked the activity of rNoxA-3 alone or after addition of FAD, FMN or both at 37°C and 60 °C (Table 4.3).

Table. 4.3. Activity (µmols of DCPIP reduced per minute per mg of enzyme) of rNoxA- 3 with and without addition of flavins (5 µM) at 37 °C and 60 °C. Experiments performed with DCPIP as the artificial electron donor, 25 µM of NADH in Kpi 50 mM pH 7.

	Activity U/mg	
	37 °C	**60 °C**
rNoxA-3	0,020	-
rNoxA-3 + FAD	0,101	1,540
rNoxA-3 + FMN	0,028	-
rNoxA-3 + FAD+FMN	0,096	1,176

After verifying that rNoxA-3 could oxidize NADH in the presence of DCPIP at 37 °C and at 60 °C, a kinetic study was performed (Figure 4.4). At 60 °C the K_m for NADH is 4.71±1.3 µM and the V_{max} is 1.6 ± 0.06 U/mg.

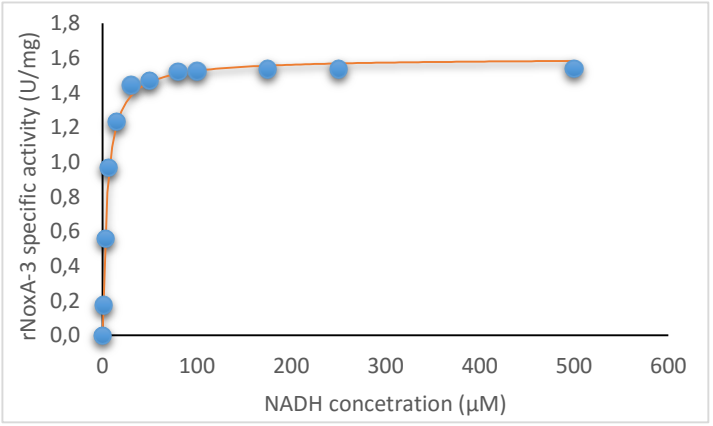

Figure. 4.4. Kinetic activity of rNoxA-3 with DCPIP at 60 °C.

Activities of DsrAB from *D. vulgaris* and *A. fulgidus* with the potential electron donors

To study the potential electron donors for the dissimilatory sulfite reductase, biochemical and biophysical techniques were employed. As discussed before, three ferredoxin oxidoreductases (PFOR, AOR and CODH) and one NADH oxidase were chosen. Concerning PFOR, Oliveira *el* al. (2011) already generated a theoretical structure model for the possible interaction between PFOR and DsrAB (*D. vulgaris*). They verified that the surface electrostatic potential for the *D. vulgaris* DsrAB protein surface is negatively charged around the region of the ferredoxin domain (DsrB), which is potentially the region for interaction with the electron donor. In the PFOR analysis, the ferredoxin binding domain is positively charged. Using Pymol as the modeling tool, they verified that the PFOR ferredoxin binding domain can be positioned in the vicinity of the *D. vulgaris* DsrAB ferredoxin domain. This analysis positioned the iron–sulfur clusters of the two domains at ~15 Å from each other, suggesting that electron transfer from the PFOR catalytic center to the DsrAB (*D. vulgaris*) [4Fe-4S] cluster is possible (Oliveira *et al.*, 2011). On the other hand, AOR, CODH and NoxA-3 were not yet analyzed as possible electron donors.

Two approaches were conducted to test these possible electron donors: i) the analysis of the sulfite consumption/product formation by DsrAB (*D. vulgaris* and *A. fulgidus*) in the presence of the different possible physiologic electrons donors in comparison to the DsrAB activity using methyl viologen as the artificial electron donor, and ii) the analysis of protein-protein interactions using Surface plasma resonance (SPR).

Ferredoxin oxidoreductases

To analyze the consumption of sulfite/product formation by DsrAB (*D. vulgaris* and *A. fulgidus*) the monobromobimane (mBbr) method was used. In this method, mBbr reacts with free thiols, such as sulfite, sulfide and thiosulfate. The first attempt was to analyze the consumption of sulfite. Unfortunately, it was impossible to extrapolate any conclusion from the sulfite consumption, as the data values for the sulfite consumption during the time period were poorly reproducible (Figure 4.5). The reason for these oscillation in the data could be due to the method of collecting the sample. The enzymatic reactions were performed in a 500 µL tube with 300 µL of total reaction. At each data point the system was opened (inside of the anaerobic chamber) and a sample of 10 µL was taken to analyze by HPLC, which accounted for a loss of 20% of total volume at the end of the experiments. The small reaction volume along with the disturbance of the atmospheric equilibrium (at 37 and 60 °C) might had led to changes in sulfite concentration, which masked the results. Therefore, we analyzed instead the product formation. In these analyzes we were expecting to find production of thiosulfate as it is found when Mv is used. As it can be

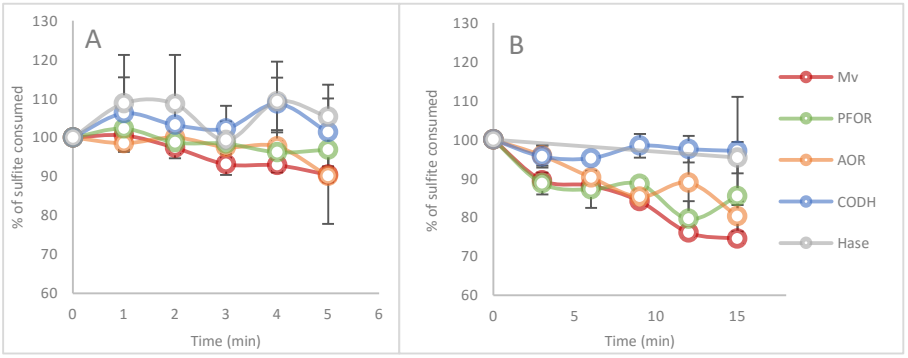

Figure. 4.5. Analysis of sulfite consumed by DsrAB of A. fulgidus (A) and D. vulgaris (B) in the presence of the possible physiological electron donors. Mv as the positive control and Hase (hydrogenase) alone as a negative control.

verified in the Figure 4.6, when we analyzed thiosulfate production none of the possible physiological electron donors behaves similarly to the artificial electron donor (Mv). Only AOR seemed to support some level of activity.

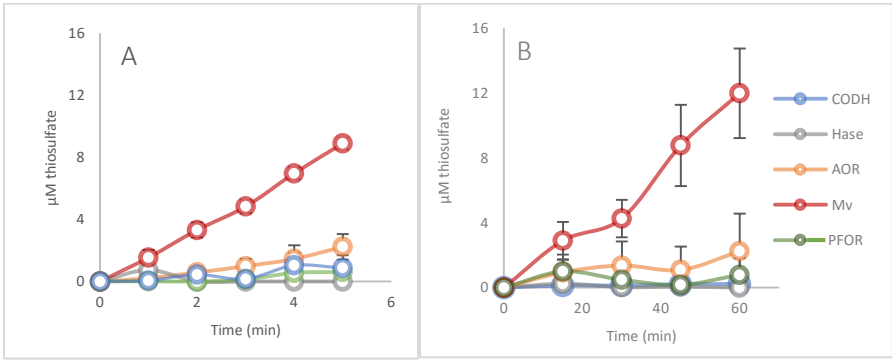

Figure. 4.6. Analysis of thiosulfate production of DsrAB of A. fulgidus (A) and D. vulgaris (B) in the presence of the possible physiological electron donors. Mv as the positive control and Hase (hydrogenase) alone as a negative control.

NADH oxidase (rNoxA-3)

To analyze the interaction of rNoxA-3, a different approach was used, as we measured instead the oxidation of NADH at 340 nm with DsrAB and sulfite as electron acceptors (Figure 4.7). However, the number of mols of NADH needed to reduce sulfite is complex as it depends on the products formed (Table 4.4).

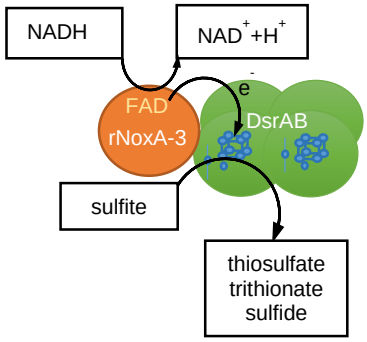

Figure. 4.7. Scheme of the activity assay of rNoxA-3 with DsrAB

Table. 4.4. Number of mols of NADH needed per sulfite product.

mols NADH	sulfite reduction product
1	1mol thiosulfate
2	1 mol trithionate
3	1mol sulfide

In many assimilatory sulfite reductases, a NADPH-dependent subunit functions as the electron donor for sulfite reduction (Crane & Getzoff, 1996). Similarly in the SOB *A. vinosum*, the reverse dissimilatory sulfite reductase is co-purified with DsrL, an NAD(P)H:acceptor oxidoreductase. Also, in *E. coli*, the cytoplasmic NirB nitrite reductase, of the same siroheme-dependent family as DsrAB, is a NADH-dependent enzyme capable of reducing nitrite to ammonium (Wang & Gunsalus, 2000). These factors suggest a probable interaction of dissimilatory sulfite reductase with an NAD(P)H-dependent oxidoreductase. This would connect sulfite reduction to the regeneration of NAD^+.

We first checked for the activity of rNoxA-3 at 37 °C and 60 °C, at pH 7 and in Kpi 50 mM buffer following the decrease of the DCPIP absorbance at 600 nm. The activities were 0.101 U/mg at 37 °C and 1.250 U/mg at 60 °C. Inside the anaerobic chamber the electron acceptor DCPIP was substituted by sulfite (0.5 mM for DsrAB from *A. fulgidus* and 2.5 mM for DsrAB of *D. vulgaris*) and the DsrAB protein of *D. vulgaris* (37 °C) and *A. fulgidus* (60 °C), and the activity as followed by NADH decrease at 340 nm. However, we observe no oxidation of NADH in these conditions, suggesting that rNoxA-3 cannot transfer electros to DsrAB in the conditions of this assay.

Surface plasma resonance (SPR)

To test protein-protein interactions independently from enzymatic assays, SPR was employed. The CM5 chip (amine binding) was selected to bind DsrAB from *D. vulgaris* and *A. fulgidus*. All the proteins previously referred were tested: PFOR, AOR, CODH and rNoxA-3. The SPR corroborated the data obtained by the *in vitro* activities experiments, as no interaction between these potential electron donors and both DsrABs was observed. Having the proteins already bound to the chip we decided to test other possible electrons donors, soluble and membrane proteins, as these proteins were already available in our laboratory. The proteins were: Tmc and Qrc from *D. vulgaris* Hildenborough, Hmc from *D. gigas*, and DsrMKJOP from *D. desulfuricans* ATTC 27774 (membrane complexes), and ferredoxin I from *D. gigas*. No interaction with these proteins was observed for DsrAB from *A fulgidus*, which presented only a week interaction with the Hmc membrane complex and with ferredoxin I. However, DsrAB from *D. vulgaris* showed some interaction with all membrane complexes and also with ferredoxin I. This difference between DsrAB from *D. vulgaris* and *A. fulgidus* is probably due to the fact that the *D. vulgaris* protein has DsrC bound to it. It was already proven by Venceslau et al. (Venceslau, 2011) that DsrC is able to bind to DsrMKJOP, and this shows that DsrC can interact with the membrane complex even when bound to DsrAB.

Genomic analysis of ferredoxin-like proteins in SPR

As referred before Larsen *et* al. did a multiple alignment analysis where they grouped together a ferredoxin (Fdx) from *D. thermocisternum* (immediately upstream of *dsrAB* genes) along with the Fdx-4 of *A. fulgidus* and Fdx-I from *D. vulgaris* (Larsen *et al.*, 1999). We decided to extend this analysis for all the available genomes present in the list for sulfate reducers at IMG. As so, we compared the Fdx-4 from *A. fulgidus* (AF0427) against the SRP list. From this comparison, forty seven genomes had at least one Fdx homologue to Fdx-4 of *A. fulgidus*. Moreover, thirteen Fdx homologues were found nearby a *dsr* gene (Figure 4.8). From this analysis, the thirteen organisms can be divided in two main groups: the Gram-negative SRP (Figure 4.8 A) and Gram-positive SRP (Figure 4.8 B). In both cases the *fdx* gene is near the *dsrAB-D* genes or *dsrMKJOP*/*dsrMK-C* genes. This results supports the proposal that this ferredoxin protein can act as the possible physiological electron donor.

In our *in vitro* experiments we tried to use the ferredoxin (Fdx) from *Clostridium tetanomorphum*, as an intermediate between AOR and DsrAB. This experiment failed to prove the interaction between DsrAB and the Fdx. Nevertheless, this Fdx may not be the best candidate for DsrAB interaction, as it has a molecular weight of ~26.7 kDa, while the ferredoxins near the *dsr* genes are smaller, ~6.6 kDa. The difference in size and the fact that the ferredoxin and the DsrAB used are from different organisms, probably influenced the interaction with the ferredoxin domain in the vicinity of the siroheme. The next step is to purify the ~6.6 kDa ferredoxin from *D. vulgaris* or *A. fulgidus* and evaluate their interaction.

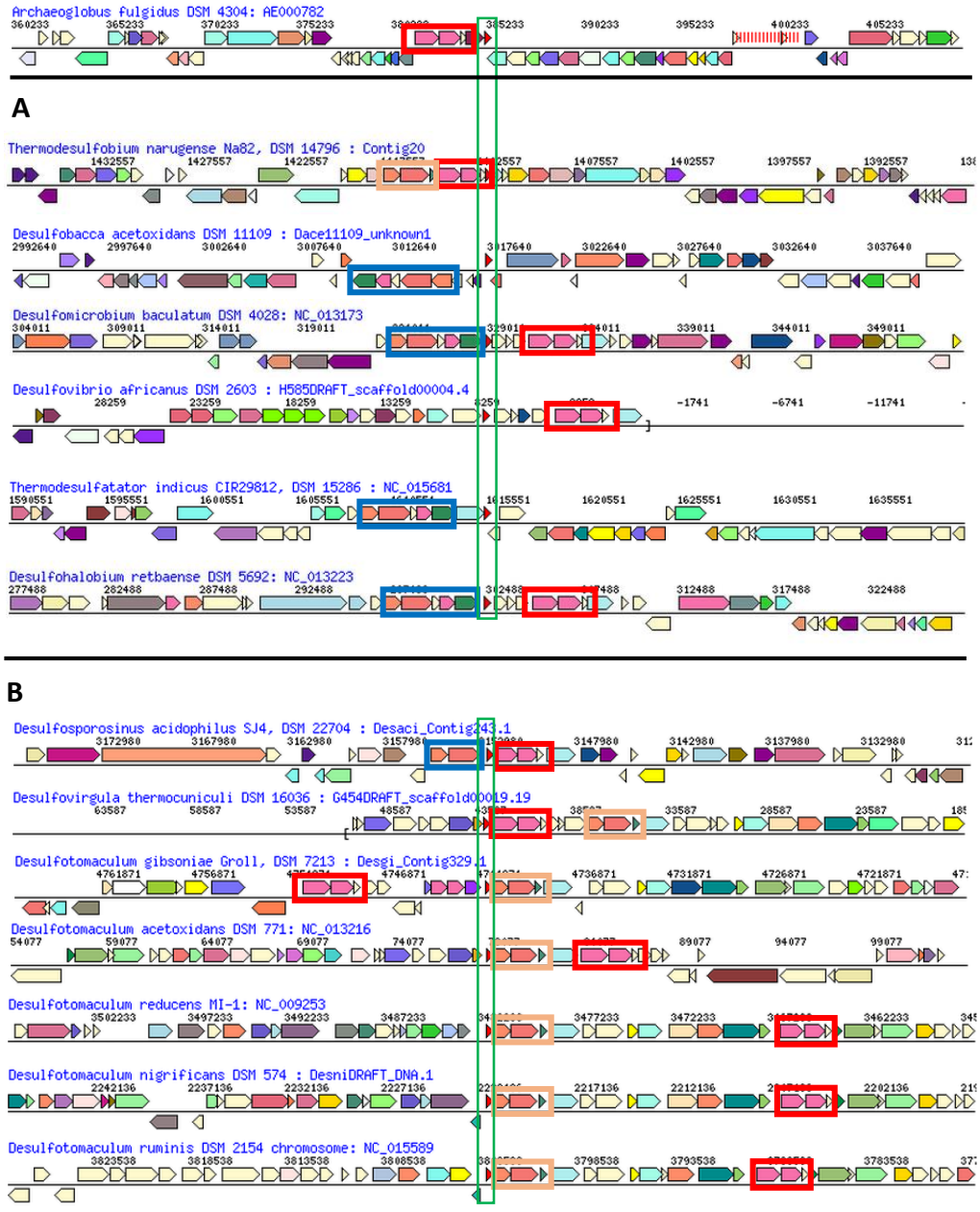

Figure. 4.8. Neighborhood organization of the genes homologous to fdx-4 gene from A. fulgidus (AF0427). (A) Gram-negative SRP, (B) Gram-positive SRP. In the green box are represented the homologues to the Fdx-4. Red, orange and blue boxes identify the dsrAB-D, dsrMK-C and dsrMKJOP genes respectively (This scheme was obtain using the IMG database website)

4.4. Conclusion

According to our experiments the ferredoxin oxidoreductases PFOR, AOR and CODH were not capable of sustaining DsrAB activity (*D. vulgaris* and *A. fulgidus*). Also, the NADH oxidase rNoxA-3 was not able to interact with DsrAB to reduce sulfite to sulfide. We also tried to use the ferredoxin (from *C. tetanomorphum*) as an intermediate between the AOR and DsrAB, also with negative results. These results do not mean that these candidates are not physiological partners, only that in the conditions in which the experiments were performed they did not succeed. In our perspective, ferredoxin is still a good candidate to be involved with DsrAB for sulfite reduction due to the fact that at least in thirteen genomes, of the total forty seven genomes, a homologue of Fdx-4 is found near *dsr* genes. The small ferredoxin from *A. fulgidus* (AF0427) would be a good candidate for heterologous expression and to test as the electron donor for DsrAB proteins. Further work needs to be performed in order to find the physiological electron donor for the DsrAB dissimilatory sulfite reductase.

References

Barata BAS, Legall J & Moura JJG (1993) Aldehyde Oxidoreductase Activity in Desulfovibrio-Gigas - in-Vitro Reconstitution of an Electron-Transfer Chain from Aldehydes to the Production of Molecular-Hydrogen. *Biochemistry* **32**: 11559-11568.

Barquera B (2014) The sodium pumping NADH:quinone oxidoreductase (Na+-NQR), a unique redox-driven ion pump. *J Bioenerg Biomembr* **46**: 289-298.

Bevers LE, Bol E, Hagedoorn P-L & Hagen WR (2005) WOR5, a Novel Tungsten-Containing Aldehyde Oxidoreductase from Pyrococcus furiosus with a Broad Substrate Specificity. *J Bacteriol* **187**: 7056-7061.

Biegel E & Muller V (2010) Bacterial Na+-translocating ferredoxin:NAD+ oxidoreductase. *Proc Natl Acad Sci U S A* **107**: 18138-18142.

Biegel E, Schmidt S, Gonzalez JM & Muller V (2011) Biochemistry, evolution and physiological function of the Rnf complex, a novel ion-motive electron transport complex in prokaryotes. *Cell Mol Life Sci* **68**: 613-634.

Brondino CD, Romao MJ, Moura I & Moura JJ (2006) Molybdenum and tungsten enzymes: the xanthine oxidase family. *Current opinion in chemical biology* **10**: 109-114.

Chabriere E, Charon MH, Volbeda A, Pieulle L, Hatchikian EC & Fontecilla-Camps JC (1999) Crystal structures of the key anaerobic enzyme pyruvate:ferredoxin oxidoreductase, free and in complex with pyruvate. *Nat Struct Biol* **6**: 182-190.

Chen L, Liu MY, Legall J, Fareleira P, Santos H & Xavier AV (1993) Rubredoxin Oxidase, a New Flavo-Hemo-Protein, Is the Site of Oxygen Reduction to Water by the "Strict Anaerobe" Desulfovibrio gigas. *Biochemical and Biophysical Research Communications* **193**: 100-105.

Correia HD, Marangon J, Brondino CD, Moura JJ, Romao MJ, Gonzalez PJ & Santos-Silva T (2015) Aromatic aldehydes at the active site of aldehyde oxidoreductase from Desulfovibrio gigas: reactivity and molecular details of the enzyme-substrate and enzyme-product interaction. *J Biol Inorg Chem* **20**: 219-229.

Crane BR & Getzoff ED (1996) The relationship between structure and function for the sulfite reductases. *Curr Opin Struc Biol* **6**: 744-756.

Dahl C, Kredich NM, Deutzmann R & Truper HG (1993) Dissimilatory sulphite reductase from Archaeoglobus fulgidus: physico-chemical properties of the enzyme and cloning, sequencing and analysis of the reductase genes. *J Gen Microbiol* **139**: 1817-1828.

Feng Y, Li W, Li J*, et al.* (2012) Structural insight into the type-II mitochondrial NADH dehydrogenases. *Nature* **491**: 478-482.

Garczarek F, Dong M, Typke D, Witkowska HE, Hazen TC, Nogales E, Biggin MD & Glaeser RM (2007) Octomeric pyruvate-ferredoxin oxidoreductase from Desulfovibrio vulgaris. *Journal of Structural Biology* **159**: 9-18.

Hadj-Said J, Pandelia ME, Leger C, Fourmond V & Dementin S (2015) The Carbon Monoxide Dehydrogenase from Desulfovibrio vulgaris. *Biochim Biophys Acta*.

Hensgens CMH, Nienhuiskuiper ME & Hansen TA (1994) Effects of Tungstate on the Growth of Desulfovibrio-Gigas Ncimb-9332 and Other Sulfate-Reducing Bacteria with Ethanol as a Substrate. *Arch Microbiol* **162**: 143-147.

Hensgens CMH, Hagen WR & Hansen TA (1995) Purification and Characterization of a Benzylviologen-Linked, Tungsten-Containing Aldehyde Oxidoreductase from Desulfovibrio-Gigas. *J Bacteriol* **177**: 6195-6200.

Hille R, Hall J & Basu P (2014) The Mononuclear Molybdenum Enzymes. *Chem Rev* **114**: 3963-4038.

Huang H, Wang S, Moll J & Thauer RK (2012) Electron bifurcation involved in the energy metabolism of the acetogenic bacterium Moorella thermoacetica growing on glucose or H2 plus CO2. *J Bacteriol* **194**: 3689-3699.

Jeoung J-H, Fesseler J, Goetzl S & Dobbek H (2014) Carbon Monoxide. Toxic Gas and Fuel for Anaerobes and Aerobes: Carbon Monoxide Dehydrogenases. *The Metal-Driven Biogeochemistry of Gaseous Compounds in the Environment,* Vol. 14 (Kroneck PMH & Torres MES, eds.), p.^pp. 37-69. Springer Netherlands.

Karkhoff-schweizer RR, Huber DPW & Voordouw G (1995) Conservation of the genes for dissimilatory sulfite reductase from *Desulfovibrio vulgaris* and *Archaeoglobus fulgidus* allows their detection by PCR. *Appl Environ Microb* **61**: 290-296.

Larsen O, Lien T & Birkeland NK (1999) Dissimilatory sulfite reductase from Archaeoglobus profundus and Desulfotomaculum thermocisternum: phylogenetic and structural implications from gene sequences. *Extremophiles* **3**: 63-70.

Lubbe YJ, Youn H-S, Timkovich R & Dahl C (2006) Siro(haem)amide in Allochromatium vinosum and relevance of DsrL and DsrN, a homolog of cobyrinic acid a,c-diamide synthase, for sulphur oxidation. *Fems Microbiol Lett* **261**: 194-202.

Melo AM, Bandeiras TM & Teixeira M (2004) New insights into type II NAD(P)H:quinone oxidoreductases. *Microbiology and molecular biology reviews : MMBR* **68**: 603-616.

Mukund S & Adams MW (1991) The novel tungsten-iron-sulfur protein of the hyperthermophilic archaebacterium, Pyrococcus furiosus, is an aldehyde ferredoxin oxidoreductase. Evidence for its participation in a unique glycolytic pathway. *J Biol Chem* **266**: 14208-14216.

Oliveira TF, Vonrhein C, Matias PM, Venceslau SS, Pereira IA & Archer M (2008) The crystal structure of Desulfovibrio vulgaris dissimilatory sulfite reductase bound to DsrC provides novel insights into the mechanism of sulfate respiration. *J Biol Chem* **283**: 34141-34149.

Oliveira TF, Franklin E, Afonso JP, Khan AR, Oldham NJ, Pereira IAC & Archer M (2011) Structural insights into dissimilatory sulfite reductases: structure of desulforubidin from Desulfomicrobium norvegicum. *Frontiers in Microbiology* **2**.

Pereira IA, Ramos AR, Grein F, Marques MC, da Silva SM & Venceslau SS (2011) A comparative genomic analysis of energy metabolism in sulfate reducing bacteria and archaea. *Front Microbiol* **2**: 69.

Pieulle L, Guigliarelli B, Asso M, Dole F, Bernadac A & Hatchikian EC (1995) Isolation and Characterization of the Pyruvate-Ferredoxin Oxidoreductase from the Sulfate-Reducing Bacterium Desulfovibrio-Africanus. *Bba-Protein Struct M* **1250**: 49-59.

Rabus R, Venceslau SS, Wohlbrand L, Voordouw G, Wall JD & Pereira IA (2015) A Post-Genomic View of the Ecophysiology, Catabolism and Biotechnological Relevance of Sulphate-Reducing Prokaryotes. *Adv Microb Physiol* **66**: 55-321.

Ragsdale SW (2003) Pyruvate Ferredoxin Oxidoreductase and Its Radical Intermediate. *Chem Rev* **103**: 2333-2346.

Ragsdale SW (2004) Life with carbon monoxide. *Critical reviews in biochemistry and molecular biology* **39**: 165-195.

Ramos AR, Grein F, Oliveira GP, Venceslau SS, Keller KL, Wall JD & Pereira IA (2015) The FlxABCD-HdrABC proteins correspond to a novel NADH dehydrogenase/heterodisulfide reductase widespread in anaerobic bacteria and involved in ethanol metabolism in Desulfovibrio vulgaris Hildenborough. **17**: 2288-2305.

Rauh D, Graentzdoerffer A, Granderath K, Andreesen JR & Pich A (2004) Tungsten-containing aldehyde oxidoreductase of Eubacterium acidaminophilum. *European Journal of Biochemistry* **271**: 212-219.

Reyes-Prieto A, Barquera B & Juarez O (2014) Origin and evolution of the sodium -pumping NADH: ubiquinone oxidoreductase. *Plos One* **9**: e96696.

Romao MJ (2009) Molybdenum and tungsten enzymes: a crystallographic and mechanistic overview. *Dalton Transactions* 4053-4068.

Roy R, Menon AL & Adams MW (2001) Aldehyde oxidoreductases from Pyrococcus furiosus. *Methods Enzymol* **331**: 132-144.

Santos H, Fareleira P, Xavier AV, Chen L, Liu MY & Legall J (1993) Aerobic Metabolism of Carbon Reserves by the "Obligate Anaerobe" Desulfovibrio gigas. *Biochemical and Biophysical Research Communications* **195**: 551-557.

Sazanov LA (2015) A giant molecular proton pump: structure and mechanism of respiratory complex I. *Nat Rev Mol Cell Biol* **16**: 375-388.

Schmehl M, Jahn A, Vilsendorf AMZ, Hennecke S, Masepohl B, Schuppler M, Marxer M, Oelze J & Klipp W (1993) Identification of a New Class of Nitrogen-Fixation Genes in Rhodobacter-Capsulatus - a Putative Membrane Complex Involved in Electron-Transport to Nitrogenase. *Mol Gen Genet* **241**: 602-615.

Soboh B, Linder D & Hedderich R (2002) Purification and catalytic properties of a CO-oxidizing:H2-evolving enzyme complex from Carboxydothermus hydrogenoformans. *Eur J Biochem* **269**: 5712-5721.

Stetter KO, Lauerer G, Thomm M & Neuner A (1987) Isolation of Extremely Thermophilic Sulfate Reducers - Evidence for a Novel Branch of Archaebacteria. *Science* **236**: 822-824.

Thapper A, Rivas MG, Brondino CD, Ollivier B, Fauque G, Moura I & Moura JJG (2006) Biochemical and spectroscopic characterization of an aldehyde oxidoreductase isolated from Desulfovibrio aminophilus. *Journal of Inorganic Biochemistry* **100**: 44-50.

Uyeda K & Rabinowitz JC (1971) Pyruvate-ferredoxin oxidoreductase. 3. Purification and properties of the enzyme. *J Biol Chem* **246**: 3111-3119.

Venceslau SS (2011) Electron transfer chains in sulfate reducing bacteria. Thesis, Universidade Nova de Lisboa.

Wang HN & Gunsalus RP (2000) The nrfA and nirB nitrite reductase operons in Escherichia coli are expressed differently in response to nitrate than to nitrite. *J Bacteriol* **182**: 5813-5822.

Wang S, Huang H, Moll J & Thauer RK (2010) NADP+ Reduction with Reduced Ferredoxin and NADP+ Reduction with NADH Are Coupled via an Electron-Bifurcating Enzyme Complex in Clostridium kluyveri. *J Bacteriol* **192**: 5115-5123.

Weghoff MC, Bertsch J & Müller V (2015) A novel mode of lactate metabolism in strictly anaerobic bacteria. *Environmental Microbiology* **17**: 670-677.

Wu M, Ren Q, Durkin AS*, et al.* (2005) Life in Hot Carbon Monoxide: The Complete Genome Sequence of Carboxydothermus hydrogenoformans Z-2901. *PLoS Genet* **1**: e65.

Chapter 5

DsrJ, the cytochrome *c* subunit of the DsrMKJOP membrane complex

Table of contents

5.1. Introduction

Membrane respiratory complexes are of extreme importance for life as they are the link to for energy conservation in living organisms. There are two essential membrane complexes for sulfate reduction present in all SRP and also some SOB, DsrMKJOP and QmoABC (Frigaard & Dahl, 2009, Pereira *et al.*, 2011). The QmoABC complex is thought to exchange electrons with the ApsBA (APS reductase) and DsrMKJOP is proposed to reduce the trisulfide form of DsrC. The DsrMKJOP membrane complex was first purified from *A. fulgidus* in 2002 by Mander and coworkers (Mander *et al.*, 2002), where it was named Hme for Hdr-like menaquinone-oxidizing enzyme (Hme). A homologue to Hme complex was also discovered in *A. vinosum* by Dahl *et* al (Dahl *et al.*, 2005). It was found to be part of an essential operon for sulfur oxidation coupled with the *dsrAB* genes, and for this reason was named DsrMKJOP complex. In 2006, Pires *et* al purified the DsrMKJOP complex from *D. desulfuricans* ATCC 27774 which was shown to be a homologue of the Hme complex of *A. fulgidus* (Pires *et al.*, 2006). This complex is formed by five subunits. One cytoplasmic subunit, DsrK, thought to be the catalytic subunit of DsrMKJOP complex due to its homology to HdrD, which is responsible for heterodisulfide reduction by the membrane-bound HdrDE complex. Two membrane bound subunits (DsrM and DsrP), possibly responsible for menaquinol interaction, and two periplasmic facing membrane bound proteins (DsrO and DsrJ) (Pires *et al.*, 2006, Grein, 2010). DsrJ contains three heme binding motives CXXCH, in which one of these hemes is characterized by an unusual His/Cys heme distal axial ligation (Pires *et al.*, 2006, Grein *et al.*, 2010). In the DsrMKJOP from *D. desulfuricans* a redox potential of - 400 mV and a very unique peak g_{max} 2.47 for the EPR spectra were attributed to this His/Cys heme ligation (Pires *et al.*, 2006). This very low redox

potential was also found in SoxXA from *Rhodovulum sulfidophilum*. SoxXA are heme-containing proteins crucial for the initiation of thiosulfate oxidation (Cheesman *et al.*, 2001). Also, EPR spectra of SoxXA showed a low-spin heme signal in the range of $g_{max} = 2.5$, characteristic for the His/Cys coordinated heme groups (Walker, 1999, Cheesman *et al.*, 2001, Kappler *et al.*, 2005). Although unusual, this heme cysteine ligation was proven not to be essential for SoxXA reaction mechanism, as the SoxXA cysteine mutant (change by a methionine) could maintain 55% of the wild type SoxXA glutathione-based activity (Kilmartin *et al.*, 2011). Also, in the mutated *A. vinosum* DsrJ strain, where the cysteine was substituted by a serine, albeit with a significantly reduced oxidation rate, the cells were still capable of oxidizing sulfur (Grein *et al.*, 2010). Nevertheless, in both SoxXA and DsrJ cysteine mutants, their activity decreased significantly pointing out that, although not crucial, these His/Cys heme ligations are extremely important for the overall function of these proteins (Grein *et al.*, 2010, Kilmartin *et al.*, 2011). Moreover, the crystallographic structure of DsrJ is still not available, which would provide the information needed to address the question of which amino acids are the distal axial ligands for the three hemes.

The work described aimed to disclose the true identity of all the ligands to the three heme of DsrJ. To accomplish this, mutants in the conserved residues that could be the distal axial heme ligands were performed, and were then analyzed by Electron paramagnetic resonance, Raman Resonance, UV-visible and Mass spectrometry.

5.2. Methods

Competent cell transformations

Plasmid DNA was inserted into *E. coli* strains by transforming chemically competent cells. Per each transformation, 1 µl of plasmid DNA or 5 µl of a ligation assay were added to 50 µl of competent cells. The preparation was first incubated for 60 min on ice followed by 90 s at 42 °C and 2 min on ice. These competent cells were then added to 500 µl of LB medium and incubated at 37 °C for 60 min with agitation. Finally, different aliquots of the assay were applied onto LB plates containing the respective antibiotic.

Sequence and ligation independent cloning (SLIC)

To produce the variants, the selected plasmid (pETJStrep or pETStrepJ) was amplified by PCR in two parts that carried the desired mutation at the (compatible) end of the fragments. Fragments were amplified using the HercII polymerase and using the following primer pairs: fragment A (forward primer introducing the mutation and reverse primer for the ampicilin gene) and fragment B (forward Ampicilin primer and reverse primer introducing mutation). The role of cysteine 46 was already studied before by replacing this amino acid by a serine (Grein, 2010, Grein *et al.*, 2010). Since it could not be excluded that serine can ligate a heme iron, the cysteine was here replaced by a glycine. The methionines M53, M58 and the histidine H57 were replaced by alanines. All possible combinations of mutants were created generating 10 different constructions. To create the respective mutation the entire plasmid was PCR amplified in two parts, where both parts carry a short overlapping sequence which carries the desired mutation. The parts

were then fused using the SLIC method (Li & Elledge, 2007). This protocol was used to insert the single point mutations. First a PCR of the plasmid fragment(s) with HercII polymerase was performed. After cleaning the PCR products with the Fermentas kit (GeneJET Gel Extraction Kit), the products were quantified using Nanodrop and their weight verified on an agarose gel. The plasmid fragments were then mixed in a tube so that there were in equal molar ratios of each and sterile water was added to make a total volume of 15 µl. To this volume, 5 µl of T4 prep mix (6 µl BSA (1 mg/ml), 6 µl NEB Buffer 2 (10x), 2.5 µl sterile deionized water and 0.5 µl T4 DNA polymerase (3 U/µl)) were added. This mix was incubate at room temperature for 30 min, after which 2 µl of dCTP (10 mM) were added. To allow proper annealing of the complement single stranded regions this final mix was incubated at 37 °C for 20 min. Finally 5 µl of the SLIC mix were transformed into *E. coli* DH5α.

DsrJ expression conditions

The expression of DsrJ from *A. vinosum* performed was described in (Grein *et al.*, 2010). Briefly, *E. coli* BL21 (DE3) was first transformed with the pEC86 plasmid to provide the expression of the genes encoded in the *ccm* operon under aerobic conditions (Arslan *et al.*, 1998), and was transformed with the appropriate plasmid used for expression of *dsrJ* gene. The fully heme-loaded DsrJ holoprotein was obtain by slow production of the recombinant protein in *E. coli*. The lacT7 promoter was used to allow the minimum expression level in the pET22b vector. No induction by IPTG was performed. 800 mL of NZCYM medium in a non-baffled Erlenmeyer flask were inoculated with a single colony of the appropriate clone or directly from a glycerol stock culture and grown at 37 °C with 150 rpm agitation for 16 hours.

DsrJ purification

Affinity tag purification. The purification of DsrJ was accomplished by affinity chromatography. In this purification buffer W (150 mM NaCl, 100 mM TrisHCl pH 8) was used to equilibrate the column. Cells from 800 mL were broken in a French Press equipment and centrifuged at 58545 × *g* for 20 min. The supernatant was then added to the Streptactin column and purified by gravity. After all the sample was applied to the column, 5 column volumes (CV) of buffer W were passed. Finally, to elute the protein from the column seven half CV of buffer E (150 mM NaCl, 100 mM TrisHCl pH 8 and 2.5 mM desthiobiotin) were passed. The column was regenerated with one CV of 0.5 M NaOH and 10 CV of buffer W.

Purification of the rDsrJ without the strep tag. The cells were broken with the French press, centrifuge 15 min at 58000 × *g* and the supernatant collected and centrifuge at 100000 × *g* for 1:30 h. The soluble fraction was applied in a Q-Sepharose 16/10 with and without detergent (SB12). The fraction with the highest 280/408 nm was applied into resource 6mL. The best fraction from the last column was applied to an HTP column.

Protein detection

For the detection of the DsrJ protein a 9% tricine-SDS-PAGE was performed was described in (Schagger, 2006). The gel were electrophoresed for 2 h at 120 mV in an Amersham electrophoresis equipment. To reveal the protein bands Coomassie and heme staining were employed.

Coomassie staining. After protein electrophoresis the stacking gel was removed, and the resolving gel was transferred into a staining solution containing 50% (v/v) methanol, 10% (v/v) acetic acid, 40% (v/v) dH_2O and 0.25% (w/v) Coomassie Brilliant Blue R250, during 30 min. Next, the staining solution was replaced by a destain solution with 20% (v/v) methanol, 10% (v/v) acetic acid and 70 % (v/v) dH_2O. The latter was exchanged several times, until the protein bands were clearly visible.

Heme staining. After the polyacrylamide gel electrophoresis the stacking gel was removed and the resolving gel incubated in the heme staining solution (4.5 mg of TMBZ dissolved in 15 mL methanol with 35 mL of 250 mM sodium acetate pH 5) for 30 min in the dark with gentle agitation. Then an incubation with 600 µl of a 30% H_2O_2 solution was added and the gel left in the solution until signals appeared. The reaction was stopped by several repeated wash steps with MilliQ water.

Mass spectrometry

The mass spectrometry measurements were carried at the Mass Spectrometry Laboratory, Analytical Services Unit, Instituto de Tecnologia Química e Biológica (ITQB), Universidade Nova de Lisboa. For each sample 5 µl of protein were desalted, concentrated and eluted using R1 (RP-C4 equivalent) microcolumns. Proteins were eluted directly onto a MALDI plate with sinapinic acid (10 mg/mL) using 50% (v/v) acetonitrile and 5% (v/v) formic acid. Mass spectra were acquired in the positive linear MS mode using a MALDI-TOF/TOF, Applied Biosystems, model 4800 (PO 01MS).

EPR spectroscopy

Electron paramagnetic resonance (EPR) spectroscopy was accomplished by Ines A. C. Pereira and Sofia S. Venceslau from the Laboratory for Bacterial Energy Metabolism of the Instituto de Tecnologia Quimica e Biologica (ITQB), Universidade Nova de Lisboa. Spectra were recorded using a Brucker EMX spectrometer equipped with an ESR 900 continuous-flow helium cryostat from Oxford Instruments.

Raman Resonance

RR spectra were recorded by Smilja Todorovic in the Laboratory for Raman Spectroscopy of Metalloproteins at the ITQB. Measurements were performed with a confocal microscope coupled to a Raman spectrometer (Jobin Yvon U1000). Samples were placed in a quartz rotating cell, excited with either 413 nm or 647 nm line from a krypton ion laser (Coherent Innova 302) and measured with 5 mW laser power and accumulation times of 60 s at room temperature. After polynomial background subtraction, the positions and line-widths of the Raman bands were determined by component analysis (Todorovic et al., 2006).

NMR experiments

NMR experiments were performed by Catarina Paquete from the Inorganic Biochemistry and NMR Laboratory at the ITQB. The buffer of the purified proteins was exchanged for 80 mM sodium phosphate buffer (pH 8.0) with NaCl (final ionic strength of 250 mM) prepared in 99.9% $^{2}H_2O$ (CIL), through ultrafiltration procedures with Amicon Ultra Centrifugal Filter Units (Millipore). Protein samples with

approximately 1 mM were placed in 3 mm Wilmad NMR tubes. The 1D ^{1}H NMR spectra were acquired on a Bruker Avance 600 MHz spectrometer with a spectral width of 30 kHz at 25 °C. ^{1}H chemical shifts were calibrated using the water signal as internal reference. All NMR spectra were processed using TopSpin™ NMR Software from Bruker Biospin.

5.3. Results and discussion

DsrJ is part of a larger membrane complex believed to be involved in sulfate respiration. This protein was already investigated by Pires *et* al. as part of the DsrMKJOP complex from *D. desulfuricans* (Pires *et al.*, 2006). Grein *et* al. had also examined the role of DsrJ in the DsrMKJOP complex of *A. vinosum* (Grein *et al.*, 2010). However, the nature and function of this cytochrome *c* was not completely revealed. DsrJ contains, by sequence analysis and confirmed by mass spectrometry, three *c*-type hemes. According to sequence alignment only one cysteine,

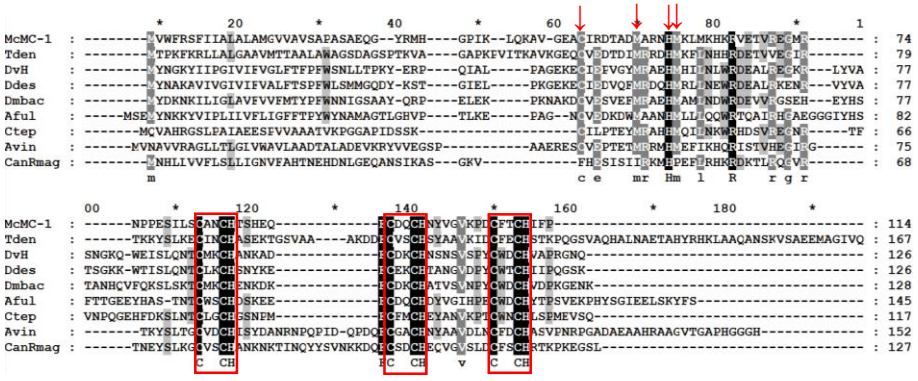

Figure. 5.1. Sequence alignment of DsrJ proteins. Heme binding motifs are boxed. Putative distal heme ligands are denoted with arrows. Strictly conserved residues are marked with black boxes. Species: A. vinosum (Avin), Magnetococcus sp. MC-1 (McMC-1), Thiobacillus denitrificans (Tden), Chlorobaculum tepidum (Ctep), Desulfovibrio vulgaris Hildenborough (Dvul), Desulfovibrio desulfuricans ATCC 27774 (Ddes), Archaeoglobus fulgidus (Aful), Desulfomicrobium baculatum (Dmbac), and Candidatus Ruthia magnifica (CandRmag) (Grein et al., 2010).

two methionines, one histidine, one serine, one arginine and one phenylalanine are conserved among DsrJ homologue sequences (Pires *et al.*, 2006, Grein *et al.*, 2010).

Considering that there are no documented cytochrome *c*- type hemes with a serine or phenylalanine as distal axial ligands, these were not considered as possible ligands. Also, in SoxXA (present in SOB and involved in thiosulfate oxidation) the conserved arginine is proposed to be responsible for the sulfur-sulfur bond polarization, providing a strong anion-binding site suitable for the substrate, thiosulfate (Bamford *et al.*, 2002). As so, only the remaining residues were considered as probable heme ligands, one cysteine, two methionines, and one histidine. Pires *et* al proposed that, the hemes have His/His, His/Met and a unique His/Cys coordination, based on sequence analysis and EPR spectroscopy. This His/Cys ligation is so unique that it has only been reported in three other proteins: SoxXA, a complex involved in thiosulfate oxidation, isolated for example from *Rhodovulum sulfidophilum* (Reijerse *et al.*, 2007), PufC; also from this organism, a protein associated with the photosynthetic reaction center (Alric *et al.*, 2004); and TsdA, a thiosulfate dehydrogenase (Denkmann *et al.*, 2012). In *A. vinosum* it was proven that DsrJ is essential for sulfur oxidation (Sander *et al.*, 2006), and it was also verified that a mutant where the conserved cysteine was changed to a serine had a severe decrease in the rate of sulfur oxidation, retaining only 19% of the wild type activity (Grein *et al.*, 2010). Although these distal axial heme ligands were assigned to DsrJ, the heme coordination was never completely established. The only evidence is for the His/Cys heme was a characteristic peak at $g_{max} = 2.47$ observed by EPR. Besides the EPR, it was not yet possible to assign the His/Cys heme-coordination by other technique. For this reason, we continued the work performed by Grein and coworkers (Grein *et al.*, 2010), using their vector we generate

several variants of DsrJ with mutations in the putative heme ligands to try to establish the heme coordination. According to Grein et al. (Grein *et al.*, 2010), the vector pETJStrep introduced in *E. coli* BL21 (DE3) gold, is able to produce a full heme loaded protein. As so, we used the same growth conditions during this work. Several approaches were used to express rDsrJ in *E. coli,* which involved the generation of the variants using different constructions: i) the rDsrJ with the Strep tag in the N-terminal, ii) rDsrJ with the Strep tag in the C-terminal position and iii) rDsrJ without the Strep tag.

rDsrJ with the Strep tag in the C-terminal

5'- MKYLLPTAAAGLLLLAAQPAMAMDEVKRYVVEGSPAAERESCVEPT
ETMRRMHMEFIKHQRISTVHEGIRGTKYSLTGCVDCHISYDANRNPQPI
DQPDQFCGACHNYAAVDLNCFDCHASVPNRPGADAEAAHRAAGVTGA
PHGGGHSAWSHPQFEK -3'

Figure. 5.2. Sequence organization with the pELB leader (blue), strep tag (green) and DsrJ gene (red).

Our first approach was to use the plasmid pETJStrep (Grein *et al.*, 2010), which is a pet22b vector in which the His tag was replaced by a pPR-IBA2 Strep tag in the C-terminal (organization in the Figure 5.2) (Grein *et al.*, 2010). This vector contains the DsrJ gene (Alvin_1260) from *A. vinosum* without the first 26 amino acids present in the N-terminal that code for a signal peptide required for the translocation of the protein via the Sec pathway. This signal peptide was removed because the plasmid already encodes an equivalent leader peptide. With this plasmid, seven variants were generated: C46G, M53A, M58A, C46GM53A, C46GM58A, M53AM58A and C46GM53AM58A.

UV-visible spectroscopic analysis. The UV-visible spectrum was similar for all the rDsrJ variants. It shows the characteristic peaks of a cytochrome *c* with the *Soret* peak at 408 nm and a δ peak at 351 nm in the oxidized state and a *Soret* peak at 417 nm and α and β peaks at 520 nm and 550 nm respectively in the reduced state (Figure 5.3). Also, a band at 650 nm appears both in the oxidized and reduced state. This band was analyzed by Grein *et* al., with resonance Raman, and it was associated with an electronic absorption band belonging to a Q-band (α/β transitions) (Grein *et al.*, 2010). The 650 nm peak is similarly detected in the spectrum of the ferric P450 cytochromes in which a Cys is a proximal ligand (Yoshioka *et al.*, 2001), in some substrate-bound LS P450 cytochromes and in Cys/His P450 mutants (Martinis *et al.*, 1996). It has also been correlated to a five-coordinated high-spin species. Due to the fact that this 650 nm band was observed in the rDsrJ Wt (which according to Grein and coworkers there was no high spin observed) and in all the variants, we did not assign this 650 nm to the presence of a high spin heme.

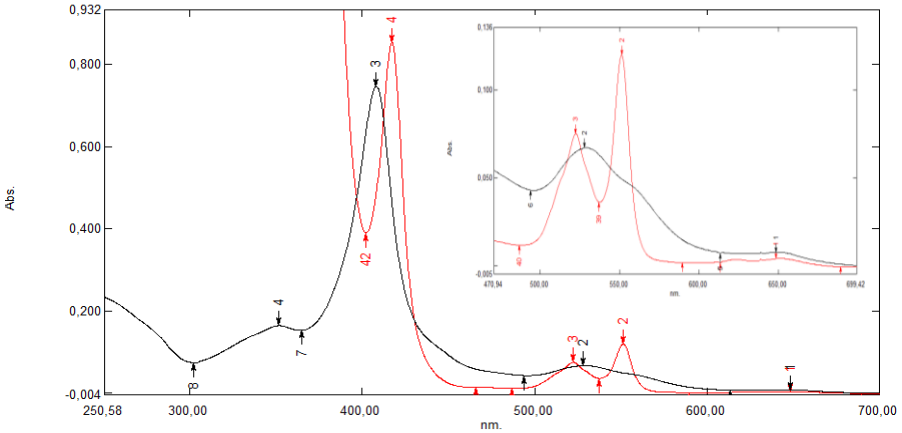

Figure. 5.3. Uv-visible spectrum of rDsrJ wild type in the oxidized state (black) and in the reduced state (red). The box on the right is a close up to α and β peaks and also to the 650nm shoulder.

Mass spectrometry analysis. According to the MS analysis the rDsrJ Wt, the rDsrJ C46G and the rDsrJ M53A all had approximately the correct molecular mass concerning the native form along with 3 hemes (Table 5.1). This suggests that the maturation time and the purification of the proteins were well established.

Table. 5.1. Mass (Da) obtained versus the theoretical mass for the variants produced and the number of hemes present per each protein. MD (Mass difference between deviation and theoretical mass of the 3 hemes (1837.5 Da)).

Mass (Da)					
	theoretical	obtained	deviation	theoretical mass of heme *c*	MD
rDsrJ wild type	14960.5	16812,2	1857.7	612,5	20
rDsrJ C46G	14914.4	16760,9	1846.5		9
rDsrJ M53A	14900.4	16760,7	1860.3		23

We also perform a more thorough analysis of the MS spectra of rDsrJ wild type and rDsrJ C46G. Comparing our results with data from Grein *et* al. 2009 (unpublished data), together these MS analyses

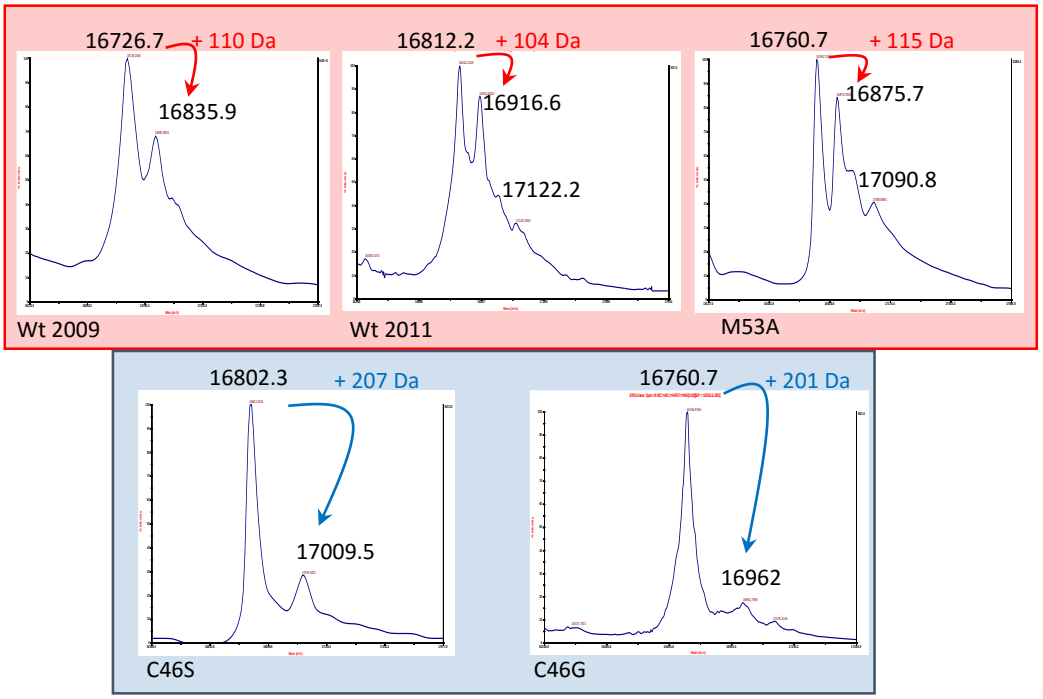

Figure. 5.4. Mass spectrometry results of rDsrJ variant proteins

indicate that there might be a modification in the wild type protein (Figure 5.4). The rDsrJ Wt protein and the rDsrJ M53A shows an additional peak that varies between 104 and 115 Dalton, besides the expected peak for DsrJ with 3 hemes. This peak is clearly missing in the C46S and C46G variants. Due to the proximity of the mass variation of this additional peak to the mass of a thiosulfate molecule (112 Da), we propose that, both rDsrJ Wt and the rDsrJ M53A, may have a thiosulfate modification of one heme. A similar modification is also observed in the heme-ligating cysteine of SoxXA, which is in a persulfide form, since the mass increased by 32 Da (Bamford *et al.*, 2002). The origin of this modification is still not clear. The persulfide form was observed in

Rv. sulfidophilum SoxXA as result of the turnover of the protein or incomplete reaction cycles and when the SoxXA was incubated with thiosulfate, dimethylsulfide (DMS) or dimethylsulfoxide (DMSO) it also give rise to additional peak increase (Kappler *et al.*, 2005).

Raman Resonance (RR) analysis. To obtain information on the redox state, spin state and ligation pattern of the hemes with RR the spectra must be at the high frequency region (1300 – 1700 cm^{-1}). In this region the spectra of the proteins are obtained upon Soret band excitation. The high frequency RR spectra were therefore recorded upon Soret band excitation at 413 nm (Figure 5.5). The ν_4 band is a marker band for the redox state of the heme iron whereas ν_3, ν_2 and ν_{10} bands are sensitive indicators of the heme spin state (Spiro & Czernuszewicz, 1995). The RR spectra of all mutants revealed a ν_4 band centered at ~1373cm^{-1} typical for ferric cytochrome *c* (Spiro & Strekas, 1974). The Raman resonance (RR) spectra of the DsrJ variant proteins are extremely similar to each other. Even the proteins missing the cysteine 46 and methionine 53 show identical spectra as the wild type protein. This was also observed for the C46S protein (Grein *et al.*, 2010). Nevertheless RR spectroscopy confirms that there is no high spin heme in any of the samples (Figure 5.5).

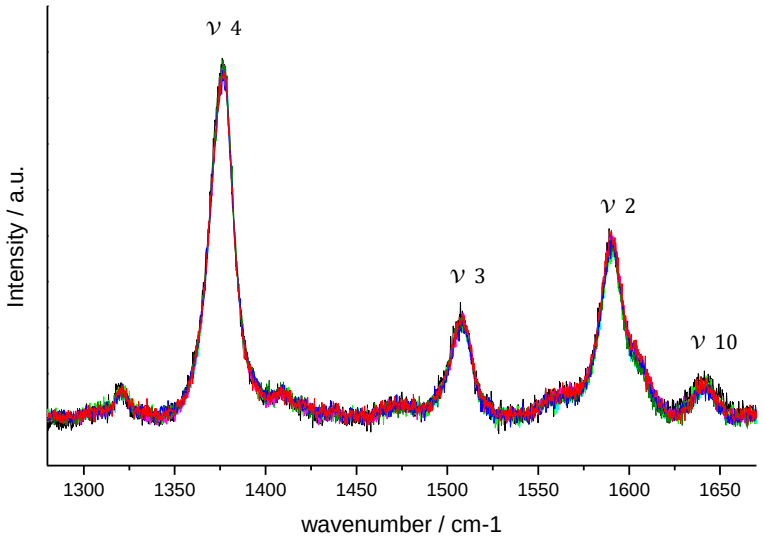

Figure. 5.5. Overlaid resonance Raman spectra overlaid of all variants analyzed, proving the absence of high spin heme in any sample.

Electron paramagnetic resonance (EPR). All DsrJ variant proteins were analyzed by EPR spectroscopy (Figure 5.6). EPR spectra also did not reveal the presence of high spin hemes. The g_{max} = 2.517 signal which was attributed to a thiolate ligated heme disappears either when C46 or M53 are missing in the protein.

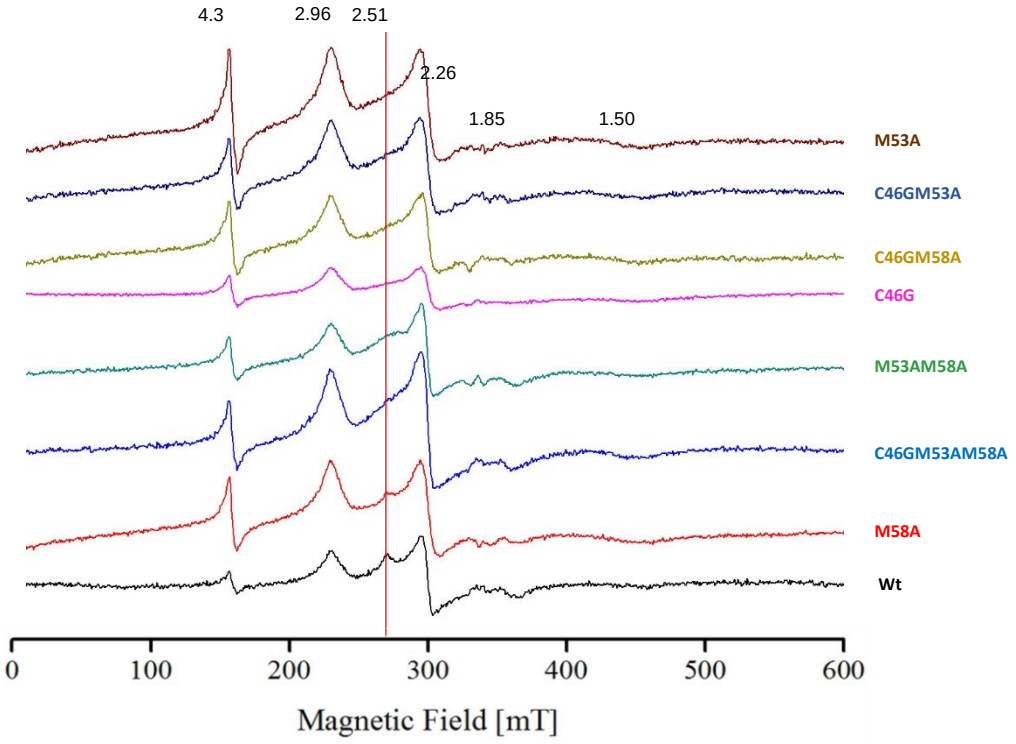

Figure. 5.6. EPR spectra of all mutants analyzed comparison. No signal is visible for a high spin heme. The only difference is the shoulder at gmax=2.517 (red line) that disappears in variants where the C46 or the M53 were modified. Experimental conditions: microwave frequency, 9.38 GHz; microwave power, 2 mW; modulation frequency, 100 kHz; and modulation amplitude, 1 mT

rDsrJ with the strep tag in the N-terminal

5’- MKYLLPTAAAGLLLLAAQPAMAMASWSHPQFEKGAGSDEVKRYVVE
GSPAAERESCVEPTETMRRMHMEFIKHQRISTVHEGIRGTKYSLTGCVD
CHISYDANRNPQPIDQPDQFCGACHNYAAVDLNCFDCHASVPNRPGAD
AEAAHRAAGVTGAPHGGGH- 3’

Figure. 5.7. Sequence organization with the pELB leader (blue), strep tag (green) and DsrJ gene (red)

During the first approach we realized that the proteins were being purified together with a second form due to the proteolytic degradation of rDsrJ (Figure 5.8 B). Since this form also stains for heme, it will distort the spectroscopic characteristics of the sample and also the protein concentration calculation. Even though this form could be removed with a S75 gel filtration column, it was decided to change the strep tag from the C-terminal to the N- terminal. In this new strategy if the proteolytic degradation of rDsrJ that binds to the Streptavidin column it will not interfere with the heme calculations as it does not contain the heme binding motif. This new approach improved the purification step without the interfering of the proteolytic degradation in the heme analysis (Figure 5.7). This new construction was named petStrepDsrJav (rDsrJ2wt), and from it seven variants were generated: C46G, H56A, C46GM53A, C46GM58A, C46GH56A and M53AM58A. Once again, there was no change in the UV-visible spectra of the variants. Intriguingly, not even the H56A variant had extra peak for a high spin heme, which is quite strange as this is the only histidine conserved among all DsrJ proteins and it should be one of the heme-ligands in this protein.

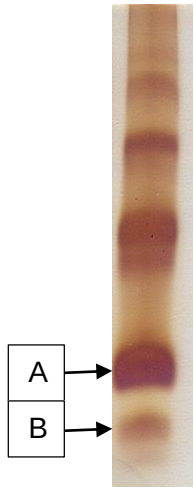

Figure. 5.8. Heme staining of rDsrJ wild type (A) and the proteolytic form (B)

Nuclear magnetic resonance (NMR). NMR is an extremely good technique to study heme ligations and heme environment changes. The samples rDsrJ2wt and the variant rDsrJ2C46G were purified and analyzed by NMR (by Doctor Catarina Paquete from Inorganic Biochemistry and NMR Laboratory at ITQB-UNL Portugal). When comparing rDsrJ2wt with rDsrJ2C46G there is no peak differences from these two samples. However, the absence of the cysteine may be affecting the heme environment. When the cysteine is modified to a glycine, in the NMR spectrum we can verify the appearance of a shoulder in the main peaks of the rDsrJ2C46G variant (Figure 5.9). According to the temperature assay (Figure 5.9), it can be observed that both samples start with the same peaks at the same ppm, with increasing temperature it can be noticed that in both cases there is a peak shift. However, in the case where the cysteine is absent (rDsrJ2C46G variant), a shoulder starts to appear (with increasing temperature) in the peaks at ~35 ppm and ~21 ppm (Figure 5.8 blue arrows). This may suggest a change in the heme environment.

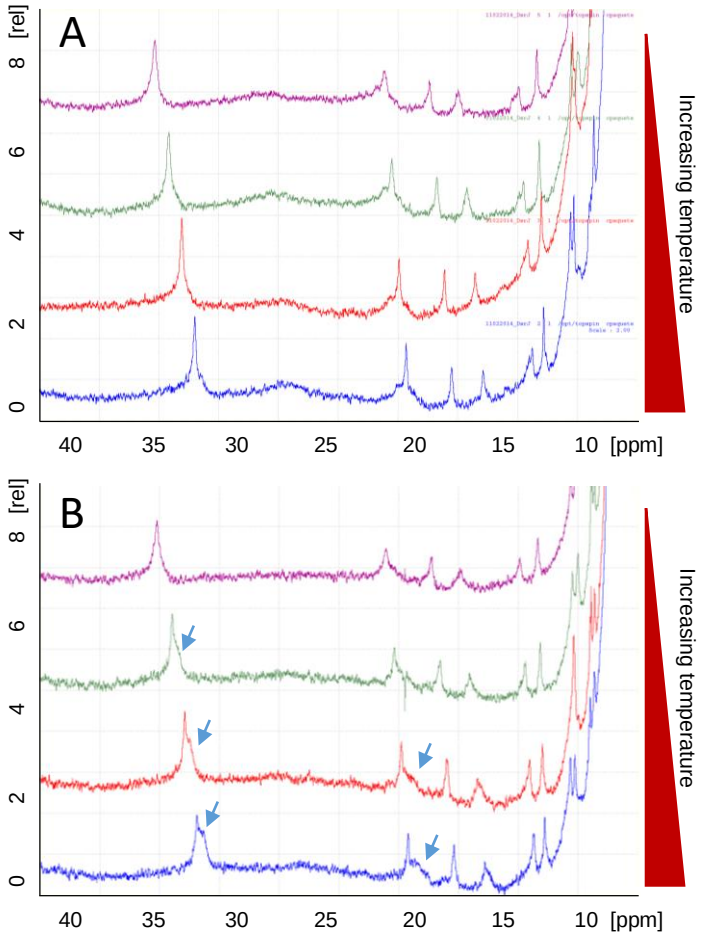

Figure. 5.9. Temperature dependence of the samples (A) rDsrJ2wt and (B) rDsrJ2C46G. The arrows in (B) indicate the appearance of the shoulders.

rDsrJ without the Strep tag

Due to the ambiguous results described above, concerning the heme ligands we thought that the strep tag could be influencing the overall structure of rDsrJ. To remove the tag we used two approaches: to simply remove it from the vector or to use a 6His-tag instead with a thrombin cutting sequence in the N-terminal to enable its removal.

The recombinant protein without any tag revealed to be extremely difficult to purify. Although three columns were performed, the pure protein had a very low 408/280 nm ratio when comparing with what is obtained when purifying the rDsrJ protein with the strep tag. This ratio was no higher than 0.26 in comparison with 5 from the strep tagged protein. Another drawback of this new approach was the fact that rDsrJ was spread through several peaks. From this strategy it was never possible to obtain pure protein to work with.

5'- MKYLLPTAAAGLLLLAAQPAMAMGSSHHHHHHSSGLVPRGSHMDE
VKRYVVEGSPAAERESCVEPTETMRRMHMEFIKHQRISTVHEGIRGTK
YSLTGCVDCHISYDANRNPQPIDQPDQFCGACHNYAAVDLNCFDCHA
SVPNRPGADAEAAHRAAGVTGAPHGGGH -3'

Figure. 5.10. Sequence organization with the pELB leader (blue), 6his tag (green), thrombin cutting site (yellow) and DsrJ gene (red)

Our last approach was to introduce the *dsrJ* gene without the first 26 amino acids into pet28c (Figure 5.10). This new pET vector contains a 6His-tag in the N-terminal position followed by a thrombin cutting sequence. The optimization of this method is still ongoing.

5.4. Conclusion

DsrJ is a very special *c*-type cytochrome. Although it has been studied since 2006 (Pires *et al.*, 2006, Grein *et al.*, 2010) the heme ligands still remain to be clearly established. Here, the continuation of the work performed by Grein and coworkers was described. We performed more than ten variants and analyzed the recombinant proteins by several techniques such as EPR, RR, NMR and UV-visible. The results were not elucidative as they do not corroborate the previous results on heme ligands assumptions (Pires *et al.*, 2006). It was predicted by Pires that the conserved cysteine 46, the histidine 57 and the methionine 58 should be the three distal axial ligands of DsrJ hemes. These proposals could not be supported by the variants performed, including the cysteine and the conserved methionines, as they did not reveal any high spin heme in any of the techniques used. This may mean that either there are other residues (not conserved among different DsrJ proteins) that can ligate the hemes in the absence of the preferred distal axial ligand (the conserve residues) predicting a “switch on/off” mechanism, or simply that something is interfering with the heme coordination, and so these results are not conclusive. Furthermore, we cannot exclude the possibility of a change in the native structure of DsrJ, due to the absence of the other subunits of the DsrMKJOP complex. Attempts to crystalize DsrJ failed, as none of the variants produced crystals. The structure of DsrJ could close the discussion, as it would answer the question of the heme ligands.

References

Alric J, Tsukatani Y, Yoshida M, Matsuura K, Shimada K, Hienerwadel R, Schoepp-Cothenet B, Nitschke W, Nagashima KVP & Vermeglio A (2004) Structural and functional characterization of the unusual triheme cytochrome bound to the reaction center of Rhodovulum sulfidophilum. *Journal of Biological Chemistry* **279**: 26090-26097.

Arslan E, Schulz H, Zufferey R, Künzler P & Thöny-Meyer L (1998) Overproduction of the *Bradyrhizobium japonicum c*-type cytochrome subunits of the *cbb*$_3$ oxidase in *Escherichia coli*. *Biochem Biophys Res Commun* **251**: 744-747.

Bamford VA, Bruno S, Rasmussen T, Appia-Ayme C, Cheesman MR, Berks BC & Hemmings AM (2002) Structural basis for the oxidation of thiosulfate by a sulfur cycle enzyme. *EMBO J* **21**: 5599-5610.

Bamford VA, Bruno S, Rasmussen T, Appia-Ayme C, Cheesman MR, Berks BC & Hemmings AM (2002) Structural basis for the oxidation of thiosulfate by a sulfur cycle enzyme. *EMBO J* **21**: 5599-5610.

Cheesman MR, Little PJ & Berks BC (2001) Novel heme ligation in a c-type cytochrome involved in thiosulfate oxidation: EPR and MCD of SoxAX from Rhodovulum sulfidophilum. *Biochemistry* **40**: 10562-10569.

Dahl C, Engels S, Pott-Sperling AS, Schulte A, Sander J, Lubbe Y, Deuster O & Brune DC (2005) Novel genes of the dsr gene cluster and evidence for close interaction of Dsr proteins during sulfur oxidation in the phototrophic sulfur bacterium Allochromatium vinosum. *J Bacteriol* **187**: 1392-1404.

Denkmann K, Grein F, Zigann R, Siemen A, Bergmann J, van Helmont S, Nicolai A, Pereira IAC & Dahl C (2012) Thiosulfate dehydrogenase: a widespread unusual acidophilic c-type cytochrome. *Environmental Microbiology* **14**: 2673-2688.

Frigaard N-U & Dahl C (2009) Sulfur Metabolism in Phototrophic Sulfur Bacteria. *Advances in Microbial Physiology, Vol 54,* Vol. 54 (Poole RK, ed.) p.^pp. 103-200.

Grein F (2010) Biochemical, biophysical and functional analysis of the DsrMKJOP transmembrane complex from *Allochromatium vinosum*. Thesis, University of Bonn

Grein F, Venceslau SS, Schneider L, Todorovic S, Hildebrandt P, Pereira IAC & Dahl C (2010) DsrJ, an essential part of the DsrMKJOP transmembrane complex in the purple sulfur bacterium *Allochromatium vinosum*, is an unusual triheme cytochrome *c*. *Biochemistry* **49**: 8290-8299.

Kappler U, Hanson GR, Jones A & McEwan AG (2005) A recombinant diheme SoxAX cytochrome - implications for the relationship between EPR signals and modified heme-ligands. *FEBS Letters* **579**: 2491-2498.

Kappler U, Hanson GR, Jones A & McEwan AG (2005) A recombinant diheme SoxAX cytochrome - implications for the relationship between EPR signals and modified heme-ligands. *FEBS Lett* **579**: 2491-2498.

Kilmartin JR, Maher MJ, Krusong K, Noble CJ, Hanson GR, Bernhardt PV, Riley MJ & Kappler U (2011) Insights into structure and function of the active site of SoxAX cytochromes. *J Biol Chem* **286**: 24872-24881.

Li MZ & Elledge SJ (2007) Harnessing homologous recombination in vitro to generate recombinant DNA via SLIC. *Nat Methods* **4**: 251-256.

Mander GJ, Duin EC, Linder D, Stetter KO & Hedderich R (2002) Purification and characterization of a membrane-bound enzyme complex from the sulfate-reducing archaeon Archaeoglobus fulgidus related to heterodisulfide reductase from methanogenic archaea. *European Journal of Biochemistry* **269**: 1895-1904.

Martinis SA, Blanke SR, Hager LP, Sligar SG, Hui Bon Hoa G, Rux JJ & Dawson JH (1996) Probing the Heme Iron Coordination Structure of Pressure-Induced Cytochrome P420cam. *Biochemistry* **35**: 14530-14536.

Pereira IA, Ramos AR, Grein F, Marques MC, da Silva SM & Venceslau SS (2011) A comparative genomic analysis of energy metabolism in sulfate reducing bacteria and archaea. *Front Microbiol* **2**: 69.

Pires RH, Venceslau SS, Morais F, Teixeira M, Xavier AV & Pereira IA (2006) Characterization of the Desulfovibrio desulfuricans ATCC 27774 DsrMKJOP complex--a membrane-bound redox complex involved in the sulfate respiratory pathway. *Biochemistry* **45**: 249-262.

Reijerse EJ, Sommerhalter M, Hellwig P, Quentmeier A, Rother D, Laurich C, Bothe E, Lubitz W & Friedrich CG (2007) The Unusal Redox Centers of SoxXA, a Novel c-Type Heme-Enzyme Essential for Chemotrophic Sulfur-Oxidation of Paracoccus pantotrophus†. *Biochemistry* **46**: 7804-7810.

Sander J, Engels-Schwarzlose S & Dahl C (2006) Importance of the DsrMKJOP complex for sulfur oxidation in Allochromatium vinosum and phylogenetic analysis of related complexes in other prokaryotes. *Arch Microbiol* **186**: 357-366.

Schagger H (2006) Tricine-SDS-PAGE. *Nat Protoc* **1**: 16-22.

Spiro TG & Strekas TC (1974) Resonance Raman spectra of heme proteins. Effects of oxidation and spin state. *J Am Chem Soc* **96**: 338-345.

Spiro TG & Czernuszewicz RS (1995) [18] Resonance Raman spectroscopy of metalloproteins. *Methods in Enzymology,* Vol. Volume 246 (Kenneth S, ed.) p.^pp. 416-460. Academic Press.

Todorovic S, Jung C, Hildebrandt P & Murgida DH (2006) Conformational transitions and redox potential shifts of cytochrome P450 induced by immobilization. *J Biol Inorg Chem* **11**: 119-127.

Walker FA (1999) Magnetic spectroscopic (EPR, ESEEM, Mössbauer, MCD and NMR) studies of low-spin ferriheme centers and their corresponding heme proteins. *Coordination Chemistry Reviews* **185–186**: 471-534.

Yoshioka S, Takahashi S, Hori H, Ishimori K & Morishima I (2001) Proximal cysteine residue is essential for the enzymatic activities of cytochrome P450cam. *European Journal of Biochemistry* **268**: 252-259.

Chapter 6

Concluding remarks

Concluding remarks

Over the decades the mechanism of sulfate respiration has been uncovered. One of the main questions was the mechanism of the six electron reduction of sulfite to sulfide by DsrAB. For several years, the mechanism proposed was based in *in vitro* assays, in which DsrAB produces three products, in relative proportions that depend on the sulfite concentration available. The enzyme produces more trithionate/thiosulfate in the presence of high concentrations of sulfite, or more sulfide in the presence of lower concentrations of sulfite. However, in 2008 Oliveira and coworkers suggested that DsrC could be crucial for this mechanism. With this, Oliveira and coworkers proposed a different mechanism for sulfite reduction based on the crystal structure of DsrAB from *D. vulgaris* Hildenborough. In this mechanism, the C-terminal conserved cysteines (Cys93 or Cys_B and Cys104 or Cys_A) of DsrC would be essential for the catalytic reduction of sulfite. According to this proposal, DsrAB would reduce sulfite to an S^0 intermediate state at the siroheme-[4Fe-4S] catalytic center, then DsrC Cys_A would interact with the S^0 intermediate and form a persulfide DsrC-Cys_A-SH intermediate. This persulfide DsrC form would be attacked by Cys_B releasing sulfide and forming a disulfide bond between Cys_B and Cys_A. Finally, it was proposed that this oxidized form of DsrC would then be reduced by the DsrMKJOP complex. This was the first proposal for a connection of sulfite reduction to energy conservation. Our new findings showed that this proposal was correct in the fact that DsrC is crucial for the DsrAB sulfite reduction, however DsrC does not form a persulfide but a trisulfide product. We now propose that four electrons from the reduced menaquinone pool will be needed for reducing this DsrC form, instead of the two proposed by Oliveira et al. (2008). According to our data, DsrAB

reduces sulfite to an S^{II} intermediate which is attacked by Cys_A of DsrC and subsequently by Cys_B to form a trisulfide bound Cys_B - S^0 - Cys_A. This DsrC-trisulfide will be then reduced at the DsrK heterodisulfide reductase-like protein (present in the DsrMKJOP) by four electrons. Thus, the soluble process accomplished by DsrAB and DsrC is coupled to energy conservation through the generation of a pH gradient driven by the DsrMKJOP. It is thought that DsrK may be able to reduce disulfide bridges and an interaction between the DsrMKJOP complex and reduced DsrC has already been shown. However, this proposal must be validated experimentally, and the redox potential of the DsrC-trisulfide should also be determined.

Furthermore, the source of the first two electrons going into DsrAB and sulfite still needs additional investigation. Based on the structure of DsrAB, which contains one ferredoxin like domain per each DsrA and DsrB subunit, we considered that DsrAB could interact with a ferredoxin oxidoreductase-like protein. Also, in the case of some aSiR and in the reverse DsrAB, NAD(P)H oxidoreductases are crucial as electron donor/acceptor. As such, three ferredoxin oxidoreductases (AOR, PFOR and CODH) and one NADH oxidase were selected as physiologic candidates to test their ability to donate electrons for DsrAB sulfite reduction. Using *in vitro* activity assays and SPR we could not observe any interaction of DsrAB with the selected electron donors. However, these are still preliminary results and further work needs to be performed in order to confirm them. Besides the need to fine tune individual reaction conditions (such as pH and buffer), the next step would be to isolate the electron donor candidates from the same organism as the DsrAB protein. Moreover, there is still the possibility that the electron donor is a ferredoxin protein similar to ferredoxin I of *D. vulgaris* (known to be present in all SRP), as in plants where the aSiR receives electrons from

a ferredoxin previously reduced by the photosystem I. The production of the recombinant 6 kDa ferredoxin from *A. fulgidus* (Fdx IV) would be of extreme importance to test in the activity assays of DsrAB and DsrC.

As referred before, the DsrC is proposed to interact with the DsrMKJOP complex for the reduction of the trisulfide bond after reacting with DsrAB S^{II} intermediate. This complex is widespread among SRP and can be divided in two modules: DsrMK (known to be present in all SRP) and DsrJOP. The DsrMK module is proposed to interact with the menaquinone pool (through DsrM) and to reduce the DsrC-trisulfide bond (through DsrK). On the other hand, the DsrJOP module is very intriguing. It was shown that a mutant lacking the DsrJ subunit was incapable of oxidizing sulfur globules in SOB, although it also exists in SRP, where no sulfur chemistry is supposed to occur in the periplasm. DsrJ is a cytochrome *c* protein with three heme binding motifs with one proposed to have an unusual cysteine/histidine ligation. To reveal the nature of the heme ligands of DsrJ we generated several variants. These variants were characterized by several techniques: EPR, RR, MNR and UV-visible. Even though we generated more than ten variants, and tested them using different approaches, all the results were inconclusive and did not clarify the nature of the heme ligands. These results suggest that probably something occurred to the recombinant protein masking the results. It could also be that the presence of the other subunits of DsrMKJOP could be extremely important for the proper folding of DsrJ. Moreover, we tried also several attempts to get a crystal structure but none of the variants formed crystals. The crystal structure of DsrJ will be important to solve the question of which are the three distal axial heme ligands. Also, the construction of a *dsrJ* deletion mutant in *D. vulgaris* could answer the question of how important this protein is in SRP.

Overall, this thesis contributed to better understand the role of DsrAB and DsrC in the mechanism of dissimilatory sulfite reduction. It is known that the predominant menaquinone in *Desulfovibrio* (MK-6) has a redox potential of ~-67 mV, while inorganic polysulfides have redox potentials in the range of ~-260 mV. So, the DsrC-trisulfide may have a redox potential too low to be reduced directly by MK-6, suggesting that a quinone bifurcating mechanism may occur in DsrMKJOP. Thus, disclosing the physiological electron donor to DsrAB and the interaction of the DsrC-trisulfide with the DsrMKJOP complex are mandatory to fully understand the sulfite reduction mechanism.